p-ISSN 3093-3137
e-ISSN 3093-3153

VIETNAM JOURNAL OF Agriculture & Environment

MINISTRY OF AGRICULTURE AND ENVIRONMENT

Volume 4
No. 9 (2025)

EDITORIAL BOARD

VIETNAM JOURNAL OF AGRICULTURE AND ENVIRONMENT

p-ISSN 3093-3137
e-ISSN 3093-3153
VOL.4 No. 9 (2025)

Head-office
No 10 Nguyen Cong Hoan
Giang Vo - Ha Noi - Vietnam
Tel: 024.37711072
Fax: 024.37711073
E-mail: tapchinnmt@mae.gov.vn
http://tapchikhoahoc.nnmt.net.vn

License No.23/GP - BVHTTDL issued by the Ministry of Culture, Sports and Tourism on April 25, 2025

Printing in Hung Ha trading production company Limited

CONTENTS

OPTIMIZING MICRO PROPAGATION OF *Asparagus officinalis* AND STIMULATING PLANTLETS USING ARBUSCULAR MYCORRHIZAL FUNGI

Bui Minh Sang[1], Nguyen Thi Pha[2], Do Thi Xuan[2,*]

[1] *Cuu Long Delta Rice Research Institute, Can Tho city*

[2] *Institute of Food and Biotechnology, Can Tho University*

**Email: dtxuan@ctu.edu.vn*

ABSTRACT

The study aimed to optimize the micropropagation process, including seed sterilization, shoot multiplication and *in vitro* rooting and to investigate the effect of arbuscular mycorrhizal fungi (AMF) inocula on the stimulation of the plantlets (*Asparagus officinalis*) growth. The results showed that the highest germination rate was 90% when the seeds were disinfected with 6% sodium hypochlorite for 10 minutes. A Murashige and Skoog medium (MS) supplemented with 2.0 mg/L kinetin and 0.1 mg/L naphtalen-acetic acid effectively promoted the shoot formation with 6.6 shoots/explant and shoot length reaching 6.24 cm. Shoots cultured on semi-MS supplemented with 0.7 mg/L indole-3-butyric acid gained the best rooting rate of 42.67%, an average of 3.73 roots/plant, root length reaching 3.93 cm and no callus formation. The plantlets treated with each of three different AMF inocula grew better and achieved a 100% survival rate. Among them, the treatments amended with either AMF-SA or AMF-SC inoculum recorded the highest performance, with an average of 13.6 and 13.2 stems and plant heights of 66.38 and 66.26 cm, respectively. The combination of the micropropagation and AMF improved the propagation efficiency and growth performance of the asparagus in the plantlet stage.

Keywords: *Asparagus officinalis, micropropagation, rooting in vitro, arbuscular mycorrhizal fungi.*

Received: 4 September 2025; revised: 6 October 2025; accepted: 2 December 2025.

1. INTRODUCTION

Asparagus species is recognized as a perennial plant with several valuable functional ingredients, and has been widely used as medicine and food since ancient times [1]. It is grown globally in various climatic conditions [2]. A green asparagus is a perennial plant that is packed with nutrients and has a delightful taste [3], is one of the top 20 vegetable crops in the world. The largest production regions are China, Western Europe, North America and Peru [4]. However, the expansion of the cultivated area in Vietnam is constrained by the growers' challenge in sourcing high-quality seedlings.

Micropropagation is a widely recognized method of vegetative propagation that allows for the production of numerous offspring plants [5]. This innovative method harnesses the potential of nutrient-rich media to efficiently replicate plant cells on a large scale, resulting in the rapid production of mature and disease-free plants [6]. For asparagus, tissue culture is especially important, the traditional propagation of the asparagus is ineffective; the seed germination rate is low, and vegetative propagation by mechanical division of the rhizome is time and money-consuming and produces a very limited number of clonal copies of the plant [7]. Despite micropropagation being practiced for a long time in the asparagus, challenges such as low multiplication rate, low root formation rate, or weak root development still exist [8]. For efficient *in vitro* propagation protocols, it is essential that

the shoots root in large proportions and the regenerated plantlets acclimatize successfully. Rooting is a difficult process in recalcitrant species and without roots, the survival rate of acclimatized plants is reduced [9].

Acclimatization is the last stage of the tissue culture technique which is crucial for the success of *'in vitro'* plant propagation [10]. The mycorrhization of *in vitro* - propagated plants using arbuscular mycorrhizal fungi (AMF) is beneficial for micro-propagated plants, especially during acclimatization [11]. The AMF can promote the growth and yield of crops by increasing the use of nutrients [12], enhance host plant tolerance to drought stress [1, 13] and vigorously increase the plantlets [14]. Several reports showed that the application of the AMF improves the development of micro-propagated plantlets such as banana, blackberry and coconut [10, 11, 15].

In Vietnam, research on the micropropagation development of the asparagus industry is quickly developing. However, researches on a combination of beneficial microorganisms including AMF inocula with micro-propagated plantlets are very few. The study was conducted to optimize the micropropagation process of the asparagus (*Asparagus officinalis*) and to determine the impact of three different AMF inocula on the survival and growth of the asparagus micropropagated plantlets under greenhouse conditions.

2. MATERIALS AND METHODS

The experiment was conducted from May to December, 2024 at laboratories of the plant genetic engineering and the agricultural microbiology, Institute of Food and Biotechnology; and the greenhouse of College of Agriculture, Can Tho University. The tissue culture room maintained suitable conditions with a photoperiod of 16 hours of light per day, temperature set at 25 ± 2°C, humidity ranging from 50 to 60% and light intensity of 3,000 Lux [16]. The study was conducted in a greenhouse under controlled conditions, with a mean temperature variation from 25°C to 35°C, minimum and maximum, respectively and relative air humidity of 45% [17].

2.1. Materials and chemicals

The F1 heat-tolerant green asparagus of varieties "Atlas" (*Asparagus officinalis* L.) seeds were provided by GAFOCO Company. Murashige and Skoog (MS) basic nutrient medium containing 30 g/L sucrose and 7 g/L agar was adjusted to a pH of 5.8 before sterilizing at 121°C, 1 atm for 30 minutes [8, 18]. Chemicals used in this study included kinetin (KIN), indol-acetic acid (IAA), naphtalen-acetic acid (NAA), indole-3-butyric acid (IBA), sodium hypochlorite (NaOCl), agar, sucrose, potassium hydroxide (KOH), acetic acid, glycerol, trypan blue. They were from Sigma Chemicals company (USA). Three AMF populations selected from an asparagus soil (AMF-SA), a maize soil (AMF-SC) and a rice soil (AMF-SR) were preserved at the agricultural microbiology laboratory, Institute of Food and Biotechnology, Can Tho University

2.2. Methods

2.2.1. Effects of different NaOCl concentrations and disinfection time periods on the seed germination

The F1 asparagus seeds were first washed with soap for 10 minutes, followed by rinsing under continuously tap water for two hours. The seeds were then shaken with sterile distilled water for 1 minute and soaked in 70% ethanol for 1 minute. Subsequently, the seeds were shaken with a 3% and 6% NaOCl solution for sterilizing for 5, 10 and 15 minutes. Finally, the seeds were rinsed three times with sterile distilled water and cultured onto a basic MS medium after sterilization. The experiment was arranged in a completely randomized design with 6 treatments, 3 replications, each replication had 5 vessels, and each vessel contained 5 seeds. The germination rate (%) was monitored at three time intervals (14, 21 and 28 days) after culture.

2.2.2. Effects of different growth regulators on shoot formation under the in-vitro experiment

The study utilized 0.5 cm uniform asparagus shoot explants, cultured on the basal MS medium with 13 treatments and 3 replications for each treatment. Each replication had 5 vessels and each

vessel contained 3 cultures. The medium was supplemented with different concentrations of KIN (0, 1, 2, 3 and 4 mg/L) in combination with different concentrations of NAA (0, 0.1 and 0.5 mg/L). The number of shoots, shoot height (cm) and shoot quality were determined after 30 days of culture. The shoot quality was assessed as described by Sallam (2019) [19] including: (+++): thick, dark green explants; (++): slightly thick, green explants; (+): thin, light green explants.

2.2.3. Effects of different plant hormones on rooting formation under the in vitro experiment

The well-developed shoots got about 4 - 5 cm in height from the 2.2.2 experiment were separated individually from the clusters of shoots. The detached shoots were placed on an MS medium containing half of the basal concentration [16], supplemented with each of NAA, IBA and IAA at different concentrations (0, 0.1, 0.3, 0.5 and 0.7 mg/L) with 3 replications and 5 vessels each, making a total of 5 cultures per vessel. After 60 days of culture, the root formation rate (%), number of roots, root length (cm), and root quality were recorded.

2.2.4. Effects of the AMF populations on the plantlet growth under in vivo acclimation

Plantlets with 1 - 2 shoots, 4 - 5 cm of height and at least 3 roots each were washed with tap water after being removed from the culture vessel to remove the adhering culture medium [16]. The plantlets were planted in perforated pots measuring 6 x 10 cm, filled with an organic substrate composted from a growing substrate of a melon plant, chicken manure, and a melon residue. The substrate had a humidity content of 12%, pH = 7.67, EC = 3.03 mS/cm, total organic matter content (OM) = 31.63% and total nitrogen (Ntot) = 1.65%. Three AMF populations of AMF-SA, AMF-SC and AMF-SR which directly applied into the roots of each plantlet with a density of 100 spores and then filled with the growing substrate to cover the roots completely [20]. The study was repeated 10 replications, each replication was one pot, each pot planted one plantlet. During the experiment, plantlets were irrigated with osmosis water twice a week for two months [20]. The control treatment was set up similarly but without AMF amendment. The record survival rate (%), number of stems and plant height (cm) were collected at four-time intervals of 15, 30, 45 and 60 days respectively after the acclimation.

2.2.5. Evaluation of the presence of arbuscular mycorrhizal fungal infection

After 60 days of the acclimatization, the young root segments of the asparagus plantlets were taken to examine the infection ability of different AMF populations according to the method of Dalpé and Séguin (2013) [21]. The stained root samples were observed under a digital microscope (Olympus CX23, Japan) with 40X magnification to identify the characteristic structures of the AMF including the presence of hyphae, of arbuscules, and of vesicles.

2.3. Statistical analysis

Data were processed using Microsoft Excel (Version 2013). The variance analysis was carried out by ANOVA to compare the differences in the means of treatments which was tested by Tukey's test at a significant level of 5% using Minitab 16 software.

3. RESULTS AND DISCUSSION

3.1. Effect of different NaOCl concentrations and disinfection time periods on *in vitro* seed germination ability

When the concentration of NaOCl solution applied was increased from 3% to 6%, the germination rate also tended to increase with an average of 76.7% and 86.7%, respectively. Additionally, increasing the sterilization time from 5 to 10 minutes seemed to increase in the seed germination rate. However, when the time period was increased to 15 minutes, the germination rate tended to decrease (Table 1). Therefore using a 6% NaOCl concentration for 10 minutes the germination rates increased steadily and gained 90.0% at 28 days, which was significantly higher than that of the rates observed with other treatments. These findings aligned with previous observations that NaOCl was not effective in disinfection at low concentrations [22] while either excessive concentrations or prolonged exposure

can damage plant tissue [23]. Moderate disinfection concentration and time were observed to stimulate seed germination through the mechanism of partial seed coat degradation [24].

Table 1. Effect of NaOCl concentration and disinfection time on germination

Concentration NaOCl (%)	Disinfection time (minute)	Germination rate (%)			
		14 days	21 days	28 days	Average (%)
3	5	50.0^{b}	60.0^{b}	63.3^{b}	76.6
	10	63.3^{ab}	80.0^{ab}	83.3^{ab}	
	15	66.7^{ab}	80.0^{ab}	83.3^{ab}	
6	5	66.7^{ab}	76.7^{ab}	86.7^{ab}	86.7
	10	80.0^{a}	86.7^{a}	90.0^{a}	
	15	66.7^{ab}	83.3^{ab}	83.3^{ab}	
P		**	**	**	
CV (%)		15.7	11.7	9.6	

*Note: In the same column, numbers followed by the same letter are not statistically different according to Tukey's test, **: difference at the 1% significance level.*

3.2. Effect of KIN and NAA on *in vitro* shoot formation

3.2.1. Number of shoots

The results in table 2 showed that the medium supplements with various concentration of KIN and NAA had different effects on shoot formation after 30 days, with values ranging from 2.27 to 6.60 shoots/explant. Notably, the culture transplanted in a medium without the plant growth regulators (PGR) produced only 2.20 shoot. In the present study, the highest number of shoots (6.60 shoots/explant) was obtained from the medium supplemented with 2.0 mg/L KIN combined with 0.1 NAA. These results showed an improvement over the 6.11 shoots reported by Thuy *et al.* (2020) [25], who used the MS medium supplemented with 2.0 mg/L KIN alone. Moreover, the findings were also consistent with the report that the MS medium without PGR gave the lowest number of shoots (1.55 shoots), while the addition of 1.0 mg/L KIN combined with 0.05 mg/L NAA increased the number of shoots (2.55 shoots) [16]. The conclusion of Dahal and Joshi (2018) [26] indicated that supplementing KIN alone was not highly effective in the asparagus shoot kernels. However, KIN and NAA were found to be essential for shoot formation and growth in *Aspagagus officinallis* [16]. Additionally, the combined effect of KIN and NAA with high shoot multiplication efficiency has been observed in *Moringa stenopetala* [27] and *Asparagus aphyllus* [28]. The likely mechanism is that the rate of auxin and cytokinin application in the plant tissue culture can control the state of cell di-or dedifferentiation [29]. The KIN could promote cell division by strengthening the meristem, whereas the NAA aids in cell elongation and stabilizes initial formation. The combination of KIN and NAA at appropriate concentrations most likely established a balance of PGR and improved the asparagus shoot multiplication.

Table 2. Effect of KIN and NAA on shoot formation after 30 days

Plant growth regulators (mg/L)	No. of shoots/explants	Shoot height (cm)	The quality of shoots
Control	2.20^{g}	7.03^{a}	+
1 KIN + 0 NAA	3.60^{cd}	4.76b^{cd}	++
1 KIN + 0.1 NAA	3.00^{efg}	4.69^{bcd}	++

1 KIN + 0.5 NAA	2.27^{g}	1.97^{e}	++
2 KIN + 0 NAA	4.80^{bc}	6.22^{ab}	++
2 KIN + 0.1 NAA	6.60^{a}	6.24^{a}	+++
2 KIN + 0.5 NAA	5.40^{ab}	3.79^{d}	++
3 KIN + 0 NAA	4.47^{bcd}	6.20^{ab}	++
3 KIN + 0.1 NAA	4.27^{bcd}	5.52^{abc}	+++
3 KIN + 0.5 NAA	3.40^{d}	4.05^{cd}	++
4 KIN + 0 NAA	4.27b^{cd}	6.06^{ab}	++
4 KIN + 0.1 NAA	4.20^{bcd}	4.01^{cd}	++
4 KIN + 0.5 NAA	2.40^{fg}	3.51^{de}	++
P	**	**	
CV (%)	14.04	14.56	

*Note: In the same column, numbers followed by the same letter are not statistically different according to Tukey's test, **: difference at the 1% significance level. Shoot quality was assessed as described by Sallam (2019) [19] including (+++): thick, dark green explants; (++): slightly thick, green explants; (+): thin, light green explants.*

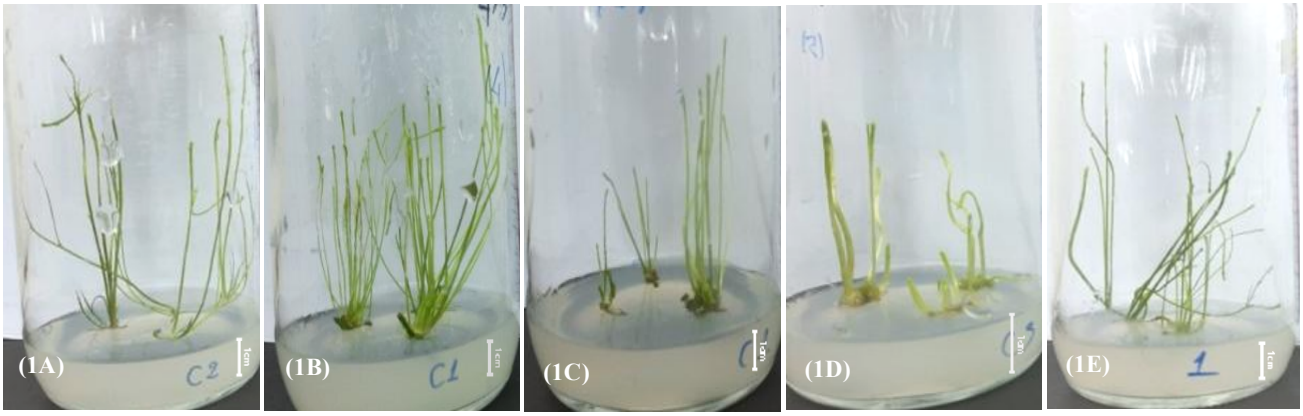

Figure 1. Shoot formation on medium supplemented with different concentrations of KIN and NAA after 30 days

Note: (1A): Control; (1B): 2 mg/L KIN + 0.1 mg/L NAA; (1C): 3 mg/L KIN + 0.1 mg/L NAA; (1D): 1 mg/L KIN + 0.5 mg/L NAA; (1E): 4 mg/L KIN.

3.2.2. Shoot height and the quality of shoot

The shoot height and quality were significantly affected by the growth regulators of KIN and NAA (Table 2). In the control treatment (without PGR), the highest shoot height was recorded at 7.03 cm, however, the shoot quality was poor with thin, light green explants and weak shoots (Figure 1A). In contrast, the treatments supplemented with KIN and NAA generally resulted in decreasing shoot height while the shoot quality was significantly improved. Plant growth regulators are known to enhance plants'

regeneration ability to form various organs and tissues by determining embryonic fate *in vivo* and boosting regeneration efficiency *in vitro* [29]. Cytokines affect the formation of lateral shoots, inhibiting the aging of plant organs and tissues [30]. According to Al Malki and Elmeer (2010) [31], the medium supplemented with cytokinin combined with auxin will inhibit the height growth of *Ficus anastasia*, while simultaneously improving overall quality. In this study, the best shoot quality with thick, dark green explant and vigorous shoots was recorded in the treatments supplemented with 2 mg/L and 3 mg/L KIN combined with 0.1 mg/L NAA, with shoot heights reaching 6.24 cm and 5.22 cm, respectively, and was not significantly different from that of the control treatment (Figures 1B and 1C). The treatment of 1 mg/L KIN + 0.5 mg/L NAA had the shoot heights ranging from 1.97 cm to 6.20 cm with slightly thick, green, and steadily growing shoots (Figure 1D). Notably, the treatment of 1 mg/L KIN + 0.5 mg/L NAA had the lowest shoot height and callus formation at the shoot base (Figure 1E). The phenomenon of callus formation happens when the accumulation of auxins at the base of the shoot and stimulation of cell division, forming callus [32]. However, the regeneration of adventitious shoots or full plantlets is a method scarcely used in the micropropagation of selected genotypes due to the possible genetic variability resulting in a high rate of progenies without the parental characteristics, which is unsuitable [33].

3.3. Effect of NAA, IBA, IAA on *in vitro* root formation

3.3.1. Roots formation rate

One of the main changes in the micropropagation of the asparagus is root formation [33]. In this study, the control treatment (without PGR) did not promote root formation of the varieties "Atlas" asparagus at 60 days after culturing (Table 3, figure 2A). Among the auxin treatments, NAA had the highest root formation rate, ranging from 20.00 to 62.67%, and the optimal result was observed at 0.7 mg/L NAA with 62.67% (Figure 3C). Comparatively, IAA exhibited a minimal root formation rate (0.00 - 0.36%), while IBA led to a moderate root formation rate (10.67 - 42.67%). However, the rooting efficiency observed in this study was lower than that in some previous publications. Specifically, Minh *et al.* (2022) [34] reported that shoots regenerated from callus cultured on medium supplemented with 0.5 mg/L NAA had a rooting efficiency of 74.59%. Similarly, Yavuz and Çömlekçioğlu (2022) [8] found that the asparagus shoots of the variety "Jersey Knight F1" achieved a rooting rate of 65% on medium supplemented with 0.5 mg/L IBA, while the "Mary Washington" variety achieved 62% under the same conditions [35]. These findings suggested that while the positive role of auxin in the direction of motility, root formation, the optimal type and concentration of auxin for rooting was plant-species-dependent and explant type [8, 32, 36].

3.3.2. Number of roots

Although the NAA had the highest root formation rate, all treatment concentrations resulted in callus formation at the root and the exact number of roots cannot be determined. Similar results on the "F1 male hybrid lines" also showed that NAA concentrations didn't record any significant values and only transparent rooted plantlets formed [19]. According to Wang *et al.* (2010) [37] highlighted that the asparagus was sensitive to NAA, so root edema often appears, affecting the growth of the plant at an acclimatized stage. In contrast, the results of this study showed that the supplementary treatments of IAA and IBA lead to a greater number of roots and root lengths at higher concentrations compared to lower concentrations. The treatment supplemented with 0.7 mg/L IBA achieved the highest number of roots, with an average of 3.73 roots, followed by 0.5 mg/L IBA with 3.00 roots. The IBA is more stable and less sensitive to auxin-degrading enzymes, which allows it to be gradually metabolized by the enzyme peroxidase. This stability may explain why it is more effective than other auxins [38]. Additionally, IBA is more biologically active than NAA and IAA in promoting root initiation because it serves as a precursor to endogenous IAA [39]. Furthermore, IBA remains significantly more stable than IAA when autoclaved [40].

Table 3. Rooting ability of asparagus in medium supplemented with NAA, IAA and IBA with different concentrations after 60 days

Auxin	Concentration (mg/L)	Root rate (%)	No. roots	Root length (cm)	The quality of roots
Control	0	0.00^{i}	0.00^{e}	0.00^{e}	-
NAA	0.1	20.00^{g}	0.00^{e}	0.45^{d}	+
	0.3	46.67^{bc}	0.00^{e}	0.49^{d}	+
	0.5	52.00^{b}	0.00^{e}	0.62^{d}	+
	0.7	62.67^{a}	0.00^{e}	0.64^{d}	+
IAA	0.1	0.00^{i}	0.00^{e}	0.00^{e}	-
	0.3	0.00^{i}	0.00^{e}	0.00^{e}	-
	0.5	24.00^{fg}	1.53^{cd}	1.69^{c}	++
	0.7	36.00^{de}	1.73^{c}	1.71^{c}	+++
IBA	0.1	10.67^{h}	1.20^{d}	1.60^{c}	+
	0.3	22.67^{g}	1.67^{cd}	1.61^{c}	++
	0.5	32.00^{ef}	3.00^{b}	3.27^{b}	+++
	0.7	42.67^{cd}	3.73^{a}	3.93^{a}	+++
P		**	**	**	
CV (%)		15.69	17.38	15.19	

*Note: In the same column, numbers followed by the same letter are not statistically different according to Tukey's test, **: Difference at the 1% significance level. (+++): Vigorous and white roots; (++): Adventitious, short and yellow-brown roots; (+): Light green callus tissue surrounding the roots and slender root tips roots; (-): No roots formed.*

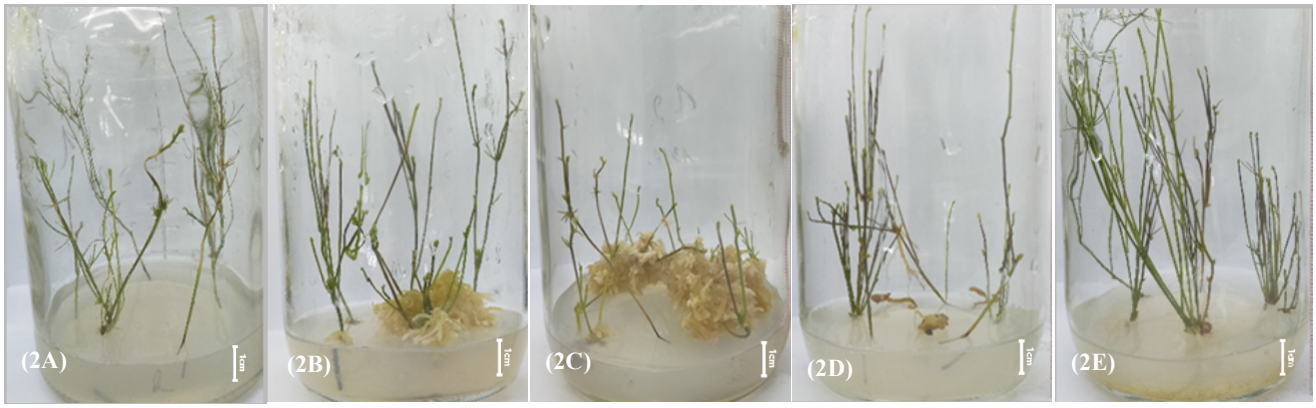

Figure 2. Roots formation in a medium supplemented with different concentrations of auxin after 60 days

Note: (2A): Control; (2B): 0.5 mg/L NAA; (2C): 0.7 mg/L NAA; (2D): 0.5 mg/L IAA; (2E): 0.7 mg/L IBA.

3.3.3. Root length and the quality of roots

Although micropropagation has been practiced for a long time in asparagus, low propagation coefficient, weak roots or lack of root formation are concerned [8]. Therefore, PGR was added into the basal culture medium to enhance root induction and promote the development of healthier asparagus roots [34]. The results presented in table 3 showed that, in contrast to the root formation rate, the treatment supplemented with NAA resulted in shorter roots lengths, ranging from 0.45 to 0.64 cm. In particular, the

treatment supplemented 0.5 mg/L of NAA resulted in poor root quality, with the formation of light green callus tissue surrounding the roots and slender root tips (Figure 2B) and the concentration of 0.7 mg/L NAA, resulted in the largest callus formation (Figure 2C). The study also revealed that a concentration of 0.5 mg/L IAA led to the formation of adventitious short, yellow-brown roots and leaf senescence (Figure 2D). This case aligned with the conclusion that IAA negatively impacted leaf development [41]. According to Sallam (2019) [19] the successful transplantation of *Asparagus officinalis in vitro* produced plantlets, it is required to improve vigorous storage roots (white root). The treatment with 0.7 mg/L IBA resulted in the longest root length, reaching 3.93 cm, with vigorous, and white root (Figure 2E). Similar findings were reported by Banharn and Kongthong (2023) [42] regarding the effectiveness of IBA in promoting asparagus root formation without abnormal root structures. Due to its stability and efficacy, IBA is frequently chosen for *in vitro* root induction in various plant species, such as *Aloe vera* and *Prunus* [5, 43].

3.4. Effect of AMF on the acclimation and growth of asparagus plantlets

3.4.1. Survival rate of plantlets

Acclimatization is the last stage of the tissue culture technique, which is crucial for the success of *in vitro* plant propagation [10]. Like other *in vitro* propagated plants, an *ex vitro* acclimatization process was required to ensure plant growth and survival of well-developed *in vitro Asparagus officinalis* plantlets when transplanted to soil or field environments [16]. The survival and performance of vegetables in the field production cycle depended on the plantlet quality and, in turn, the substrate [17]. The results presented in figure 4A showed that in the control treatment without AMF inoculation, plant death began to appear after 30 days of the acclimatization (DAA), with the percentage of surviving plants recorded at 60% and continued to decrease to 40% after 60 days. In contrast, the treatments inoculated with arbuscular mycorrhizal fungi (AMF-SA, AMF-SC and AMF-SR) maintained a survival rate of 100% at both survey stages. The results reported by Gómez-Falcón *et al.* (2023) [15] on coconut (*Cocos nucifera* L.) and Widijanto *et al.* (2024) [10] on kepok banana (*Musa paradisiaca* L.) also showed that AMF improved the survival of plantlets produced by the micropropagation. The superior survival in AMF-supplemented treatments clearly highlights the beneficial role for AMF in supporting the recovery of asparagus plantlets after *in vitro* culture.

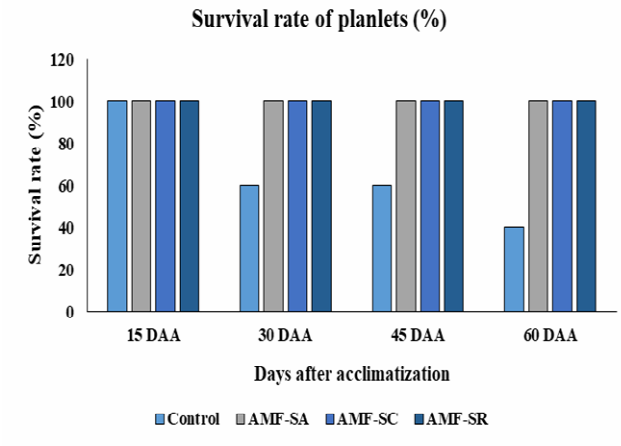

Figure 3. Plantlets survival rate at 40 and 60 days after acclimatization

3.4.2. Characteristics of arbuscular mycorrhizal fungi infection

Microscopic observations of the roots revealed the presence of all three typical infection structures e.g. hyphae (Figure 4A), arbuscules (Figure 4B) and vesicles (Figure 4C), indicating good compatibility between all three AMF preparation and asparagus roots. This result is consistent with previous descriptions by Spinoso-Castillo *et al.* (2023) [20], which showed hyphae were observed between the central cylinder and the parenchyma, along with the presence of arbuscular structures are inside the cells; forming hyphal extensions outside the cells was observed. Vesicles, on the other hand, are storage structures formed by AMF within plant cells. The vesicles contain nutrient reserves that act as a sustained supply for fungi and plants [44]. These structures are widely recognized as a key indicator of successful AMF symbiosis, which helps plants absorb water and nutrients, especially phosphorus [45].

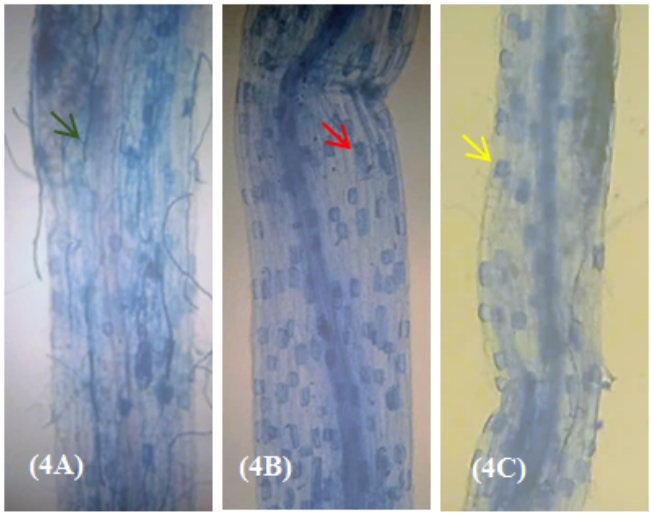

Figure 4. Root infection characteristics of asparagus plantlets by different AMF populations

Note: (4A): hyphae; (4B): arbuscules; (4C): vesicles.

3.4.3. Number of stems and plant height

The results presented in table 4 indicated that at the 15 DAA stage, there were no statistically significant differences in the number of stems or plant height among the treatments. The number of stems ranged from 2.4 to 3.2, while the plant height was between 6.72 and 8.76 cm. However, a significant difference emerged starting from the 30 DAA stage. The treatment without arbuscular mycorrhizal fungi (AMF) application significantly exhibited fewer in the number of stems (1.2 stems) and a plant height got significantly shorter with 12.66 cm than those of other treatments. In contrast, the treatments applied with AMF included AMF-SA (6.6 stems; 19.08 cm), AMF-SC (6.2 stems; 18.96 cm) and AMF-SR (5.0 stems; 17.60 cm) were shown significantly increase in both the number of stems and plant height, compared to those of the control treatment. Dewir *et al.* (2023) [11] reported that AMF improved acclimation in micro-propagated of *Philodendron bipinnatifidum* by enhancing photosynthetic activity. Similarly, Mohan and Joshi (2024) [13] indicated that AMF could improve plant tolerance to stress by improving nitrogen fixation, water uptake, soil structure, and pathogen resistance. In sugarcane plantlets, Spinoso-Castillo *et al.* (2023) [20] demonstrated that AMF enhanced water absorption and improved root systems by extending fungal hyphae to access to water and nutrient resources under artificial drought conditions. At the 45 DAA stage, the control treatment showed the slowest growth, recording 1.4 stems and a height of 16.98 cm, while the AMF-applied treatments demonstrated significant differences. Among these, AMF-SA (9.4 stems; 37.34 cm, respectively) and AMF-SC (9.2 stems; 37.04 cm) resulted in significantly higher growth compared to the AMF-SR treatment (7.6 stems; 29.32 cm). This trend continued through to the 60 DAA stage, where the best growth was observed in the AMF-SA (13.6 stems; 66.38 cm) and AMF-SC (13.2 stems; 66.26 cm) treatments, both outperforming the other treatments. Although all three treatments were treated with AMF, the marked differences in asparagus plantlets growth reflected the uneven symbiotic efficacy among the AMF preparations. AMF have a wide host range [46], however, plant species are known to respond differently to AMF [47]. This difference is reflected in the ability to colonize, transport nutrients, and trigger physiological responses in the host plant, which depends on the fungal species, the source of isolation, and the specific physiology of the plant. According to Navarro and Morte (2024) [14], careful selection of the appropriate AMF strain is an important step in the inoculation process to ensure compatibility between the fungus and the host plant. The superior performance of AMF-SA and AMF-SC can likely be attributed to their higher specificity and compatibility with *Asparagus officinalis*. These fungi were isolated from the rhizosphere of asparagus (AMF-SA) and maize (AMF-SC), both of which thrive in aerobic soil environments and share similar root characteristics. This facilitates the colonization and diversity of AMF communities within the host roots. Host plants may benefit from more diverse communities of AMF because they are more likely to match with an ideal AMF symbiont and because AMF's functional complementarity may facilitate greater resource acquisition [48]. In contrast, the AMF-SR, originating from rice soil, may be less adapted to the root physiology of asparagus. This could lead to lower colonization efficiency and a reduced

ability to promote growth. Moreover, AMF also indirectly improve soil nutrient cycling and plant health by releasing organic acids, glomalin and signaling molecules that influence the structure and function of host rhizosphere bacterial communities [49]. The effectiveness of AMF-SR may be reduced due to its limited ability to interact with the rhizosphere bacterial community of asparagus. This limitation arises because the AMF-SR community is primarily adapted to anaerobic conditions found in flooded rice soil. When these strains were exposed to aerobic conditions in the substrate, their interaction performance with the aerobic rhizosphere bacterial community became less stable. As a result, while AMF are a valuable unit for sustainable agriculture, their application requires careful adaptation to local agroecosystems in order to maximize benefits while avoiding potential drawbacks [50].

Table 4. The effect of AMF population on the number of stems and the height of plantlets

Treatment	Number of stems				Plant height (cm)			
	15 DAA	30 DAA	45 DAA	60 DAA	15 DAA	30 DAA	45 DAA	60 DAA
Control	2.4	1.2^{d}	1.4^{c}	1.8^{c}	6.72	12.66^{b}	16.98^{c}	23.56^{c}
AMF-SA	3.2	6.6^{a}	9.4^{a}	13.6^{a}	8.76	19.08^{a}	37.34^{a}	66.38^{a}
AMF-SC	3.2	6.2^{ab}	9.2^{a}	13.2^{a}	8.70	18.96^{a}	37.04^{a}	66.26^{a}
AMF-SR	3.2	5.0^{bc}	7.6^{b}	10.2^{b}	8.46	17.60^{a}	29.32^{b}	50.52^{b}
P	ns	**	**	**	ns	**	**	**
CV (%)	28.54	20.78	13.45	7.48	18.57	8.60	15.66	14.80

*Note: In the same column, numbers followed by the same letter are not statistically different according to Tukey's test, **: difference at the 1% significance level; ns: not statistically significantly different; DAA: days after acclimation.*

4. CONCLUSION

Seeds sterilized with 6% NaOCl for 10 minutes achieved the highest germination rate of 90.00% after 28 days. In the shoot formation stage, the medium supplemented 2.0 mg/L KIN + 0.1 mg/L NAA produced the highest number of shoots, reaching 6.60 shoots with an average shoot height of 6.44 cm. In the rooting stage, the highest root generation rate was from the medium supplemented with 0.7 mg/L NAA, reaching 62.67%. However, the number of roots (3.73), root length (3.93 cm) and root quality were recorded at 0.7 mg/L IBA concentration gave the best results. In the acclimatization stage, two treatments applied with either AMF-SA or AMF-SC population, resulted in a 100% plantlets survival rate, with the highest observed average values for the number of shoots (13.6 and 13.2 shoots, respectively) and plant height (66.38 and 66.26 cm, respectively).

ACKNOWLEDGMENT

The research was granted by the Department of Science and Technology of Can Tho city (Contract number: 20-HĐ-KHCN).

REFERENCES

1. Zhang, F., Chen, S., Zhang, J., Thakur, K., Battino, M., Cao, H., Farag, M. A., Xiao, J. and Wei, Z. (2024). *Asparagus saponins*: effective natural beneficial ingredient in functional foods, from preparation to applications. *Critical Reviews in Food Science and Nutrition*, 64(33), 2284 - 12302.

2. Drost, D. (2023). Asparagus breeding: Future research needs for sustainable production. *Frontiers in Plant Science*, 14, 1148312.

3. Chen, H., Guo, A., Wang, J., Gao, J., Zhang, S., Zheng, J., Huang, X., Xi, J. and Yi K. (2020). Evaluation of genetic diversity within asparagus germplasm based on morphological traits and ISSR markers. *Physiology and Molecular Biology of Plants*, 26(2), 305 - 315.

4. Pegiou, E., Mumm, R., Acharya, P., de Vos, R. C. and Hall, R. D. (2019). Green and white asparagus (*Asparagus officinalis*): A source of developmental, chemical and urinary intrigue. *Metabolites*, 10(1), 17.

5. Yasemin, S. and Beruto, M. (2024). A Review on flower bulb micropropagation: Challenges and Opportunities. *Horticulturae*, 10(3), 284.

6. Thakur, S., Hashmi, S., Mishra, S., Ekka, S. K., Kushwaha, A. and Kujur, R. (2024). A Review on plant tissue culture. *Asian Journal of Biology*, 20(2), 14 - 18.

7. Lopez-Granero, M., Arana, A., Regalado, J. J., Encina, C. L. and Ochatt, S. J. (2023). Mass micropropagation and *in vitro* flowering of *Mammillaria vetula ssp. gracilis* var. Arizonica Snowcap. *Plant Cell, Tissue and Organ Culture,* 155, 759 - 771.

8. Yavuz, H. B. and Çömlekçİoğlu, N. (2022). Effects of donor plant age and explant types on Asparagus (*Asparagus officinalis* L.) micropropagation. *International Journal of Agriculture, Forestry and Life Sciences*, 6(1), 12 - 17.

9. Radomir, A. M., Stan, R., Florea, A., Ciobotea, C. M., Bănuță, F. M., Negru, M., Neblea, M. A. and Sumedrea, D. I. (2023). Overview of the success of *in vitro* culture for ex situ conservation and sustainable utilization of endemic and subendemic native plants of Romania. *Sustainability*, 15(3), 2581.

10. Widijanto, H., Tetrani S. A. and Salsabill, S. (2024). Application of organic fertilizers and 'arbuscular mycorrhiza' dosage to increase the growth of Kepok banana seedlings ('*Musa paradisiaca* L.') derived from tissue culture. *Australian Journal of Crop Science*, 18(5), 253 - 258.

11. Dewir, Y. H., Al-Qarawi, A. A., Alshahrani, T., Bansal, Y., Mujib, A., Murthy, H. N., Alebidi, A. I., Almutairi, K. F. and Al-Saif, A. M. (2023). Influence of arbuscular mycorrhizal fungi on the growth and development of micropropagated *Rubus fruticosus* 'P45' plants during acclimatization. *HortScience*, 58(8), 871 - 876.

12. Xue, J., Guo, L., Li, L., Zhang, Z., Huang, M., Cai, J. and Zhou, Q. (2024). Effects of arbuscular mycorrhizal fungi on uptake, partitioning and use efficiency of nitrogen in wheat. *Field Crops Research*, 306, 109244.

13. Mohan, V. K. and Joshi, S. R. (2024). Mycorrhizal fungi as ecofriendly interventions for crop productivity. In *Industrial Microbiology and Biotechnology: An Insight into Current Trends,* 663 - 677. Singapore: Springer Nature Singapore.

14. Navarro, J. M. and Morte, A. (2024). Arbuscular mycorrhizal fungi as biofertilizers to increase the plant quality of Sour-Orange seedlings. *Agronomy*, 14(1), 230.

15. Gómez-Falcón, N., Sáenz-Carbonell, L. A., Andrade-Torres, A., Lara-Pérez, L. A., Narváez, M. and Oropeza, C. (2023). Arbuscular mycorrhizal fungi increase the survival and growth of micropropagated coconut (*Cocos nucifera* L.) plantlets. *In vitro Cellular & Developmental Biology-Plant*, 59(3), 401 - 412.

16. Klanrit, P., Lila, K., Netsawang, P., Siangsanor, P., Thanonkeo, P. and Thanonkeo, S. (2023). Effect of organic additives on the micropropagation of *Asparagus officinalis*. *Horticulturae*, 9(11), 1244.

17. Tavares, I. N., Alves, J. M. A., Uchôa, S. C. P., Iuit, C. E. C., Guedes, Y. A. and Silva, D. C. O. (2023). Characterization of substrates and their influence on germination and growth of asparagus seedlings. *Revista De Agricultura Neotropical*, 10(1), e7254-e7254.

18. Murashige, T. and Skoog, F. (1962). A revised medium for rapid growth and bio assays with tobacco tissue cultures. *Physiologia plantarum*, 15(3), 473.

19. Sallam, A. (2019). *In vitro* propagation of F1 male hybrid lines in *Asparagus officinalis*. *Egyptian Journal of Desert Research*, 69(1), 67 - 86.

20. Spinoso-Castillo, J. L., Moreno-Hernández, M. D. R., Mancilla-Álvarez, E., Sánchez-Segura, L.,

Sánchez-Páez, R. and Bello-Bello, J. J. (2023). Arbuscular mycorrhizal symbiosis improves ex vitro acclimatization of sugarcane plantlets (*Saccharum* spp.) under drought stress conditions. *Plants*, 12(3), 687.

21. Dalpé, Y. and Séguin, S. M. (2013). Microwave-assisted technology for the clearing and staining of arbuscular mycorrhizal fungi in roots. *Mycorrhiza*, 23, 333 - 340.

22. Hsiao, A. I. and Quick W. A. (1984). Actions of sodium hypochlorite and hydrogen peroxide on seed dormancy and germination of wild oats, *Avena fatua* L. *Weed Research*, 24, 411 - 419.

23. Yildiz, M., Fatih Ozcan, S., T Kahramanogullari, C. and Tuna, E. (2012). The effect of sodium hypochlorite solutions on the viability and *in vitro* regeneration capacity of the tissue. *The Natural Products Journal*, 2(4), 328 - 331.

24. Yildiz, M. and Celal, E. (2002). The effect of sodium hypochlorite solutions on *in vitro* seedling growth and shoot regeneration of flax (*Linum usitatissimum*). *Naturwissenschaften*, 89(6), 259 - 261.

25. Thuy, H. T., Hang, C. B., Hoa, M. T. P. and Vinh, D. T. (2020). Micropropagation of *Asparagus officinalis* L. *Journal of Science and Technology - Nguyen Tat Thanh University*, 3(1), 33 - 38.

26. Dahal, K. K. and Joshi, S. D. (2018). Comparative study of *in vitro* root and shoot proliferation from the node explants of *Asparagus racemosus* Willd. J*ournal of the Institute of Agriculture and Animal Science*, 35(1), 121 - 125.

27. Adugna, A. Y., Feyissa, T. and Tasew, F. S. (2020). Optimization of growth regulators on *in vitro* propagation of Moringa stenopetala from shoot explants. *BMC biotechnology*, 20(1), 60.

28. Salman, S. (2021). *In vitro* propagation and secondary metabolites production in the wild rare *Asparagus aphyllus* L. plant. *Egyptian Journal of Desert Research*, 71(2), 149 - 161.

29. Asghar, S., Ghori, N., Hyat, F., Li, Y. and Chen, C. (2023). Use of auxin and cytokinin for somatic embryogenesis in plant: a story from competence towards completion. *Plant Growth Regulation*, 99(3), 413 - 428.

30. Sosnowski, J., Truba, M. and Vasileva, V. (2023). The impact of auxin and cytokinin on the growth and development of selected crops. *Agriculture*, 13(3), 724.

31. Al Malki, A. A. H. and Elmeer, K. M. S. (2010). Influence of auxin and cytokinin on *in vitro* multiplication of *Ficus anastasia*. *African Journal of Biotechnology*, 9(5), 635 - 639.

32. Abdalla, N., El-Ramady, H., Seliem, M. K., El-Mahrouk, M. E., Taha, N., Bayoumi, Y., Shalaby, T. A. and Dobránszki, J. (2022). An academic and technical overview on plant micropropagation challenges. *Horticulturae*, 8(8), 677.

33. Encina, C. L. and Regalado, J. J. (2022). Aspects of *in vitro* plant tissue culture and breeding of Asparagus: a review. *Horticulturae*, 8(5), 439.

34. Minh, L. N., Nhat, T. N. T., Diem, S. L. H., Mironov, A., Vorobyev, M. and Orlova, E. (2022). Micropropagation of *Asparagus officinalis* L. through callus development. *In BIO Web of Conferences* (Vol. 47, p. 04001). EDP Sciences.

35. Sargsyan, E., Vardanyan, A., Parsaeimehr, A. and Bekyan, A. (2015). Elaboration of *Asparagus officinalis* L. by *in vitro* and hydroponic. *American Journal of Microbiology and Biotechnology*, 2(6), 82 - 86.

36. Nayak, S. S., Chakraborty, S., Roy, S., Roy, S., Ghosh, K., Ghorui, A., Sarkar, S. and Sarkar, S. G. S. (2023). The role of plant hormone on root development. *Journal of Survey in Fisheries Sciences*, 10(1S), 6401 - 6407.

37. Wang, J. Y., Zhang, X. P., Yang, R. and Li, X. F. (2010). Effects of auxins on the propagation of *Asparagus officinalis* L. *Journal of East China Normal University (Natural Science)*, (6), 101 - 108.

38. Dobránszki, J. and Silva, J. A. T. (2010). Micropropagation of apple-A review. *Biotechnology Advances*, 28(4), 462 - 488.

39. Liu, C., Zhu, J., Liu, Z., Li, L., Pan, R. and Jin, L. (2002). Exogenous auxin effects on growth and phenotype of normal and hairy roots of *Pueraria lobata* (Wild.) Ohwi. *Plant Growth Regul*, 38, 37 - 43.

40. Nissen, S. J. and Sutter, E. G. (1990). Stability of IAA and IBA in nutrient medium to several tissue culture procedures. *HortScience*, 25(7), 800 - 802.

41. Lakho, M. A., Jatoi, M. A., Solangi, N., Abul-Soad, A. A., Qazi, M. A. and Abdi, G. (2023). Optimizing *in vitro* nutrient and *ex vitro* soil mediums-driven responses for multiplication, rooting, and acclimatization of pineapple. *Scientific Reports*, 13(1), 1275.

42. Banharn, S. and Kongthong, S. (2023). *In vitro* shoot induction and shoot multiplication of Asparagus (*Asparagus officinalis*). *Burapha Science Journal*, 28(1), 422 - 438.

43. Lawson, J. D., Bridges, W. C. and Adelberg, J. W. (2023). IBA delivery technique and media salts affected *in vitro* rooting and acclimatization of eight *Prunus genotypes*. *Plants*, 12(2), 289.

44. Torres, M. J., Moreira, G., Bhadha, J. H. and McLamore, E. S. (2024). Arbuscular mycorrhizal fungi as inspiration for sustainable technology. *Encyclopedia*, 4(3), 1188 - 1200.

45. Bennett, A. E. and Groten, K. (2022). The costs and benefits of plant-arbuscular mycorrhizal fungal interactions. *Annual Review of Plant Biology*, 73, 649 - 672.

46. Dowarah, B., Gill, S. S. and Agarwala, N. (2022). Arbuscular mycorrhizal fungi in conferring tolerance to biotic stresses in plants. *Journal of Plant Growth Regulation*, 41(4), 1429 - 1444.

47. Brundrett, M. C. and Tedersoo, L. (2018). Evolutionary history of mycorrhizal symbioses and global host plant diversity. *New Phytologist*, 220(4), 1108 - 1115.

48. Weber, S. E., Bascompte, J., Kahmen, A. and Niklaus, P. A. (2025). AMF diversity promotes plant community phosphorus acquisition and reduces carbon costs per unit of phosphorus. *New Phytologist,* 248(2), 886 - 896.

49. Deveau, A., Bonito, G., Uehling, J., Paoletti, M., Becker, M., Bindschedler, S., Hacquard, S., Hervé, V., Labbé, J., Lastovetsky, O. A., Mieszkin, S., Millet, L. J., Vajna, B., Junier, P., Bonfante, P., Krom, B. P., Olsson, S., van Elsas, J. D. and Wick, L. Y. (2018). Bacterial-fungal interactions: ecology, mechanisms and challenges. *FEMS Microbiology Reviews*, 42(3), 335 - 352.

50. Igiehon, N. O. and Babalola, O. O. (2017). Biofertilizers and sustainable agriculture: exploring arbuscular mycorrhizal fungi. *Applied microbiology and biotechnology,* 101(12), 4871 - 4881.

SELECTION AND EVALUATION OF SILKWORM (*Bombyx mori* L.) BREEDS FOR HYBRIDIZATION IN SERICULTURE IMPROVEMENT

Nguyen Thi Nhai[1,*], Dinh Thi Xuan[1], Tran Thi Binh Nguyen[2], Nguyen Mai Phuong[2], Nguyen Hoang Thinh[3]

[1]*Vietnam Sericulture Research Centre*

[2]*Faculty of Biotechnology, Vietnam National University of Agriculture*

[3]*Faculty of Animal Science, Vietnam National University of Agriculture*

**Email: nguyennhaidt@gmail.com*

ABSTRACT

Considered a decisive factor in the sericulture agro-industry, the development of high-yielding, healthy silkworm hybrids, robust silkworm hybrids are essential for commercially successful and sustainable production. Therefore, screening and prioritizing and superior parental lines for breeding program must be accordingly. This study aims to systematically evaluate the performance of diverse silkworm germplasm comprising 10 bivoltine and 5 multivoltine breeds, preserved and maintained at the Vietnam Sericulture Research Centre (VIETSERI) from which promising parental breeds used for future heterosis breeding would be suitably identified. The multivoltine breeds (VBL, RVTB, HLS, etc) exhibited excellent health characteristics, presented by good hatching (up to 97.83%, much higher than usual), higher survival (up to 92.15%) and pupation rates (up to 97.85%) whereas the bivoltine ones (e.g., TQ10, HQ2, IN03, IN02) demonstrated significantly better cocoon quality, excelling in SCW, CSW and CSR (up to 21.13%). As a results, the bivoltine breed TQ10 (50.78), followed by HQ4 (50.50), VN7 (50.43), IN03 (50.43), IN02 (50.30) and TQ1 (50.18) was selected based on the Evaluation Index. The study's results showed that the bivoltine breeds coded TQ10, HQ4, VN7, IN03, and IN02 were screened as elite parental breeds for improving silk yield and quality. The multivoltine breeds were considered valuable genetic resources for enhancing hardiness and can be used for recommend specific crossing strategies to develop high-performance hybrids for Vietnam's sericulture industry.

Keywords: *Silkworm, germplasm, parental line, breeding program.*

Received: 19 August 2025; revised: 8 October 2025; accepted: 2 December 2025.

1. INTRODUCTION

The practice of rearing silkworms (*Bombyx mori* L.) to produce raw silk plays an important role in sericulture production, especially in Asian countries where sericulture has been considered not only a traditional craft but also a sophisticated agricultural and industrial sector with notable economic and social impacts. Sericulture is consistently cited as a significant tool for poverty reduction and inclusive growth in developing nations, offering substantial employment - especially for rural women and youth and helping to curb rural-to-urban migration [1, 2].

A major focus of current breeding efforts is the creation of "dual-tolerance" or "multi-tolerance" hybrids. Recent publications indicate that silkworm F1 and double hybrids, identified through properly screened evaluation, can be significantly tolerant to both high temperatures and major diseases for commercial exploitation in

subtropical and tropical regions [3, 4, 5]. In this direction, researchers continue to screen and select new parental breeds and hybrids to identify supperior combinations that consistently excel in reeling and raw silk quality characteristics under challenging farmer-level field conditions, thus ensuring both high yield and quality for the reeling sector [6, 7].

The selection of parents is regarded as a decisive factor in the breeding program in terms of genetic material supply for the pure lines to be utilized. Consequently, parental lines are accordingly evaluated using a combination of traditional quantitative and qualitative traits, often integrated into a Multi-Trait Evaluation Index (EI) to identify the most commercially viable lines [3, 5, 6, 8, 9]. As a result, the success of breeding programs is closely linked with the selection of parents to be hybridized.

This study aims to identify promising parental combinations of silkworm on the basic of a systematic evaluation of pure silkworm breeds. This evaluation covers crucial quantitative and qualitative economic traits from which the genetic diversity, inter-relationship among selected breeds and desired genetic divergence for future heterosis exploitation in breeding programs can be recommended.

2. MATERIALS AND METHODS

2.1. Materials

The experiments were conducted at Vietnam Sericulture Research Centre (VIETSERI) during spring (March - April) in 2023. Fifteen silkworm breeds including 10 bivoltine and 5 multivoltine ones were selected from germplasm bank maintained at VIETSERI.

Silkworm breed	Symbol	Origin
Bivoltine silkworm breeds		
IN01	IN01	India
IN02	IN02	India
IN03	IN03	India
B42	VN2	Vietnam
QĐ7	VN7	Vietnam
A1	TQ1	China
526	TQ9	China
75 xin	TQ10	China
Keumok	HQ2	Korea
KoC	HQ4	Korea
Multivoltine silkworm breeds		
Vang Bao Loc	VBL	Vietnam
Re vang Thai Binh	RVTB	Vietnam
Re vang Ha Tinh	RVHT	Vietnam
Hoang Lien Son	HLS	Vietnam
Do Son Khoang	DSK	Vietnam

2.2. Methods

2.2.1. Experimental design

The experiment was conducted using a completely randomized block design. Fifteen silkworm breeds reared by a standard method, served as the treatments with three replications. Each replication raised 300 larvae (after third moult).

2.2.2. Measurements

Cocoons were harvested on the fifth day of spinning. Yield and quality traits were evaluated, including fercudity, hatching rate, survival rate, pupation rate, single cocoon weight (SCW), cocoon shell weight (CSW), cocoon shell rate (CSR), cocoon yield per 300 larvae.

The relevant data and information were collected and analyzed in accordance with TCVN 13474-2:2022 Testing and appraisal procedures for animal breed - Part 2: Silkworm [10]

Evaluation index (EI) value for silkworm breed performance was calculated using the following formula [11].

$$EI = (A - B)/C \times 10 + 50$$

Where, A is mean of the particular trait; B is overall mean of particular trait; C is standard deviation; 50 is constant.

2.2.3. Data analysis

Analysis of variance (ANOVA) was performed using "Statistix 10". The significance of means values was analysed using LSD 0.05.

3. RESULTS AND DISCUSSIONS

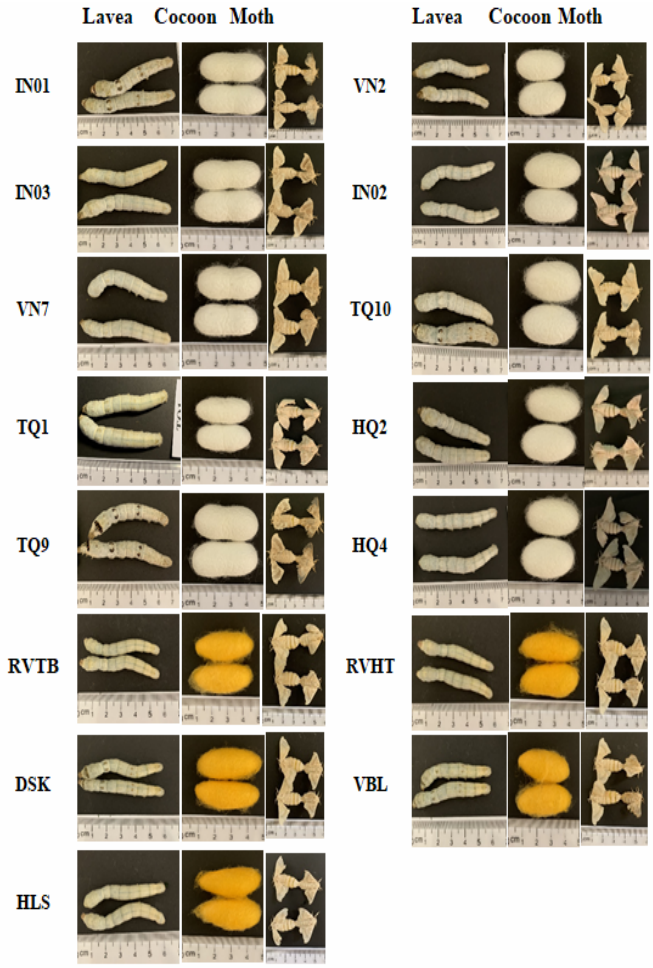

Figure 1. The pictures of larva, cocoon and adult of 15 silkworm breeds of *B. mori*

The morphological characteristics of silkworm breeds studied were presented in figure 1. Out of 15 silkworm breeds, 5 breeds had white, peanut-shaped cocoons, 5 breeds had white, oval - shaped cocoons and 5 breeds had yellow, spindle-shaped cocoons. Among 10 white cocoon breeds, 7 breeds had plain larvae, 2 breeds had marked larvae and one had sex-limited marking. In the 5 yellow cocoon breeds, 2 breeds had marked larvae and the remaining 3 were plain larvae.

Analysis of Variance (ANOVA) revealed statistically significant differences ($p < 0.05$) among the 15 breeds for all economic traits studied, as indicated by the LSD test. It is also mentioned that substantial genetic variation within the germplasm is essential for effective selection and breeding.

Results also showed that a clear difference in rearing performance between multivoltine and bivoltine groups was recognized. The multivoltine breeds (VBL, RVTB, RVHT, HLS and DSK) had significantly lower quantity of egg (268 - 344 eggs) compared to the bivoltine ones (455 - 567 eggs). The multivoltine breeds were, however, reported to be healthy. RVTB recorded the highest hatching rate (97.83%), followed by HLS (92.15%) and VBL (91.35%) which also demonstrated the highest survival rates. This proved their good adaptation to the conditions and hardiness. In contrast, the bivoltine breed IN01 had the lowest survival rate (41.71%). The pupation rate was also highest in the multivoltine group, with VBL (97.85%), HLS (97.60%), and RVTB (96.86%) performing exceptionally well (Table 1).

Table 1. Mean performance of economic traits of silkworm breeds

No.	Breeds	Fecundity (No)	Hatching rate (%)	Survival (%)	Pupation rate (%)	Cocoon yield (g)	SCW (g)	CSW (g)	CSR (%)
1	VBL	268^{c}	94.23^{abc}	91.35^{a}	97.85^{a}	266^{ef}	1.001^{f}	0.125^{e}	12.49^{d}
2	RVTB	322^{c}	97.83^{a}	90.56^{ab}	96.86^{a}	277^{ef}	1.008^{f}	0.126^{e}	12.49^{d}
3	RVHT	324^{c}	96.51^{abc}	86.11^{c}	96.22^{a}	256^{f}	0.979^{f}	0.131^{e}	13.38^{c}
4	HLS	344^{c}	95.46^{abc}	92.15^{a}	97.60^{a}	277^{ef}	0.978^{f}	0.129^{e}	13.19^{cd}
5	DSK	309^{c}	97.32^{ab}	86.44^{bc}	96.29^{a}	274^{ef}	1.105^{e}	0.141^{e}	12.76^{cd}
6	IN01	455^{b}	85.41^{ef}	41.71^{h}	78.05^{cde}	178^{g}	1.482^{b}	0.312^{c}	21.08^{a}
7	IN03	567^{a}	93.87^{abc}	76.01^{e}	83.86^{bcd}	353^{b}	1.590^{a}	0.332^{ab}	20.89^{a}
8	VN7	546^{a}	94.39^{abc}	87.07^{bc}	92.03^{ab}	340^{bc}	1.335^{c}	0.261^{d}	19.55^{b}
9	VN2	536^{a}	91.97^{bcd}	85.82^{c}	87.64^{abc}	310^{cd}	1.246^{d}	0.260^{d}	20.84^{a}
10	TQ1	519^{a}	91.21^{cd}	85.59^{c}	90.18^{abc}	325^{bc}	1.299^{cd}	0.257^{d}	19.80^{b}
11	TQ9	557^{a}	86.42^{de}	71.45^{f}	72.21^{de}	317^{cd}	1.508^{b}	0.311^{c}	20.62^{a}

12	TQ10	532 [a]	96.62 [abc]	85.65 [c]	89.07[abc]	393[a]	1.588[a]	0.329[abc]	20.73[a]
13	HQ2	540 [a]	93.17 [abc]	61.46[g]	68.51[e]	287[de]	1.612[a]	0.335[a]	20.76[a]
14	HQ4	566[a]	94.77 [abc]	80.72 [d]	87.18[abc]	348[b]	1.487[b]	0.313[bc]	21.07[a]
15	IN02	558[a]	93.84 [abc]	73.22[è]	81.48[bcd]	332[bc]	1.588[a]	0.330[abc]	21.13[a]

** The values in the same column followed by the same letter are not significantly different at the level of $_{0.05}$*

Data in table 1 showed that the bivoltine breeds were highly evaluated in all cocoon-related traits. And the multivoltine ones had significantly lower cocoon yield, SCW, CSW and CSR. The highest cocoon yield (per 300 larvae) was recorded in TQ10 (393 g) followed by IN03 (353 g) and HQ4 (348 g). Meanwhile, the heaviest single cocoon weight was reported in HQ2 (1.612 g) followed by IN03, TQ10 and IN02. Cocoon shell rates (CSR), a critical trait for raw silk recovery, varied slightly from breed to breed IN02 (21.13%) was reported as the highest, followed by IN01 (21.08%), HQ4 (21.07%), IN03 (20.89%), VN2 (20.84%), HQ2 (20.76%), and TQ10 (20.73%). The multivoltine breeds had very low CSRs, ranging from 12.49% to 13.38%.

To assess the overall commercial viability and identify the best parental lines, a Multi-Trait Evaluation Index (EI) was calculated (Table 2). This index provides a balanced score across all measured economic traits.

Table 2. Evaluation index values of selected traits

No.	Breeds	Fecundity	Hatching rate	Survival	Pupation	Cocoon yield	SCW	CSR	Average	Rank
1	VBL	48.28	50.06	50.85	51.09	49.30	48.72	48.55	49.55	15
2	RVTB	48.76	51.06	50.80	50.99	49.53	48.75	48.55	49.78	11
3	RVHT	48.78	50.70	50.47	50.92	49.00	48.63	48.78	49.61	14
4	HLS	48.95	50.40	50.91	51.07	49.53	48.63	48.73	49.75	12
5	ĐSK	48.64	50.92	50.49	50.93	49.45	49.14	48.62	49.74	13
6	IN01	49.93	47.62	47.19	48.97	47.62	50.64	50.79	48.97	10
7	IN03	50.91	49.96	49.72	49.59	50.99	51.08	50.74	50.43	4
8	VN7	50.73	50.11	50.54	50.47	50.73	50.06	50.39	50.43	3
9	VN2	50.65	49.44	50.45	50.00	50.15	49.70	50.73	50.16	7
10	TQ1	50.50	49.23	50.43	50.27	50.44	49.91	50.46	50.18	6
11	TQ9	50.83	47.90	49.39	48.34	50.28	50.75	50.67	49.74	10
12	TQ10	50.61	50.73	50.43	50.15	51.76	51.07	50.70	50.78	1
13	HQ2	50.67	49.77	48.65	47.94	49.71	51.17	50.71	49.80	8
14	HQ4	50.91	50.21	50.07	49.95	50.89	50.67	50.79	50.50	2
15	IN02	50.84	49.96	49.52	49.34	50.57	51.07	50.81	50.30	5

Generally, the bivoltine breeds could be ranked on the top in terms of all criteria. TQ10 (50.78) was evaluated as the most promising breed, which resulted in the best EI score. This reflects its outstanding performance in cocoon yield combined with excellent SCW and CSR. It was followed closely by HQ4 (50.50), VN7 (50.43), IN03(50.43), IN02 (50.30) and TQ1 (50.18).

4. CONCLUSION

Out of 15 silkworm breeds evaluated from VIETSERI germplasm bank, the bivoltine breeds (TQ10, HQ4, VN7, IN03, IN02 and TQ1) were screened as elite parental breeds, indicated by superior performance in cocoon yield, single cocoon weight and cocoon shell rate. Conversely, the multivoltine breeds (RVTB, HLS and VBL) were recorded to have lower silk yield but can be used as valuable genetic resource for breeding programs aimed at producing varieties with excellent hatching, survival, and pupation rate.

The primary recommendation for future breeding programs proposed by this study is to utilize the top-ranked EI breeds for hybridization. Specifically, crosses such as HQ4 x TQ10, HQ4 x IN02, IN03 x VN7 and IN03 x TQ1 should be use in bivoltine x bivoltine crosses to maximize silk

yield. Meanwhile TQ10 x HLS, HQ4 x RVTB, IN03 x RVTB should be used in bivoltine x multivoltine crosses for producing healthy, high-yielding hybrids adapted to changeable field condition

ACKNOWLEDGEMENTS

The authors are thankful to the Vietnam Sericulture Research Centre (VIETSERI) for providing the germplasm and facilities needed for our research. Our best regards should be also sent to technical staff of the Faculty of Biotechnology and Faculty of Animal Science, Vietnam National University of Agriculture, for their useful support.

REFERENCES

1. Madiga Parasuramudu *et al.* (2025). A Sustainable approach to sericulture enterprise and rural youth empowerment. *International Journal of Enviroment and Agriculture Research,* 11(7): 136 - 1463. (Source 3.5)

2. Mavilashaw VP, Aruna N and Menaka D (2025). Sericulture by-products and their economic importance: A review. *International Journal of Agriculture Extension and Social Development*, 8(8): 30 - 36 (Source 3.3)

3. Attri, M., Gupta, R. K., & Bali, K. (2025). Evaluation of Bivoltine Silkworm (*Bombyx mori* L.) Hybrids for Disease Resistance and Suitability in Subtropical Conditions. *Journal of Advances in Microbiology*, 25(1), 57 - 61. (Source 1.1)

4. Kankanawadi, N. *et al.* (2025). Reeling and raw silk assessment of new bivoltine silkworm double hybrids tolerant to high temperature and muscardine disease. *Journal of Advances in Biology & Biotechnology*, 28(8), 114 - 122. (Source 1.3).

5. Ghulam Ali Bajwa *et al.* (2023). Identifying hybrid genotypes of mulberry silkworm (*Bombyx mori*) using heterosis for biological and silk yielding traits. *Pakistan J.Zool,* 55(1): 85 - 91. (Source 2.3)

6. Singh, B. D. & Mishra, A. K. (2020). Heterosis Evaluation of Some Local and Imported Hybrids of Silkworm, *Bombyx mori* L. *Egyptian Academic Journal of Biological Sciences A Entomology*, 13(2), 77 - 95. (Source 2.5).

7. Pankaj Lushan Dutta *et al.* (2025). Global perspective on silk: An economic analysis of international sericulture trade. *Agriculture Association of Textile Chemical and Critical Reviews Journal,* 33(2): 231 - 238. (Source 3.2)

8. Prashanth Javanegowda *et al.* (2024) Seasonal performance of new bivoltine lines of Bombyx mori evolved from heat shock technology and identification of potent breed for tropical conditions. *Journal of Insect Biotechnology and Sericology*, 92, 17 - 27.

9. Raviraj VS, Md. Akib Hussain, Anu Sonowal and Y. Surjalata Devi (2024). Identification of bivoltine breeds tolerant to high temperature and humidity using marker assisted selection in silkworm bombyx mori. *International Journal of Zoology and Applied Biosciences*, 9(5): 8 - 14.

10. TCVN 13474-2:2022: Testing and appraisal procedures for animal breed - Part 2: Silkworm (in Vietnamese).

11. Mano, Y., Nirmal Kumar, S., Basavaraja, H. K., Mal Reddy N. and Datta, R. K. (1993). A new method to select promising silkworm breeds/combinations. *Indian Silk*, 31(10): 53.

ENZYME SCREENING FROM *Pleurotus* spp. STRAINS UNDER SUBMERGED CONDITIONS AS A BASIS FOR FUTURE AGRO-WASTE BIOCONVERSION STUDIES

Doan Chi Cuong[1,*], Munehiro Tanaka[2], Vo Chau Tuan[1], Bui Duc Thang[1], Nguyen Thi Bich Hang[1]

[1] *Faculty of Biology, Agriculture and Environmental Science, University of Science and Education, The University of Danang*

[2] *Faculty of Agriculture, Saga University, Japan*

[*] *Email: dccuong@ued.udn.vn*

ABSTRACT

Bioconversion efficiency of agricultural waste into value-added products relies on robust microbial strains capable of producing a broad of extracellular enzymes. Among edible mushrooms, *Pleurotus* species are recognized for their enzymatic diversity and potential in solid-state fermentation processes. This study aimed to evaluate and compare the extracellular enzymatic profiles of four *Pleurotus* species, including *P. ostreatus*, *P. pulmonarius*, *P. djamor*, and *P. citrinopileatus* to identify the most suitable strain for agro-waste bioconversion. Each species was cultivated under identical conditions and the activities of four key enzymes (laccase, cellulase, protease, and chitinase) were quantified using standardized colorimetric assays. Statistical analysis was performed using one-way ANOVA followed by Tukey's HSD test ($p<0.05$). The results showed that *P. pulmonarius* exhibited the most balanced enzymatic profile, with high laccase (59.9 ± 5.5 U/mL) and cellulase (5.39 ± 0.38 U/mL) activities, moderate protease activity (14.4 ± 3.4 U/mL) and strong chitinase activity (7.59 ± 0.85 U/mL). Unlike other species that showed specialization in one or two enzymes, *P. pulmonarius* performed consistently across all categories, enabling it to degrade lignin, cellulose, proteins and chitin. Hence, *P. pulmonarius* is identified as the optimal candidate for integrated agro-waste valorization via SSF, offering significant potential for applications in circular bioeconomy frameworks and sustainable bioprocess development.

Keywords: *Agro-waste, bioconversion, enzyme activity, enzyme screening, Pleurotus* spp.

Received: 10 September 2025; revised: 6 November 2025; accepted: 2 December 2025.

1. INTRODUCTION

The increasing global demand for sustainable agricultural practices has encouraged a transition toward circular bioeconomy models that emphasize waste minimization and biomass valorization. Agricultural residues, which are generated in vast quantities worldwide, represent an abundant resource of carbon-based polymers such as lignocellulose and chitin. Mismanagement of these residues contributes significantly to environmental degradation through greenhouse gas emissions, soil nutrient imbalances and water pollution. Therefore, developing eco-friendly and cost-effective bioconversion strategies to transform agro-waste into high-value products are important [1].

Solid-state fermentation (SSF) has been recognized as a viable biotechnological platform for the transformation of agricultural byproducts into valuable compounds due to its low moisture requirements, high productivity, and compatibility with filamentous fungi [2]. Among these fungi,

members of the *Pleurotus* genus (oyster mushrooms) are of interest due to their fast growth, adaptability to diverse lignocellulosic substrates, and high yield of extracellular enzymes [3]. These mushrooms produce an extensive range of hydrolytic and oxidative enzymes, including laccase, cellulase, protease and chitinase, which decompose the complex organic matter such as straw, husks, bran and seafood waste [4, 5].

Laccases are multi-copper oxidase that catalyzes the oxidation of phenolic and non-phenolic substrates, playing a central role in lignin depolymerization. Due to broad substrate specificity, laccases have applications in paper pulping, dye decolorization, wastewater treatment and biosensor development [6]. Cellulases are a group of synergistic enzymes that hydrolyze cellulose into glucose, making them essential for biomass saccharification, bioethanol production and animal feed processing [7]. Proteases break down proteinaceous materials into peptides and amino acids and have important roles in organic waste valorization, feed enhancement, and pharmaceuticals [8]. Chitinases degrade chitin, a major component of crustacean shells and fungal cell walls, contributing to waste management, antifungal biocontrol and biomedical applications [9].

While the enzyme-producing potential of *Pleurotus* spp. is well documented with numerous advantages regarding enzyme production levels, substrate preferences and environmental tolerance. Recent studies have screened wild and commercial *Pleurotus* strains to identify those with superior enzyme productivity. For example, Mikiashvili *et al.* (2006) demonstrated strain-dependent variability in cellulase and laccase production when *P. ostreatus* grew on different lignocellulosic substrates [10]. Kachlishvili *et al.* (2006) observed that *P. eryngii* and *P. pulmonarius* exhibited distinct enzymatic profiles under SSF, underscoring the need for targeted screening and selection [11]. However, studies on investigating multi-enzyme production, particularly for combinations of laccase, protease, cellulase and chitinase, which together enable the comprehensive degradation of mixed agro-waste streams are still limited. Moreover, the majority of enzyme-related studies focus on enzyme extraction for industrial use rather than in situ application of enzyme-producing fungi in SSF systems. Utilizing native *Pleurotus* strains that exhibit high enzymatic activity in SSF could enhance the efficiency of agro-waste bioconversion while reducing processing costs. Such approaches not only yield nutrient-enriched fermented products but also align with sustainability goals through circular material flows [12, 13].

Herein, the present study aims to isolate and characterize native *Pleurotus* strains capable of producing high levels of laccase, protease, cellulase and chitinase. The selected strains were also evaluated for their suitability in SSF of agricultural residues, which are rich in lignocellulose and protein/chitin components but remain largely underutilized in many developing countries. This research supports the principles of circular agriculture, which promotes the reuse and recycling of organic matter within agricultural systems. Incorporating enzyme-rich fungi into SSF offers a practical, low-cost and decentralized strategy for managing waste, improving soil health and producing feed additives or biofertilizers. It also contributes to local bioeconomy development, particularly in regions where agricultural residues and seafood byproducts are plentiful but poorly exploited [14].

2. MATERIALS AND METHODS

2.1. Materials

The strains *P. ostreatus*, *P. pulmonarius*, *P. djamor* and *P. citrinopileatus* were purchased from the Lam Dong Center for Science and Technology Application (Hamlet 5, Cam Ly Ward, Da Lat city, Lam Dong province). After acquisition, the strains were reactivated, cultivated to produce fruiting bodies and subsequently re-isolated to ensure purity. Strain identities were confirmed through ITS region sequencing using primers ITS1/ITS4. BLASTn comparison against GenBank revealed > 99% sequence similarity to the corresponding *Pleurotus* species, which was further supported by morphological observations.

Then *P. pulmonarius*, *P. citrinopileatus*, *P. ostreatus* and *P. djamor* were cultured and preserved at the Mushroom Technology Laboratory, Faculty of Biology. Agriculture and Environment Science, University of Science and Education, The University of Danang.

2.2. Propagation on agar and liquid media

After pouring the prepared agar medium into test tubes in appropriate volumes, sterilization is carried out at 121°C for 20 minutes. The tubes are then allowed to cool before inoculation. The fungal cultures are subsequently incubated at 25 - 28°C for 5 to 7 days. Primary spawn of *Pleurotus* was propagated in glass test tubes (F1, Ø8 cm, 180 mm) containing a medium composed of potato extract (200 g/L), glucose (20 g/L) and agar (15 g/L) and incubated at 27°C for 10 days. Subsequently, mycelial cultivation experiments were conducted by transferring 150 mL of PDB^{+} medium (composed of potato extract: 200 g; glucose: 20 g; yeast extract: 2 g; peptone: 2 g; distilled water: 1 L) into 250 mL Erlenmeyer flasks. The media were sterilized using autoclaving at 121°C for 30 minutes. After cooling, equal amounts of mycelial inoculum from the primary spawn tubes were transferred into each flask. The cultures were incubated on a rotary shaker at 150 rpm, at a temperature ranging from 25 - 27°C.

2.3. Determination of laccase activity

Laccase activity was determined spectrophotometrically by measuring the rate of oxidation of 2,2'-azino-bis(3-ethylbenzothiazoline-6-sulphonic acid) (ABTS), a commonly used chromogenic substrate. The assay was conducted according to the method described by Niku-Paavola *et al.* (1990) with slight modifications. The standard reaction mixture (total volume: 3.0 mL) consisted of: 2.7 mL of 100 mM sodium acetate buffer (pH 4.5), 0.2 mL of 1.0 mM ABTS solution, and 0.1 mL of appropriately diluted enzyme sample [15]. The reaction was initiated by the addition of the enzyme extract and monitored by the increase in absorbance at 420 nm using Shimadzu UV-1800UV-Vis spectrophotometer. The oxidation of ABTS by laccase results in the formation of a green-colored cation radical (ABTS•$^{+}$), which exhibits strong absorbance at 420 nm (ε = 36,000 $M^{-1}cm^{-1}$). The assay was performed at 27°C and the change in absorbance was recorded for 3 minutes. One unit (U) of laccase activity was defined as the amount of enzyme required to oxidize 1 µmol of ABTS per minute under the assay conditions. Laccase activity (U/mL) was calculated using the equation (1):

$$\text{LacA}\left(\frac{\text{U}}{\text{mL}}\right) = \frac{\Delta A_{420} \times V_{total}}{\varepsilon \times d \times V_{enzyme} \times T} \quad (1)$$

Where: ΔA_{420}: change in absorbance per minute at 420 nm; V_{total}: total reaction volume (mL); ε: molar extinction coefficient of ABTS at 420 nm (36,000 $M^{-1}cm^{-1}$); d: path length of the cuvette (1 cm); V_{enzyme}: volume of enzyme extract used (mL); T: incubation time (minutes).

2.4. Determination of protease activity

Protease activity was determined based on the method recommended by Sigma-Aldrich, which measures the hydrolysis of casein as a substrate under alkaline conditions. The assay quantifies the release of soluble peptides and amino acids, particularly tyrosine, which remain in solution after precipitation of undigested proteins with trichloroacetic acid (TCA). This method is widely used for estimating general proteolytic activity in crude enzyme extracts. The standard reaction mixture contained: 2.5 mL of 0.65% (w/v) casein solution prepared in 50 mM glycine-NaOH buffer (pH 9.0); 0.5 mL of appropriately diluted enzyme extract [16]. The reaction was initiated by adding the enzyme solution to the prewarmed substrate mixture and incubated at 37°C for 10 minutes. The enzymatic reaction was terminated by the addition of 2.5 mL of 110 mM trichloroacetic acid (TCA) to precipitate the undigested casein. The mixture was then allowed to stand for 30 minutes at room temperature to ensure complete precipitation, followed by centrifugation at 10,000 g for 10 minutes. The absorbance of the supernatant was measured at 280 nm against a reagent blank using Shimadzu UV-1800UV-Vis spectrophotometer. One unit (U) of protease activity was defined as the amount of enzyme that liberates 1 µmol of

tyrosine equivalent per minute under the assay conditions. Protease activity (U/mL) was calculated using the equation (2):

$$\text{ProA}\left(\frac{\text{U}}{\text{mL}}\right) = \frac{\Delta A_{280} \times V_{\text{total}}}{\varepsilon \times d \times V_{\text{enzyme}} \times T} \quad (2)$$

Where: ΔA_{280}: change in absorbance per minute at 280 nm; V_{total}: total reaction volume (mL); ε: extinction coefficient for tyrosine at 280 nm (~1.1 mLU'µmol^{-1}U'cm^{-1}); d: path length of the cuvette (1 cm); V_{enzyme}: volume of enzyme extract added (mL); T: incubation time (minutes).

2.5. Determination of cellulase activity

Cellulase activity was determined using the filter paper assay described by Ghose (1987), which is the internationally recognized standard protocol for measuring total cellulase activity. This method estimates the amount of reducing sugars released from a standardized strip of filter paper by the action of cellulase enzymes under defined conditions [17]. The assay mixture contained: 1.0 mL of appropriately diluted enzyme solution; 1.0 mL of 0.05 M citrate buffer (pH 4.8); 1 pre-weighed strip of Whatman No. 1 filter paper (50 mg). The reaction was initiated by immersing the filter paper into the reaction tube and incubating at 50°C for 60 minutes in a water bath. After incubation, the reaction was terminated by adding 3.0 mL of DNS reagent to the tube and placing it in a boiling water bath for 5 minutes to develop color. After cooling to room temperature, the absorbance of the reaction mixture was measured at 540 nm using Shimadzu UV-1800UV-Vis spectrophotometer. The amount of reducing sugar released was determined by comparing to a glucose standard curve. One unit (U) of cellulase activity is defined as the amount of enzyme required to release 2.0 mg of glucose equivalents from filter paper in 60 minutes under the specified assay conditions. If the released glucose is less than 2.0 mg, the enzyme is diluted further and the cellulase activity is calculated using the equation (3):

$$\text{CellA}\left(\frac{\text{U}}{\text{mL}}\right) = 0.37 \times \frac{\textit{reducing sugar (mg)}}{\text{volume of enzyme used (mL)}} \quad (3)$$

Where: The factor (0.37) is a constant derived from the IUPAC standard that normalizes the unit to the amount of enzyme that releases exactly 2.0 mg of glucose in 60 minutes under assay conditions. The reducing sugar released (in mg) is calculated using a glucose standard curve, typically via DNS assay (absorbance at 540 nm). The volume of enzyme used is usually 0.5 or 1.0 mL.

2.6. Determination of chitinase activity

Chitinase activity was assayed by quantifying the amount of N-acetyl-β-D-glucosamine (GlcNAc) released from colloidal chitin as substrate during enzymatic hydrolysis. The method is based on colorimetric detection of reducing sugars using the 3,5-dinitrosalicylic acid (DNS) reagent and is adapted from established protocols with modifications to increase specificity for chitinolytic activity [18]. Colloidal chitin was prepared by slowly adding 10 g of purified chitin powder to 100 mL of cold concentrated HCl (12 N) under constant stirring at 4°C. After overnight incubation, the mixture was filtered and washed repeatedly with distilled water until the filtrate reached neutral pH. The final colloidal chitin suspension was stored at 4°C and adjusted to 1% (w/v) concentration before use. The standard reaction mixture (final volume: 1.0 mL) contained: 0.5 mL of 1% (w/v) colloidal chitin in 50 mM sodium acetate buffer (pH 5.0); 0.4 mL of 50 mM sodium acetate buffer (pH 5.0); and 0.1 mL of enzyme extract.

The reaction mixture was incubated at 37°C for 60 minutes. The enzymatic reaction was terminated by adding 1.0 mL of DNS reagent, followed by boiling the tubes in a water bath for 5 minutes to color development. After cooling to room temperature, the absorbance was measured at 540 nm using Shimadzu UV-1800UV-VIS spectrophotometer. The amount of reducing sugar released was determined using a GlcNAc standard curve (ranging from 0 to 500 µM). The GlcNAc standard curve regression equation: y = 0.0003x - 0.0317, with R^2 = 0.99. One unit (U) of chitinase activity is defined as the amount of enzyme required to release 1 µmol of GlcNAc per minute

under the assay conditions, the chitinase activity is calculated using the equation (4):

$$ChiA\left(\frac{U}{mL}\right) = \frac{C \times K \times V_{total}}{t \times V_{enzyme} \times 10^3} \quad (4)$$

Where: C: Concentration of GlcNAc released (μM), determined from the GlcNAc standard curve using the absorbance at 540 nm; K: dilution factor; 10^3: conversion factor from L to mL; V_{total}: total reaction volume (mL), typically 1.0 mL; t: incubation time (min), typically 60 min; V_{enzyme}: volume of enzyme extract used (mL), typically 0.1 mL.

2.7. Data analysis

All enzyme activity assays (laccase, protease, cellulase and chitinase) were conducted in triplicate and results are expressed as mean ± standard deviation. Enzyme activities were calculated using appropriate equations based on the amount of product formed, as determined from standard curves prepared for each assay. Statistical analyses were performed using IBM SPSS v20. Differences in enzyme activities among fungal isolates or treatment conditions were assessed using one-way ANOVA, followed by Tukey's HSD post hoc tests to identify statistically significant differences at $p < 0.05$. Graphs and data visualizations were generated using MS Excel 365, with error bars representing standard deviations.

3. RESULTS AND DISCUSSION

3.1. Laccase activity

Laccase activity among the *Pleurotus* species showed substantial interspecies variation (Figure 1). The highest activity was recorded in *P. ostreatus* and *P. pulmonarius*, both about 60 U/mL. One-way ANOVA revealed a statistically significant difference in laccase activity among the species ($F = 1146.38$, $p < 0.001$). Post hoc analysis using Tukey's HSD indicated that *P. ostreatus* and *P. pulmonarius* belonged to the same group "a", significantly different from *P. djamor* (group "b") and *P. citrinopileatus* (group "c"). This finding aligns with trends observed by Couto and Herrera, where basidiomycetes like *Pleurotus* typically exhibit robust laccase production [6]. *P. ostreatus* and *P. pulmonarius*'s high laccase level suggests strong ligninolytic potential, positioning it aptly for pretreatment of lignin-rich substrates such as straw, husks, or wood chips, consistent with the oxidative polymer breakdown reported by Baldrian [19].

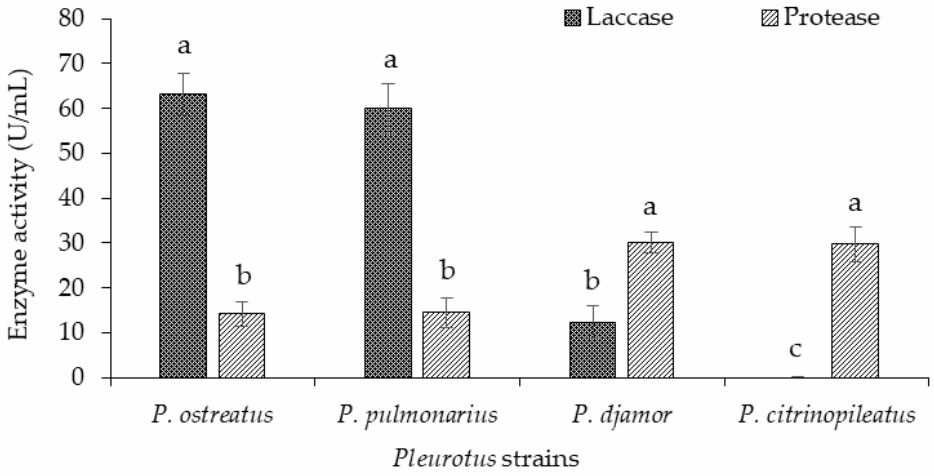

Figure 1. Comparative enzyme activities of laccase and protease among different *Pleurotus* strains (Different letters (a, b, c, d) in the same pattern chart indicate statistically significant differences at $p < 0.05$ by Tukey's HSD)

High laccase activity in *P. ostreatus* and *P. pulmonarius* holds significant promise for biomass pretreatment applications. Laccases are known to oxidize phenolic lignin substructures, reducing structural recalcitrance and enhancing enzymatic hydrolysis efficiency in downstream processes [20]. Crude laccases from both *P. ostreatus* and *P. pulmonarius* have been successfully applied to

degrade bisphenol A, demonstrating their robust oxidative capacity and potential for lignin modification [21]. Moreover, *P. ostreatus* exhibits superior laccase production on lignocellulosic substrates under solid-state fermentation, underlining its suitability for low-cost enzyme sourcing [22]. While direct comparisons of *P. pulmonarius* are limited, both species clearly function as efficient ligninolytic enzyme sources, with *P. pulmonarius* likely matching *P. ostreatus* in laccase-driven biomass deconstruction, particularly when considering its broader enzymatic capacities observed in preliminary studies [23].

3.2. Protease activity

The protease activity assay (Figure 1) demonstrated significant variation ($F = 42.62$, $p < 0.001$). *P. djamor* and *P. citrinopileatus* exhibited the highest protease activities (~30 U/mL), forming group "a" in the Tukey post hoc test. *P. pulmonarius* and *P. ostreatus* showed moderate protease activity (~14 U/mL), categorized as group "b".

In this study, general protease activities reached approximately 14 U/mL for *P. ostreatus* and *P. pulmonarius*, and around 30 U/mL for *P. djamor* and *P. citrinopileatus*. This is broadly consistent with previously reported values of Ravikumar *et al.* documented about 28 U/mL protease activity from *P. sajor-caju* fermentation on finger millet, whereas corn flour substrate produced about 45 U/mL [24]. By contrast, a study by Santana *et al.* (2024) measured a much higher fibrinolytic protease activity of 71.5 U/mL for *P. ostreatus*, though differences in assay specificity and enzyme type likely account for this discrepancy [25]. Meanwhile, an engineered *P. sajor-caju* strain (CTM10057) demonstrated an extraordinarily high output of 10,500 U/mL under optimized conditions, highlighting how strain selection and process optimization can drastically amplify enzyme yield [26]. Overall, our findings support moderate-level protease production in *Pleurotus* species under typical liquid fermentation, while also indicating the potential for markedly higher yields with targeted strain and condition enhancements.

Despite not being the highest protease producer, *P. pulmonarius* displayed consistent protease activity sufficient to hydrolyze proteinaceous biomass in mixed-substrate fermentation systems. The presence of protease within high ligninolytic and cellulolytic enzymes is beneficial for degrading composite agro-residues, where lignin and proteins often occur. This enables more holistic substrate valorization and protein enrichment of fermented materials. In addition, *P. pulmonarius* did not lead in protease production, its moderate activity is comparable to commercial strains used in fungal protein enrichment [24]. Furthermore, the presence of ligninolytic and cellulolytic enhances substrate breakdown efficiency in composite feedstock, pathogenically beneficial in strain selection for mixed agro-residue fermentation [27].

3.3. Chitinase activity

The chitinase activity of all four fungal species is presented in Figure 2. In contrast to the pronounced variability observed for the other enzymes, the chitinase activity among the strains remained relatively uniform, ranging from 7.0 to 8.0 U/mL. One-way ANOVA revealed no statistically significant differences among species ($F = 1.29$, $p > 0.05$), indicating that chitin hydrolysis capacity is a common and stable characteristic within the surveyed *Pleurotus* genus.

This quantitative assessment provides an important reference dataset and represents the first report of specific chitinase activity for *P. ostreatus*, *P. pulmonarius*, *P. djamor*, and *P. citrinopileatus* under liquid fermentation conditions. Previous literature on *Pleurotus* chitinase has been largely qualitative or focused on gene identification, with very few studies offering quantitative enzyme activity measurements. Compared with the limited earlier study on *P. eryngii* (approximately 3.57 U/mL), the values obtained here are more than twice as high, reinforcing the notion that Pleurotus species possess an inherent chitinase system with moderate basal activity. In another study involving a different fungal group, under optimized

environmental conditions, *Aspergillus sydowii* exhibited the highest reported chitinase activity, reaching 1,667 U/mL.

The consistent production of chitinase across all strains carries important practical implications. This trait enhances their potential applications, particularly for *P. pulmonarius*, the strain exhibiting a well-balanced overall enzymatic profile in the bioconversion of chitin-rich waste from the aquaculture industry (e.g., crustacean shells) or insect biomass. Ecologically, this capability enables *Pleurotus* species to participate actively in nutrient cycling and to compete effectively within natural ecological niches.

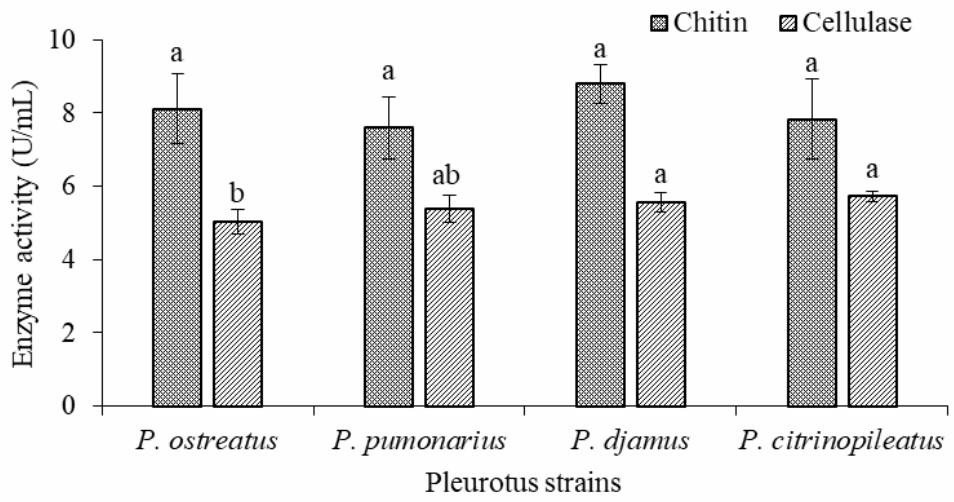

Figure 2. Comparative enzyme activities of chitinase and cellulase among different *Pleurotus* strains (Different letters (a, b, c, d) in the same pattern chart indicate statistically significant differences at $p < 0.05$ by Tukey's HSD)

3.4. Cellulase activity

The data presenting in figure 2 showed that, *P. djamor* and *P. citrinopileatus* exhibited the highest cellulase activity (about 5.03 - 5.73 U/mL), followed by *P. pulmonarius* (about 5.39 U/mL), and *P. ostreatus* (~5.03 U/mL). One-way ANOVA confirmed significant differences ($F = 7.022$, $p < 0.001$), with Tukey's HSD grouping *P. djamor*, *P. citrinopileatus* and *P. pulmonarius* together as group "a" and *P. ostreatus* as group "b". The cellulase performance of *P. pulmonarius* is notably within 3% of the highest producers, affirming its efficacy in saccharifying cellulosic feedstocks. Ghose's standardized method supports this quantitative analysis, ensuring reproducibility [17]. While not the top cellulase producer, *P. pulmonarius* exhibits high enough activity to be grouped statistically with the leading strains. This, in combination with its laccase output, enables efficient decomposition of both lignin and cellulose, a critical requirement for full exploitation of lignocellulosic residues.

Comparative enzymatic assessments consistently identify *P. pulmonarius* as the optimal strain for valorizing agro-industrial waste. Its balanced yet potent ligninolytic, chitinolytic, cellulolytic and proteolytic activities collectively establish its suitability for integration into circular agriculture and biorefinery systems.

3.5. Selection strain for agro-waste bioconversion

Degradation of complex agro-waste relies on enzyme synergy: Laccase initiates lignin removal; cellulase hydrolyzes cellulose; protease processes proteins; chitinase attacks chitinous content. *P. pulmonarius* presents a balanced multi-enzyme profile: top-tier laccase, robust cellulase, and sufficient protease and chitinase. This contrasts with the other species: *P. ostreatus*, which shows exceptionally high laccase but subpar protease and cellulase; *P. djamor*/ *P. citrinopileatus*, which excel in protease and cellulase but have deficient ligninolytic ability. The integrated profile endorses *P. pulmonarius* for solid-state fermentation setups

aimed at valorizing heterogeneous biomasses. Previous studies underscore the importance of such balanced enzymatic systems in improving bioconversion yields in SSF [28, 29].

The comprehensive performance of *P. pulmonarius* across all four enzymatic activities distinguishes it from the other strains. *P. ostreatus*, despite high laccase activity, had the lowest cellulase output. *P. djamor* and *P. citrinopileatus*, while excelling in protease and cellulase, had significantly lower laccase activity, limiting their efficiency in delignification. In contrast, *P. pulmonarius* maintains high laccase and chitinase levels, along with moderately high cellulase and protease activities. Its enzyme profile is therefore balanced, ensuring synergistic degradation of structurally diverse agro-residues, including those rich in lignin, cellulose, proteins, and chitin. The enzyme synergy is critical in solid-state fermentation, where moisture content is low and nutrient availability is restricted. Under SSF conditions, strains with balanced extracellular enzyme systems are more likely to adapt and maintain high bioconversion efficiency. The multifunctionality of *P. pulmonarius* also reduces the need for strain consortia, simplifying process control and reducing production costs.

From a bioeconomic perspective, the adoption of *P. pulmonarius*-based bioprocesses aligns with circular bioeconomy principles by converting diverse agro-residues into valuable bioproducts such as biofertilizers, enzyme-rich feed and compost [30]. FAO emphasizes transforming conventional waste streams through local biotechnology to enhance rural livelihoods and promote environmental sustainability [14]. The multifunctional enzymatic capability may also generate value-added compounds like antioxidants or polysaccharides, boosting economic outcomes. Moreover, its generally recognized as safe status, rapid mycelial growth and adaptability to a variety of lignocellulosic substrates make it scalable and industrially viable [31]. Its ability to produce bioactive compounds during fermentation further enhances the functional value of the bioproducts.

Integrating comparative enzyme activity profiles with the corresponding statistical evaluations indicates that *P. pulmonarius* represents the most promising strain for broad-spectrum bioconversion of agro-industrial residues. Its diverse enzymatic repertoire that is characterized by robust ligninolytic and chitinolytic capacities alongside consistently high cellulase and protease activities confers a distinct functional advantage, underscoring its potential as a key biological agent in circular agricultural systems and biorefinery platforms.

4. CONCLUSION

This study evaluated four *Pleurotus* species for their extracellular enzyme activities to identify a suitable strain for agro-waste biodegradation. Among them, *P. pulmonarius* exhibited a well-balanced enzymatic profile, with high laccase and cellulase activities, moderate protease production, and strong chitinase activity. These findings indicate its superior capacity for degrading lignin, cellulose, proteins and chitin - major components of agro-industrial residues. Statistical analyses confirmed that *P. pulmonarius* performed comparably or significantly better than the other species in most enzyme categories. Unlike strains that excelled in only one or two enzyme types, *P. pulmonarius* demonstrated consistent activity across all four, highlighting its potential for integrated biomass conversion. Given its enzymatic versatility and known adaptability in cultivation, *P. pulmonarius* is a strong candidate for use in solid-state fermentation systems aimed at converting agricultural by-products into value-added materials. Its application supports circular bioeconomy goals by facilitating waste valorization and sustainable bioprocess development. Future research should focus on scaling up fermentation, optimizing process parameters and exploring downstream applications of the resulting products.

ACKNOWLEDGEMENT

This study was conducted with financial support from the Vietnam Ministry of Education and Training. Grant code: B2024.DNA.11.

REFERENCES

1. Liu, R., Yu, Z., Chen, C. (2021). Circular bioeconomy: Current status and future direction. *J Clean Prod*, 280, 124278. doi: 10.1016/j.jclepro.2020.124278.

2. Pandey, A., Soccol, C. R., Mitchell, D. (2000). New developments in solid state fermentation: I - bioprocesses and products. *Process Biochemistry*, 35, 1153 - 1169. doi: 10.1016/S0032-9592(00)00152-7.

3. Zervakis, G. I., Koutrotsios, G., Katsaris, P. (2017): Mushroom breeding and cultivation. In: Petre, M. (ed.) Advances in mushroom biotechnology, 1 - 20. IntechOpen.

4. Adebayo, E. A., Oloke, J. K., Ayandele, A. A. (2021). Screening of *Pleurotus* species for extracellular enzyme production. *J Environ Biol.* 42, 563 - 571. doi: 10.22438/jeb/42/3/MRN-1596.

5. Isikhuemhen, O. S., Mikiashvili, N. A. (2009). Lignocellulolytic enzymes activity during vegetative growth of *Pleurotus ostreatus* on different lignocellulosic materials. Mycoscience. 50, 439 - 445. doi: 10.1007/s10267-009-0015-5.

6. Couto, S. R., Herrera, J. L. T. (2006). Industrial and biotechnological applications of laccases: A review. Biotechnol Adv, 24, 500 - 513. doi: 10.1016/j.biotechadv.2006.04.002.

7. Singhania, R. R., Sukumaran, R. K., Patel, A. K., Larroche, C., Pandey, A. (2010): Advancement and comparative profiles in the production technologies using solid-state and submerged fermentation for microbial cellulases. Enzyme Microb Technol, 46, 541 - 549. doi: 10.1016/j.enzmictec.2010.02.002.

8. Rao, M. B., Tanksale, A. M., Ghatge, M. S., Deshpande, V. V. (1998). Molecular and biotechnological aspects of microbial proteases. Microbiology and Molecular Biology Reviews, 62, 597 - 635. doi: 10.1128/MMBR.62.3.597-635.1998.

9. Patil, R.S., Ghormade, V., Deshpande, M. V (2000). Chitinolytic enzymes: An exploration. Enzyme Microb Technol, 26, 473 - 483. doi: 10.1016/S0141-0229(00)00134-4.

10. Mikiashvili, N., Elisashvili, V., Wasser, S. P., Nevo, E. (2006). *Lentinus edodes* and *Pleurotus* species lignocellulolytic enzyme activity. Bioresour Technol. 97, 775 - 781. doi: 10.1016/j.biortech.2005.04.013.

11. Kachlishvili, E., Penninckx, M.J., Tsiklauri, N., Elisashvili, V. (2006). Effect of nitrogen source on enzyme production by white-rot fungi. *World J Microbiol Biotechnol*, 22, 391 - 397. Doi: 10.1007/s11274-005-9054-7.

12. Mata, G., Savoie, J. M., Royse, D. J. (2017). Recycling of spent mushroom substrate. In: Zied, D. C. and Pardo-Gim'enez, A. (eds.) Mushroom biotechnology: developments and applications, 313 - 332. John Wiley& Sons.

13. Shankar, T., Gopinath, R.M., Sridevi, M. (2021). Solid-state fermentation of agro-wastes by white-rot fungi: Enzyme production and biotransformation potential. *Bioresour Bioprocess*, 8, 27. doi: 10.1186/s40643-021-00367-3.

14. FAO (2021). The state of the world's land and water resources for food and agriculture - Systems at breaking point.

15. Niku-Paavola, M. L., Karhunen, E., Salola, P., Raunio, V. (1988). Ligninolytic enzymes of the white-rot fungus Phlebia radiata. *Biochem J*, 254, 877 - 883. doi: 10.1042/bj2540877.

16. Sigma-Aldrich (1999). Protease from *Aspergillus oryzae* - Product Information and Assay Procedure. Technical Bulletin.

17. Ghose, T. K. (1987). Measurement of cellulase activities. Pure & Appl. Chem, 59, 257 - 268. doi: 10.1351/pac198759020257.

18. Monreal, J., Reese, E. T. (1969). The chitinase of *Serratia marcescens*. *Can J Microbiol*, 15, 689 - 696. doi: 10.1139/m69-122.

19. Baldrian, P. (2006): Fungal laccases - occurrence and properties. FEMS Microbiol Rev. 30, 215 - 242. doi: 10.1111/j.1574-4976.2005.00010.x

20. Haq, I. ul, Saleem, A., Chaudhary, R., Alessa, A.H., Nawaz, A., Du, C. (2024). Role of

microbial laccases in valorization of lignocellulosic biomass to bioethanol. Front Bioeng Biotechnol. 12. doi: 10.3389/fbioe.2024.1441075.

21. De Freitas, E. N., Bubna, G. A., Brugnari, T., Kato, C. G., Nolli, M., Rauen, T. G., Peralta Muniz Moreira, R. de F., Peralta, R.A., Bracht, A., de Souza, C. G. M., Peralta, R. M. (2017): Removal of bisphenol A by laccases from *Pleurotus ostreatus* and *P. pulmonarius* and evaluation of ecotoxicity of degradation products. *Chemical Engineering Journal*. 330, 1361-1369. doi: 10.1016/ j.cej.2017.08.051.

22. An, Q., Liu, Z. -Y., Wang, C. -R., Yang, J., Chen, S. -Y., Chen, X., Zhang, Y. -J., Bian, L. -S., Han, M. -L. (2021) : Laccase activity from *P. ostreatus* and *Flammulina velutipes* strains grown on agro - and forestry residues by solid-state fermentation. Bioresources, 16, 7337 - 7354. doi: 10.15376/ biores.16.4.7337-7354.

23. Stajić, M., Persky, L., Friesem, D., Hadar, Y., Wasser, S. P., Nevo, E., Vukojević, J. (2006): Effect of different carbon and nitrogen sources on laccase and peroxidases production by selected *Pleurotus* species. Enzyme Microb Technol, 38, 65 - 73. doi: 10.1016/j.enzmictec.2005.03.026.

24. Ravikumar, G., Gomathi, D., Kalaiselvi, M., Uma, C. (2012). A protease from the medicinal mushroom *P. sajor-caju*, production, purification and partial characterization. *Asian Pac J Trop Biomed*, 2, S411 - S417. doi: 10.1016/S2221-1691(12) 60198-1.

25. Santana, R. da S., Mendes, F. de S., Paula da Silva, B. J., Lima, E. S., Nascimento, T. P., Carneiro da Cunha, M. N., Porto, A. L. F., Teixeira, M. F. S., Carvalho, R. P., Gomes, W. R. (2024). Recovery and partial purification of fibrinolytic protease from *P. ostreatus* and *P. eryngii* and cytotoxic and antioxidant activity of their extracts. Prep Biochem Biotechnol. 54, 545 - 552. doi: 10.1080/10826068.2023.2253466.

26. Omrane Benmrad, M., Mechri, S., Zaraî Jaouadi, N., Ben Elhoul, M., Rekik, H., Sayadi, S., Bejar, S., Kechaou, N., Jaouadi, B. (2019). Purification and biochemical characterization of a novel thermostable protease from the oyster mushroom *P. sajor-caju* strain CTM10057 with industrial interest. BMC Biotechnol, 19, 43. doi: 10.1186/s12896-019-0536-4.

27. Pandey, A. (2003). Solid-state fermentation. Biochem Eng J. 13, 81 - 84. doi: 10.1016/S1369-703X(02)00121-3.

28. Dao T. M. L., Nguyen, T. Q. M., Bui, T. K. T., Nguyen, D. T. V., Nguyen, D. K., Son, T. N., Kieu, Y. V., Tran, Q. H. (2019). Selecting and investigating the effects of environment on characteristics of chitinase from soil fungi. *Journal of Science, Technology and Food*, 19, 38 - 49.

29. Zhou, S., Raouche, S., Grisel, S., Navarro, D., Sigoillot, J. -C., Herpoël-Gimbert, I. (2015). Solid-state fermentation in multi-well plates to assess pretreatment efficiency of rot fungi on lignocellulose biomass. Microb Biotechnol. 8, 940 - 949. Doi: 10.1111/1751-7915.12307.

30. Gkountani, V. A., Tsoulfas, G. T. (2023): Circular Bioeconomy: A Review on the Current State and Future Opportunities BT - Digital Economy and the Green Revolution. Presented at the.

31. Wu, N., Tian, F., Moodley, O., Song, B., Jia, C., Ye, J., Lv, R., Qin, Z., Li, C. (2019). Optimization of agro-residues as substrates for *P. pulmonarius* production. AMB Express. 9, 184. doi: 10.1186/s13568-019-0907-1.

MORPHOLOGICAL CHARACTERIZATION OF MEDICINAL *Coleus amboinicus* L. IN VIETNAM

Tran Thi Trang[1], To Minh Tu[1] , Tran Thi Kim Dung[1], Dao Xuan Quang[1], Dang Minh Tu[1], Dao Viet Quoc[1], Lo Duc Viet[1], Nguyen Thi Mai Phuong[1,*]

[1] *National Institute of Medicinal Materials*

**Email: phuong.nguyen.crs@gmail.com*

ABSTRACT

This study evaluated the morphological diversity, fresh biomass, and essential oil content of 15 *Coleus amboinicus* L. accessions collected in various regions in Vietnam. Based on standardized UPOV descriptors on key vegetative and reproductive traits, including plant height, petiole coloration, flower characteristics, the accessions were classified into three distinct morphological groups. Individual fresh biomass ranged from 1,974.0 to 2,804.3 g/plant while the essential oil content, determined using the Vietnamese Pharmacopoeia V protocol, ranged from 0.30% to 0.48%, with HC5 exhibiting the highest content. These findings highlight the potential of selecting promising accessions, particularly in Group II and III for breeding programs at enhancing biomass productivity and essential oil yield of *C. amboinicus*.

Keywords: *Coleus amboinicus Lour., morphological characteristics, yield, oil yield, UPOV.*

Received: 24 September 2025; revised: 10 November 2025; accepted: 4 December 2025.

1. INTRODUCTION

Coleus amboinicus (Lour.*)*, also known by its synonyms *Plectranthus amboinicus* L.*, Coleus aromaticus* B.*,* is a versatile aromatic herb, belonging to the family Lamiaceae. This species is native to the tropics and warm regions in Africa, Asia and Australia, but has been introduced and domesticated in many parts of the world, including the Americas and the Caribbean [1 - 3]. In Vietnam, commonly the species is known as "Hung chanh" or "Tan day la" and by various names worldwide including Indian borage, Cuban oregano or Mexican mint [4 - 6]. *C. amboinicus* L. is characterized by its thick, fleshy and highly aromatic leaves, which are traditionally valued in traditional and folk medicine remedies to treat respiratory, digestive and skin ailments, as well as for their antimicrobial, anti-inflammatory and antioxidant properties [7 - 13].

Historically, *C. amboinicus* L. cultivation in Vietnam has been limited to small household gardens, with minimal expansion into large-scale production. However, in recent years, its health-promoting properties have drawn increasing attention from the pharmaceutical and functional food industries, particularly highlighted during the Covid-19 pandemic. This growing demand has underlined the need for expansion of cultivation areas and to ensure a stable supply of raw materials for medicinal production. Despite the extensive research on the chemical constituents and pharmacological effects of *C. amboinicus* L., there remains a significant gap in the development of high-yielding and high-quality varieties, especially in Vietnam, where propagation is achieved primarily through stem cuttings due to the rare seed set of the plant. Therefore, this study aims to conduct a systematic evaluation based on morphological characterization of *C. amboinicus* L. and to preliminarily evaluate agronomic potentials of these accessions collected across Vietnam. Such efforts would contribute to the expansion of cultivation areas to meet market demand and facilitate the production of *C. amboinicus* L. according to the GACP-WHO standards.

2. MATERIALS AND METHODS

2.1. Materials

Fifteen accessions of *C. amboinicus* L. were collected from various agro-ecological locations in

Vietnam for evaluation. The collection site for each accession was described in table 1. Fresh stem cuttings or whole plants were collected from each collection site.

Table 1. List of *C. amboinicus* L. accessions collected in various regions in Vietnam

No.	Name	Collection sites	The common name in Vietnam	Collected time
1	HC1	My Ha commune, Lang Giang district, Bac Giang province	"Hung chanh"	20/11/2022
2	HC2	Thang Loi commune, Van Giang district, Hung Yen province	"Hung chanh"	10/3/2023
3	HC3	Ngu Hiep commune, Thanh Tri district, Hanoi city	"Hung chanh"	14/02/2023
4	HC4	Dien Hung commune, Dien Chau district, Nghe An province	"Hung chanh"	11/02/2023
5	HC5	Hoa An commune, Phung Hiep district, Hau Giang province	"Tan day la"	24/02/2023
6	HC6	An Tien commune, My Duc district, Ha Noi city	"Hung chanh"	11/02/2023
7	HC7	Tan Chau town, An Giang province	"Tan day la"	11/02/2023
8	HC8	Tan Lam Huong commune, Thach Ha district, Ha Tinh province	"Hung chanh"	13/02/2023
9	HC9	Dong Hoa town, Phu Yen province	"Tan day la"	13/02/2023
10	HC10	Tam Phuong commune, Bien Hoa district, Dong Nai province	"Tần dày lá"	24/02/2023
11	HC11	Phuoc Long, Thu Duc, Ho Chi Minh city	"Tan day la"	24/02/2023
12	HC12	Truc Chinh commune, Truc Ninh district, Nam Dinh province	"Hung chanh"	13/02/2023
13	HC13	Nhon Ai commune, Phong Dien district, Can Tho city	"Tan day la"	13/02/2023
14	HC14	Thach Ban ward, Long Bien district, Ha Noi city	"Hung chanh"	12/02/2023
15	HC15	Dak To town, Dak To district, Kon Tum province	"Hung chanh"	12/02/2023

The common names were provided by the providers and the location of the collected genotypes was presented in table 1.

2.2. Methods

2.2.1. Cultivation method

All fifteen accessions were cultivated under uniform field conditions; each was planted in a 20 m^2 plot. The plots were arranged in a randomized design without replications.

The experiment was conducted in Field experimental site - National research Center for Medicinal plant Germplasm and Breeding in Thanh Tri district, Ha Noi city in 2023.

2.2.2. Morphological characterization

The morphological characterization was evaluated according to the International Union for The Protection of New Varieties of Plant - UPOV guideline TG/315/1 for the botanical name *Coleus* Lour. or *Plectranthus* L'Hér. A list of 36

descriptors is presented in table 2 including 3 descriptors in the plant, 17 in the leaf, 16 in the flower. In addition, other distinctive traits of each accession were evaluated based on field phenotypic characterizations. Each trait was evaluated based on observations from at least five plants per accession.

2.2.3. Yield and Essential oil evaluation

Individual fresh biomass, essential oil yield was recorded at harvest, 180 days after transplanting as recommended by Sabra *et al.*, (2018) [14].

2.2.4. Essential oil analysis

100 g-sample of each accession was harvested simultaneously and quantified using the hydro distillation method in 4 hours following the protocols outlined in Vietnam Pharmacopoeia V - Supplementary Edition, 2023 [15]. Essential oil yield was calculated as the percentage of oil weight relative to the dry leaves weight.

2.2.5. Data analysis

Data were processed using Microsoft Excel software for descriptive statistics.

3. RESULTS AND DISCUSSION

3.1. Morphological characterization using UPOV descriptors

The summarized morphological characterization of fifteen *C. amboinicus* L. accessions is shown in table 2. Based on the growth habit, plant height and plant width, leaf blade characteristics and floral traits, there were 3 tentative plant types among the accessions (Figure 1).

The group I consisted of seven accessions characterized by a semi-upright growth habit, short to medium plant height (less than 80 cm) and medium canopy width, namely HC1, HC4, HC6, HC8, HC9, HC10, HC15. The group's leaf blades were consistently thick, with biserrate margins and shallow incisions. The base and apex were predominantly truncate and obtuse, respectively, and pubescence was sparse. The upper leaf surface exhibited light green coloration, with no anthocyanin pigmentation. Floral traits included purple corolla coloration with medium purple markings, long corolla length, high corolla height, and short corolla tube dimensions. These accessions exhibited a late onset of flowering (Figure 1A; figure 2).

The second group (group II) possessed a spreading growth habit type (including HC2, HC3, HC7, HC11, HC12, HC13, HC14) with tall plant height ranging from 82.4 cm to 88.2 cm and broadly spreading canopy. Leaf blades were thick, with crenate margins and medium incision depth. The leaf base was truncate and the apex was rounded, with medium pubescence and moderate blistering. The upper leaf surface was medium green in color, and anthocyanin pigmentation was absent. Flowers were pale purple with weak markings. Some flower traits such as corolla length, height, and tube dimensions were similar to Group I. These accessions flowered earlier than group I, with a medium onset of flowering (Figure 1B; figure 2).

Group III consisted solely of accession HC5, which displayed a semi-upright growth habit, the tallest recorded plant height (98.3 cm), and a broad canopy. Leaf blades were long and thick, with dentate margins and medium incision depth. The base was truncate and the apex rounded, with dense pubescence and moderate blistering. The leaf surface was light green, and anthocyanin pigmentation was absent. Floral data were not available for this accession under the duration of experiment. A transition from vegetative to reproductive development was observed. However, the floral initiation did not progress into a visible inflorescence (Figure 1C; figure 2).

Beside UPOV morphological descriptors, other characteristics relating to stem traits were observed. Group I presented green-light purple stem with a quadrangular cross-sectional shape, in low density of trichomes. Group II's stem exhibited a color range from light to deep reddish purple, with a circular transverse section with dense pubescence. The last group III of HC5 was categorized with lighter green stem, quadrangular transverse shape, high density of trichomes along stem surface (Figure 2).

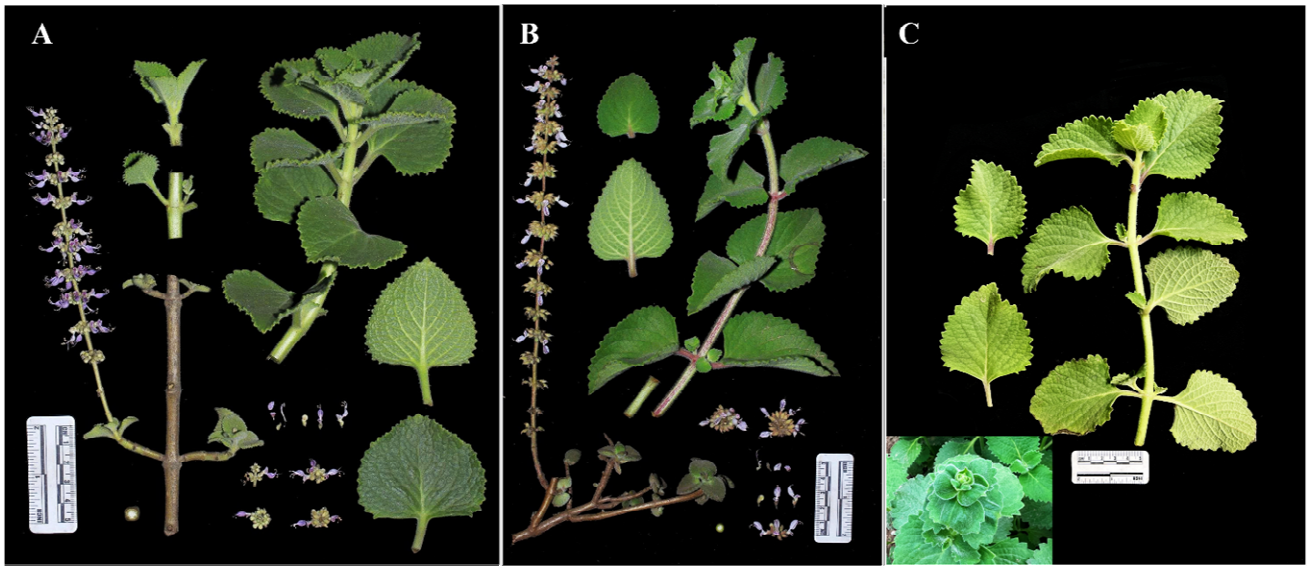

Figure 1. Representative morphological traits of collected *C. amboinicus* L. accessions. A: Group I includes HC1, HC4, HC6, HC8, HC9, HC10 and HC15 accessions; B: Group II includes HC2, HC3, HC7, HC11, HC12, HC13 and HC14 accessions; C: Group III comprises HC5 only, the inset image in group III highlights the floral primordium observed during the early stage of reproductive initiation

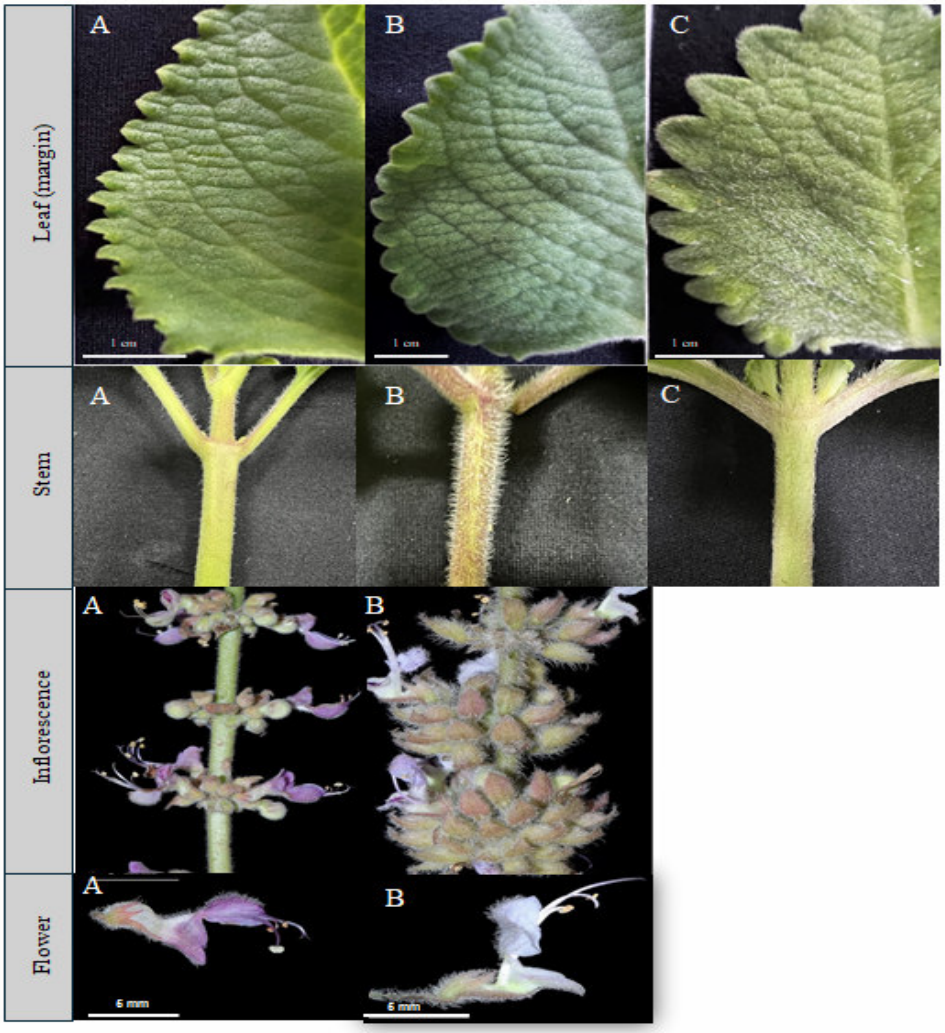

Figure 1. Morphological traits of *C. amboinicus* L. of A: Group I; B: Group II; C: Group III

Table 2. Morphological descriptors for *C. amboinicus* L. accessions (Group I) according to UPOV [16]

Descriptor No.	Character group	Descriptors	Group I						
			HC1	HC4	HC6	HC8	HC9	HC10	HC15
1	Growth habit	Growth habit	Semi-upright	Semi-upright	Semi-upright	Semi-upright	Semi-upright	Semi-upright	Semi-upright
2*	Plant height	Height	78.8	67.8	66.6	66.9	69.3	68.2	68.5
3	Plant width	Width	Medium	Medium	Medium	Medium	Medium	Medium	Medium
4	Petiole length	Petiole length	Medium	Medium	Medium	Medium	Medium	Medium	Medium
5	Leaf blade	Length	Medium	Medium	Medium	Medium	Medium	Medium	Medium
6		Width	Medium	Medium	Medium	Medium	Medium	Medium	Medium
7		Length/width ratio	Low	Low	Low	Low	Low	Low	Low
8		Thickness	Thick	Thick	Thick	Thick	Thick	Thick	Thick
9		Base shape	Truncate	Truncate	Truncate	Truncate	Truncate	Truncate	Truncate
10		Apex shape	Obtuse	Obtuse	Obtuse	Obtuse	Obtuse	Obtuse	Obtuse
11		Broadest part position	At middle	At middle	At middle	At middle	At middle	At middle	At middle
12		Variegation	Absent	Absent	Absent	Absent	Absent	Absent	Absent
13		Green color intensity (upper side)	Light	Light	Light	Light	Light	Light	Light
14		Anthocyanin (Upper side)	Absent	Absent	Absent	Absent	Absent	Absent	Absent
15		Anthocyanin (Lower side)	Absent	Absent	Absent	Absent	Absent	Absent	Absent
16		Anthocyanin distribution (Lower side)	Absent	Absent	Absent	Absent	Absent	Absent	Absent
17		Margin incision type	Biserrate	Biserrate	Biserrate	Biserrate	Biserrate	Biserrate	Biserrate
18		Margin incision depth	Shallow	Shallow	Shallow	Shallow	Shallow	Shallow	Shallow
19		Blistering	Weak	Weak	Weak	Weak	Weak	Weak	Weak
20		Pubescence	Sparse	Sparse	Sparse	Sparse	Sparse	Sparse	Sparse
21	Flower branch	Flower density	Medium	Medium	Medium	Medium	Medium	Medium	Medium
22		Pubescence	Dense	Dense	Dense	Dense	Dense	Dense	Dense
23		Anthocyanin coloration	Absent	Absent	Absent	Absent	Absent	Absent	Absent
24	Flower	Main color	Purple	Purple	Purple	Purple	Purple	Purple	Purple

Descriptor No.	Character group	Descriptors	Group I						
			HC1	HC4	HC6	HC8	HC9	HC10	HC15
25		Corolla length	Long	Long	Long	Long	Long	Long	Long
26		Corolla height	High	High	High	High	High	High	High
27		Corolla tube length	Short	Short	Short	Short	Short	Short	Short
28		Corolla tube height	Short	Short	Short	Short	Short	Short	Short
29		Corolla tube: ratio of length/height	Low	Low	Low	Low	Low	Low	Low
30		Corolla tube: longitudinal curving	Weak	Weak	Weak	Weak	Weak	Weak	Weak
31		Corolla tube: main color of outer side	Purple	Purple	Purple	Purple	Purple	Purple	Purple
32		Upper corolla lobe: main color of outer side	Purple	Purple	Purple	Purple	Purple	Purple	Purple
33		Upper corolla lobe: main color of inner side	Purple	Purple	Purple	Purple	Purple	Purple	Purple
34		Upper corolla lobe: prominence of purple spots or markings	Medium	Medium	Medium	Medium	Medium	Medium	Weak
35		Lower corolla lobe: main color of outer side	Purple	Purple	Purple	Purple	Purple	Purple	Purple
36		Flowering time (beginning)	Late	Late	Late	Late	Late	Late	Late

** In centimeters*

Table 3. Morphological descriptors for *C. amboinicus* L. accessions (Group II and Group III) according to UPOV [16]

No.	Character group	Descriptors	Group II							Group III
			HC2	HC3	HC7	HC11	HC12	HC13	HC14	HC5
1	Growth habit	Growth habit	Spreading	Spreading	Spreading	Spreading	Spreading	Spreading	Spreading	Semi-upright
2*	Plant height	Height	88.2	87.4	86.0	82.8	82.4	84.9	87.5	98.3

No.	Character group	Descriptors	Group II							Group III
			HC2	HC3	HC7	HC11	HC12	HC13	HC14	HC5
3	Plant width	Width	Broad	Broad	Broad	Broad	Broad	Broad	Broad	Broad
4	Petiole length	Petiole length	Short	Short	Short	Short	Short	Short	Short	Short
5	Leaf blade	Length	Medium	Medium	Medium	Medium	Medium	Medium	Medium	Long
6		Width	Medium	Medium	Medium	Medium	Medium	Medium	Medium	Long
7		Length/ width ratio	Low	Low	Low	Low	Low	Low	Low	Low
8		Thickness	Thick	Thick	Thick	Thick	Thick	Thick	Thick	Thick
9		Base shape	Truncate	Truncate	Truncate	Truncate	Truncate	Truncate	Truncate	Obtuse
10		Apex shape	Rounded	Rounded	Rounded	Rounded	Rounded	Rounded	Rounded	Obtuse
11		Broadest part position	At middle	At middle	At middle	At middle	At middle	At middle	At middle	At middle
12		Variegation	Absent	Absent	Absent	Absent	Absent	Absent	Absent	Absent
13		Green color intensity (upper side)	Medium	Medium	Medium	Medium	Medium	Medium	Medium	Light
14		Anthocyanin (Upper side)	Absent	Absent	Absent	Absent	Absent	Absent	Absent	Absent
15		Anthocyanin (Lower side)	Absent	Absent	Absent	Absent	Absent	Absent	Absent	Absent
16		Anthocyanin distribution (Lower side)	Absent	Absent	Absent	Absent	Absent	Absent	Absent	Absent
17		Margin incision type	Crenate	Crenate	Crenate	Crenate	Crenate	Crenate	Crenate	Dentate
18		Margin incision depth	Medium	Medium	Medium	Medium	Medium	Medium	Medium	Mediu m
19		Blistering	Medium	Medium	Medium	Medium	Medium	Medium	Medium	Mediu m
20		Pubescence	Medium	Medium	Medium	Medium	Medium	Medium	Medium	Dense
21	Flower branch	Flower density	Medium	Medium	Medium	Medium	Medium	Medium	Medium	N/A
22		Pubescence	Dense	Dense	Dense	Dense	Dense	Dense	Dense	N/A
23		Anthocyanin coloration	Absent	Absent	Absent	Absent	Absent	Absent	Absent	N/A
24	Flower	Main color	Pale purple	Pale purple	Pale purple	Pale purple	Pale purple	Pale purple	Pale purple	N/A

No.	Character group	Descriptors	Group II							Group III
			HC2	HC3	HC7	HC11	HC12	HC13	HC14	HC5
25		Corolla length	Long	Long	Long	Long	Long	Long	Long	N/A
26		Corolla height	High	High	High	High	High	High	High	N/A
27		Corolla tube length	Short	Short	Short	Short	Short	Short	Short	N/A
28		Corolla tube height	Short	Short	Short	Short	Short	Short	Short	N/A
29		Corolla tube: ratio of length/ height	Low	Low	Low	Low	Low	Low	Low	N/A
30		Corolla tube: longitudinal curving	Weak	Weak	Weak	Weak	Weak	Weak	Weak	N/A
31		Corolla tube: main color of outer side	Pale purple	Pale purple	Pale purple	Pale purple	Pale purple	Pale purple	Pale purple	N/A
32		Upper corolla lobe: main color of outer side	Pale purple	Pale purple	Pale purple	Pale purple	Pale purple	Pale purple	Pale purple	N/A
33		Upper corolla lobe: main color of inner side	White - pale purple	White - pale purple	White - pale purple	White - pale purple	White - pale purple	White - pale purple	White - pale purple	N/A
34		Upper corolla lobe: prominence of purple spots or markings	Weak	Weak	Weak	Weak	Weak	Weak	Weak	N/A
35		Lower corolla lobe: main color of outer side	Pale purple	Pale purple	Pale purple	Pale purple	Pale purple	Pale purple	Pale purple	N/A
36		Flowering time (beginning)	Medium	Medium	Medium	Medium	Medium	Medium	Medium	N/A

** In centimeters. N/A: not available at the time of observation.*

3.2. Yield and essential oil yield of collected *C. amboinicus* L.

All accessions were harvested simultaneously 180 days after planting. The average fresh biomass per individual ranged from 1,974.0 (HC10) to 2,804.3 g/plant (HC2) (Table 4). Considering the distinctive morphological traits of each group, distinct pattern in yield and essential oil were observed. Group I exhibited the lowest fresh biomass range, with yield from 1,974.0 to 2,244.0 g/plant with the corresponding essential oil ranged from 0.3% to 0.41%. Group II showed a broader and higher yield variation from 2,089.6 to 2,804.3 g/plant. The essential oil of this group varied between 0.3% and 0.45%. Group III, consisting of only HC5 was the second highest in yield of 2,796.6 g/plant with highest essential oil content of 0.48%. The results indicate that group II and group III are the most promising for attaining high fresh biomass and essential oil yield. They would be the ideal candidates for selection and breeding programs.

With an average of essential oil content of 0.4% on dry weight basis across all accessions, the results are significantly higher than those reported in previous studies. Dung *et al.* (1990) reported a range of 0.002% and 0.003% [17] while Lu (2016) documented a broader value and in range from 0.03% and 0.12% [18].

Table 4. Individual fresh biomass and total essential oil content of collected *C. amboinicus* L.

Accession	Individual fresh biomass (g/plant)	Total essential oil content (%)
HC1	1.982.2 ± 75.3	0.30 ± 0.01
HC2	2.804.3 ± 137.4	0.43 ± 0.01
HC3	2.372.9 ± 122.9	0.42 ± 0.02
HC4	2.244 ± 97.3	0.32 ± 0.01
HC5	2.796.6 ± 113.6	0.48 ± 0.01
HC6	2.020.9 ± 89.2	0.38 ± 0.01
HC7	2.606.5 ± 123.8	0.45 ± 0.02
HC8	2.060.1 ± 99.9	0.34 ± 0.01
HC9	2.019.1 ± 96.4	0.41 ± 0.01
HC10	1.974 ± 86	0.37 ± 0.01
HC11	2.465.6 ± 114.6	0.32 ± 0.01
HC12	2.089.6 ± 90.1	0.44 ± 0.02
HC13	2.412.7 ± 117.5	0.30 ± 0.02
HC14	2.442.9 ± 117.2	0.42 ± 0.01
HC15	1.978.8 ± 101.3	0.38 ± 0.01
Average	2.284.7	0.40

4. CONCLUSION

4.1. Conclusion

UPOV descriptors have been successfully applied for classifying collected accessions in the previous studies [19 - 21]. As in this study, the application of international standard UPOV guidelines is particularly appropriate for characterization of *C. amboinicus* L. accessions. The integration of UPOV guidelines and some visual observations has successfully classified 15

collected accessions into 3 tentative morphological groups (Group I, II and group III). Group differentiation was primarily based on plant growth habit, plant height, petiole coloration, stem shape, stem color, stem trichomes and flower color and structures. Significant variation in fresh biomass and essential oil yield also demonstrated potential of each group for cultivation and breeding, particularly accessions in group II and III. These finding contribute valuable insights for the selection and development of high yielding varieties of *C. amboinicus* L., supporting its broader applications in medicinal industry.

On the dry weight basis, the essential oil content of all accession ranged from 0.3% to 0.48%. When the observed fresh: Dry ratio of approximately 15: 1 is applied, the essential oil content correspond to a range of 0.02 - 0.032% on a fresh-weight basis. This converted range aligns with the previous studies and prove the differences with the previous studies with significant higher essential oil content.

4.2. Recommendation

Further evaluation of yield and quality should be conducted in subsequent growing seasons of the potential accessions in group II and group III. In addition to agronomic assessment, conducting chemical profiling of essential oil components across accessions is recommended to support the selection of superior genotypes for cultivation and medicinal use.

REFERENCES

1. Arumugam, G., Swamy, M. K. & Sinniah, U. R. (2016). *Plectranthus amboinicus* (Lour.) Spreng: Botanical, Phytochemical, Pharmacological and Nutritional Significance. *Molecules*, 21(4), 369. https://doi.org/10.3390/molecules21040369.

2. Morton, J. F. (1992). Country borage (*coleus amboinicus lour.*): A potent flavoring and medicinal plant. *Journal of Herbs, Spices and Medicinal Plants*, 1(1 - 2), 77 - 90. https://doi.org/10.1300/J044v01n01_09.

3. Paul, K., Gowda, B. H. J., Hani, U., Chandan, R. S., Mohanto, S., Ahmed, M. G., Ashique, S. & Kesharwani, P. (2024). Traditional Uses, Phytochemistry, and Pharmacological Activities of *Coleus amboinicus*: A Comprehensive Review. *Current Pharmaceutical Design*, 30(7), 519 - 535. https://doi.org/10.2174/0113816128283267240130062600.

4. Leesombun, A., Thanapakdeechaikul, K., Suwannawiang, J., Mukto, P., Sungpradit, S., Bangphoomi, N., Changbunjong, T., Thongjuy, O., Weluwanarak, T. & Boonmasawai, S. (2022). Effects of *Coleus amboinicus* L. Essential Oil and Ethanolic Extracts on Planktonic Cells and Biofilm Formation of Microsporum canis Isolated from Feline Dermatophytosis. *Antibiotics*, 11(12). https://doi.org/10.3390/antibiotics11121734.

5. Ślusarczyk, S., Cieślak, A., Yanza, Y. R., Szumacher-Strabel, M., Varadyova, Z., Stafiniak, M., Wojnicz, D. & Matkowski, A. (2021). Phytochemical profile and antioxidant activities of *coleus amboinicus lour*. Cultivated in Indonesia and Poland. *Molecules*, 26(10), 2915. https://doi.org/10.3390/molecules26102915.

6. Winter, K., Virgo, A., Garcia, M., Aranda, J. & Holtum, J. A. M. (2021). Constitutive and facultative crassulacean acid metabolism (CAM) in Cuban oregano, *Coleus amboinicus* (Lamiaceae). *Functional Plant Biology*, 48(7), 647 - 654. https://doi.org/10.1071/FP20127.

7. Maldaner, J., Oliveira, M. N., Santos, D. de A., Garcia, P. de T., Silva, S. Y. S., Silva, S. da C., Lima, L. E. P. & Silva, F. dos S. (2021). Chemical and thermal profile of *Plectranthus amboinicus* essential oil for its application as a bioherbicide. *Scientia Plena*, 17(11), 278 - 285. https://doi.org/10.14808/sci.plena.2021.731102.

8. Ananthi T. & Ramya V. (2021). HPTLC analysis and anti-inflammatory activity of *Plectranthus amboinicus* (Lour.) leaves. *International Journal of Research in Pharmaceutical Sciences*, 12(3), 2077 - 2082. https://doi.org/10.26452/ ijrps.v12i3.4816.

9. Gurning, K. (2020). Determination antioxidant activities methanol extracts of bangun-bangun (*Coleus amboinicus* L.) Leaves with DPPH method. *Jurnal Pendidikan Kimia*, 12(2), 62 - 69. https://doi.org/10.24114/jpkim.v12i2.19397.

10. Rani N, M., Shetty, P. K., Rao, S. N. & Nayak, R. P. (2020). Screening for anti-inflammatory and peripheral analgesic activity of *Coleus amboinicus* leaves using wistar albino rats. *Indian Journal of Pharmacy and Pharmacology*, 7(3), 164 - 167. https://doi.org/10.18231/j.ijpp.2020.028.

11. Pinheiro, G. P., Ferreira da Silva, G. & Frankland Sawaya, A. C. H. (2023). Effect of leaf development on the composition of *Coleus amboinicus* Lour. hydroethanolic extracts. *Biochemical Systematics and Ecology*, 111. https://doi.org/10.1016/j.bse.2023.104738.

12. Pinheiro, P. F., Costa, A. V., De Assis Alves, T., Galter, I. N., Pinheiro, C. A., Pereira, A. F., Oliveira, C. M. R. & Fontes, M. M. P. (2015). Phytotoxicity and Cytotoxicity of Essential Oil from Leaves of *Plectranthus amboinicus*, Carvacrol, and Thymol in Plant Bioassays. *Journal of Agricultural and Food Chemistry*, 63(41), 8981 - 8990. https://doi.org/10.1021/acs.jafc.5b03049.

13. Santos, F. A. V., Serra, C. G., Bezerra, R. J. A. C., Figueredo, F. G., Edinardo, Matias, F. F., Menezes, I. R. A., Costa, J. G. M. & Coutinho, H. D. M. (2016). Antibacterial activity of *Plectranthus amboinicus* Lour (Lamiaceae) essential oil against Streptococcus mutans. *European Journal of Integrative Medicine*, 8(3), 293 - 297. https://doi.org/10.1016/j.eujim.2015.11.021.

14. Sabra, A. S., Astatkie, T., Alataway, A., Mahmoud, A. A., Gendy, A. S. H., Said - Al Ahl, H. A. H. & Tkachenko, K. G. (2018). Response of Biomass Development, Essential Oil, and Composition of *Plectranthus amboinicus* (Lour.) Spreng. to Irrigation Frequency and Harvest Time. *Chemistry & Biodiversity*, 15(3). https://doi.org/10.1002/cbdv.201800005.

15. Ministry of Health. (2023). *Vietnamese Pharmacopoeia V - Supplementary Edition. 1.*

16. UPOV. (2016). Plectranthus. Guidelines for the conduct of test for distinctness, uniformity and stability.TG/315/1. International union for the protection of new varieties of plan. https:// www.upov.int/ edocs/ tgdocs/en/tg315.pdf.

17. Dung, N. X., Sothy, N., lo, V. N., Leclercq, P. A. & Moi, L. D. (1990). Chemical composition of the essential oil of *Coleus amboinicus* Lour. From Vietnam and Lampuchea.. *Proceeding of the National Center for Scientific Research of Vietnam*, 2, 123 - 127.

18. Lu, T. M. Thy. (2016). The study on the extraction of *Plectranthus amboinicus* (Lour) Spreng essential oil by the steam distillation. *Journal of Science Technology and Food*, 10, 14 - 17.

19. Díaz-Delgado, G. L., Rodríguez-Rodríguez, E. M., Ríos, D., Cano, M. P. & Lobo, M. G. (2024). Morphological Characterization of Opuntia Accessions from Tenerife (Canary Islands, Spain) Using UPOV Descriptors. *Horticulturae*, 10(7), 1 - 17. https://doi.org/10.3390/horticulturae10070662

20. Sahin, E. C., Kaya, E., Tuyel, U., Aydin, Y., Ozhatay, N. & Uncuoglu, A. A. (2021). An assessment on the floristic variety of Colchicum genus of Turkey in terms of morphological characteristics. *Scientia Horticulturae*, 287. https://doi.org/10.1016/j.scienta.2021.110251.

21. Bernhardt, B., Fazekas, G., Ladányi, M., Inotai, K., Zámbori-Németh, É., Bernáth, J. & Szabó, K. (2014). Morphological-, chemical- and RAPD-PCR evaluation of eight different *Ocimum basilicum* L. gene bank accessions. *Journal of Applied Research on Medicinal and Aromatic Plants*, 1(1), e23 - e29. https://doi.org/10.1016/J.JARMAP.2014.03.002.

QUANTIFICATION AND IN-HOUSE REFERENCE STANDARD PREPARATION OF TANSHINONE IIA FROM DANSHEN (*Salvia miltiorrhiza* Bunge) ROOTS COLLECTED IN LAI CHAU, GIA LAI, AND LAM DONG PROVINCES

Le Thi Thao An[1, 2], Tran Minh Phuong[3], Nguyen Thi Thinh[3], Nguyen Thi Y Nhi [1, 2, *]

[1] *Faculty of Chemistry, University of Science, Vietnam National University, Ho Chi Minh city*

[2] *Vietnam National University, Ho Chi Minh city*

[3] *Institute of Drug Quality Control, Ho Chi Minh city*

* *Email: ntynhi@hcmus.edu.vn*

ABSTRACT

Salvia miltiorrhiza Bunge., commonly known as Đan sâm or Danshen, is a valuable medicinal herb widely used for cardiovascular disorders. The raw materials of Danshen, originating in Vietnam, however, have remained uncommon and poorly characterized. Tanshinone IIA, one of the major and attractive components of Danshen, has been used as a key bioactive marker that is required by multiple pharmacopoeias. This compound is still available only as a costly imported reference standard, which is a hindrance for both the materials' quality evaluation and the phytochemical study of Vietnamese Danshen. In this study, the reference standard of tanshinone IIA was in-house prepared from Vietnamese Danshen root materials (labelled as IH-TIIA). This standard evolved into the validated UFLC/PDA method that is used for the quantification of tanshinone IIA in roots and extracts. The procedure for preparing IH-TIIA was also applied to the tanshinone IIA isolated from all of the Vietnamese Danshen materials. All IH-TIIA samples were achieved with high purity, being 98.62% (Lai Chau), 98.68% (Gia Lai) and 98.77% (Lam Dong), respectively. The quantification results indicated a clear regional variation of tanshinone IIA yield, with the roots from Lai Chau containing the highest content (1.24%). Known to be relatively unstable, tanshinone IIA was also subjected the stability evaluation under different storage conditions. The obtained results demonstrated that the preservation at 4°C without light exposure was ideal for tanshinone IIA.

Keywords: *Salvia miltiorrhiza, tanshinone IIA, nuclear magnetic resonance, UFLC/PDA.*

Received: 25 September 2025; revised: 4 November 2025; accepted: 8 December 2025.

1. INTRODUCTION

Salvia miltiorrhiza Bunge. is a traditional Chinese medicinal herb prescribed for promoting blood circulation, resolving stasis, nourishing the heart, calming the spirit, and detoxifying. Thanks to these beneficial effects, Danshen has been cultivated in Vietnam and other countries for the constant yield of its typical red roots [1]. In modern medicine, its roots exist in the treatment of cardiovascular disorders such as atherosclerosis, thrombosis, and angina pectoris. Clinical studies further demonstrated the protective effects of Danshen on cartilage, anti-apoptotic and platelet aggregation inhibitory activities, and vascular function improvement [2 - 8]. Regarding the phytochemistry, Danshen has been indicated to contain lipophilic diterpenoids and phenolic acids. Among these, tanshinone IIA is the main bioactive diterpenoid that is used as a recognized marker for quality control [9]. It is included in the

pharmacopoeias of China, EU, Japan, Korea, USA, and Vietnam, specified as a minimum content of 0.20% in root materials (HPLC, dry basis). The content of tanshinone IIA is one of the most important criteria for evaluating the quality of Danshen materials. Some previous studies in Vietnam have simultaneously quantified tanshinone IIA and salvianolic acid B using modern technologies such as HPLC-MS/MS or UPLC-DAD [10 - 11]. A complete and effective procedure for preparing tanshinone IIA at the reference grade has remained left-open. However, the high cost of the reference standard has still been a limitation for Vietnamese Danshen materials evaluation. The phytochemistry of Danshen originating from Vietnam remains poorly understood, with tanshinone I, tanshinone IIA, and cryptotanshinone being the reported constituents [12]. In this study, tanshinone IIA was in-house prepared at the reference standard grade, labelled as IH-TIIA, and this product evolved in a standardized UFLC/PDA procedure for tanshinone IIA quantification of Danshen roots harvested in Lai Chau, Gia Lai, and Lam Dong provinces. With this in-house preparation and large-scale quantification, a strong, traceable solution for evaluating Vietnamese Danshen was significantly supported, reducing the dependence on imported standards and establishing a framework for pharmaceutical quality control and future pharmacological research.

2. MATERIALS AND METHODS

2.1. Plant materials

Fresh Danshen roots were collected in October 2023 from three provinces in Northern and Central Vietnam: Lai Chau (LC), Gia Lai (GL), and Lam Dong (LD) (Figure 1). The LD and GL Danshen were cultivated for 18 months following the VietGAP standard, with controlled irrigation and nutrient management; while LC Danshen (at undetermined age) was wildly collected from mountainous areas of Muong Te commune. For phytochemical comparison with Vietnamese Danshen, 1.3 kg of Danshen roots were purchased from the Dai Loc Trading, Manufacturing, and Construction Company, Ltd. LC, GL, and LD Danshen roots were botanically identified via chloroplast gene sequencing (Apollo Biotek Co., Ltd., with sequence comparisons against the NCBI database), macroscopy, and powder microscopy (the Institute of Drug Quality Control, Ho Chi Minh city, in accordance with Vietnamese Pharmacopoeia V (VPV)).

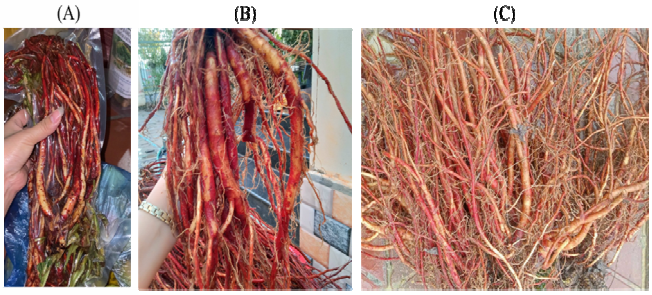

Figure 1. Danshen roots collected in Lai Chau (A), Gia Lai (B), and Lam Dong (C) provinces

2.2. Reagents and standards

Acetonitrile and methanol (HPLC-grade) were obtained from Supelco Inc. (Massachusetts, United States). Organic solvents, including *n*-hexane, chloroform, ethyl acetate, toluene, *n*-butanol, ethanol 96%, formic and sulfuric acids, were purchased from Chemsol (Vietnam). Distilled water was internally prepared. A commercial tanshinone IIA standard was supplied by the Institute of Drug Quality Control, Ho Chi Minh City (99.7817% pure (UFLC/PDA)) and was used for the quality evaluation of IH-TIIA.

2.3. UFLC/PDA analysis

The UFLC/PDA analysis was performed on a SPD-M20A (Shimadzu) system, using a Gemini-NX C18 column (250 × 4.6 mm, 5 µm) and a guard column. The mobile phase was acetonitrile-water (60: 40, v/v), 1.0 mL/min, injection volume of 20 µL, column temperature of 25°C, PDA detection at 270 nm, and a run time of 30 min.

2.4. Preparation of IH-TIIA from purchased Chinese Danshen roots

Scheme 1 of the Supplementary Materials section shows the process of preparing IH-TIIA from the purchased Chinese Danshen roots. Briefly, the roots were ground to obtain powder, which was macerated in ethanol 96% (*v/v*) at room temperature (three times of repetition, interval of

24 h) to obtain extract. The ethanolic extract was liquid-liquid extracted with a series of organic solvents (*n*-hexane, ethyl acetate, and *n*-butanol) to obtain the corresponding extracts. A residue was observed in the *n*-hexane extract, which was separated by mixing the extract with chloroform, filtering, and drying. After being eliminated, the residue, the *n*-hexane extract, was taken to the sephadex® LH-20 gel filtration and silica gel column chromatography (the gradient mobile phase of *n*-hexane–chloroform–ethyl acetate), yielding 41 fractions (A1-A41). A precipitate was observed in the A4 fraction, which was subsequently isolated and recrystallized in *n*-hexane–chloroform (1.5: 1, *v/v*) mixture at 0°C to obtain a dark brown solid. This solid was completely dried and taken to NMR and ESI-MS recordings for structural evaluation (IH-TIIA).

2.5. Quantification of tanshinone IIA in LC, GL, and LD Danshen roots

Before the quantification of tanshinone IIA, in LC, GL, and LD Danshen roots, the method was validated via the parameters of specificity, system suitability, linearity, accuracy, precision, LOD, and LOQ. Recovery tests (110–140 % levels) and six replicate injections of the standard confirmed analytical reliability. The ethanolic extract of LC, GL, and LD Danshen roots were prepared following the same process as the Chinese one. Approximately 25 mg of each extract was dissolved in methanol (10: 5, *w/v*), sonicated for 10 min, and filtered via 0.45-µm PTFE membrane. IH-TIIA was used to prepare the calibration solutions (concentration ranging from 0.00005 to 0.05 mg/mL). Scheme 2 of the Supplementary Materials section shows the process of quantifying tanshinone IIA from LC, GL, and LD Danshen roots, while figure 2 is the summary of the preparation of IH-TIIA and the quantification of tanshinone IIA in LC, GL, and LD Danshen roots.

2.6. Establishing a complete protocol for preparing IH-TIIA from Vietnamese Danshen roots and investigation on the storage conditions of tanshinone IIA

A complete protocol for preparing in-house reference tanshinone IIA was established for further quantification of tanshinone IIA for Vietnamese Danshen roots. Specifically, the extraction process was aided by sonication, using methanol and ethanol as extraction solvents. The isolated tanshinone IIA was investigated the stability under different storage conditions (at 4°C and ambient temperature) in the solid form.

2.7. Statistical analysis

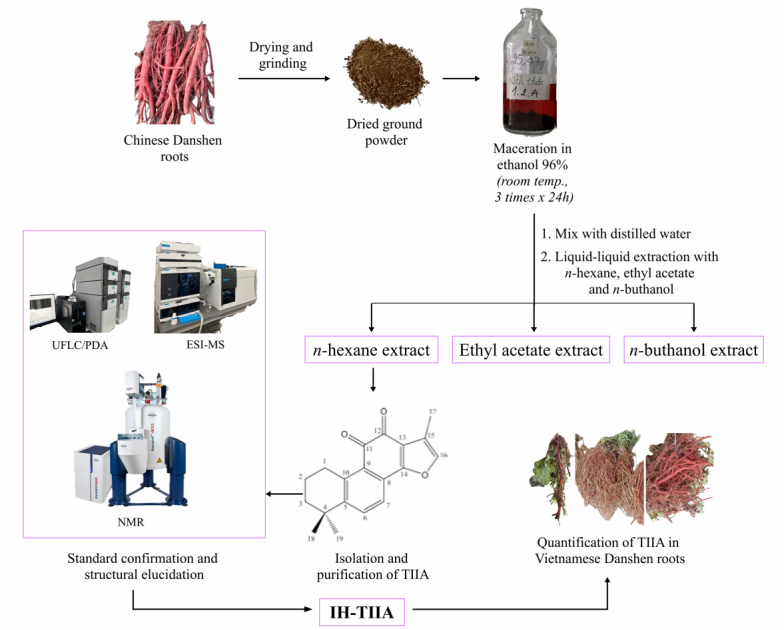

Figure 2. IH-TIIA preparation and TIIA quantification on LC, GL, and LD Danshen roots

The statistical analysis was performed in Microsoft Excel using ANOVA followed by Tukey's post-hoc test. Data are presented as mean ± SD (n = 3). The value of $p < 0.05$ was determined to be statistically significant.

3. RESULTS AND DISCUSSIONS

3.1. Botanical identification for LC, GL, and LD Danshen roots

3.1.1. Chloroplast DNA sequencing

Figures S1-S4 of the non-separative Supplementary Materials are the result of chloroplast DNA sequencing for the collected Danshen samples. Based on this result, the LD sample was identified as *Salvia miltiorrhiza*, whereas the species-level identification of the LC and GL samples was inconclusive.

3.1.2. Morphological observations

Figure 3. Morphological features of the identified Danshen samples

The LC roots were observed to be thinner and darker reddish-brown on the surface than those of the other two samples. On the other hand, the LD and GL roots had a more uniform cylindrical form and brighter periderms (Figure 1). Histological and powder microscopy revealed typical VPV diagnostic features, including multilayered cork, concentric vascular rings, lignified vessels, and resinous deposits. The vascular tissues were better organized in LD and GL samples, whereas resin was more abundant in LC roots, indicating wild-growing conditions. The purchased roots from China showed dense cork layers and highly differentiated vessels, which were possibly a consequence of a different processing manner. Figure 3 shows the morphological features of the identified Danshen samples. All samples met VPV criteria for *Salvia miltiorrhiza*, ensuring their suitability for subsequent extraction and standard preparation experiments.

3.2. Isolation, purification, and characterization of IH-TIIA and AD02

From 1.3 kg of Chinese Danshen roots, 5.55 g of *n*-hexane extract and 64.54 g of ethyl acetate extract were obtained, respectively. After the gel filtration on sephadex® LH-20, silica gel column chromatography, and further purification, 319.78 mg of a reddish-orange solid (AD02) was obtained. AD02 was subjected to thin-layer chromatography (TLC) together with the crystallized IH-TIIA at an earlier stage; the results are shown in Figure 4. Compound AD02 was structurally elucidated via ^{1}H-NMR, ^{13}C-NMR, COSY, HSQC, HMBC, and HR-ESI-MS spectra.

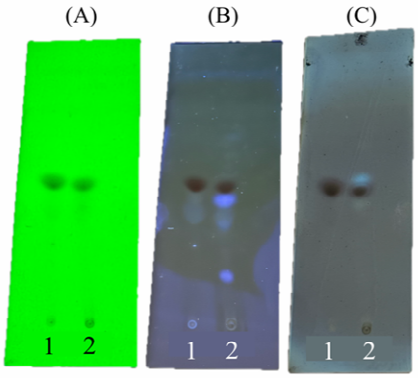

Figure 4.TLC results of crystallized IH-TIIA (1) and AD02 (2) [(A): under UV_{254} light, (B): under UV_{365} light, (C): reaction with H_2SO_4 25% reagent]

Its ^{1}H-NMR spectrum showed the signal of aromatic protons at δ_H (ppm) 7.63 (1H, d, 8.1, H-6) and 7.55 (1H, d, 8.2, H-7), an olefinic proton at δ_H (ppm) 7.22 (1H, q, 1.4, H-16), methyl protons at δ_H (ppm) 2.26 (3H, d, 1.4, H-17), 1.31 (3H, s, H-18 and H-19), and methylene protons at δ_H (ppm) 3.18 (2H, t, 6.4), 1.80 (2H, m), and 1.66 (2H, m). The ^{13}C-NMR spectrum of AD02 yielded 19 signals, including methyl carbons at δ_C (ppm) 8.8 (C-17), 31.8 (C-18 and C-19), aromatic carbons at δ_C (ppm) 144.5 (C-5), 133.5 (C-6), 120.2 (C-7), 127.5 (C-8), 126.5 (C-9), and 150.1 (C-10), olefinic oxygen-bearing carbons at δ_C (ppm) 161.7 (C-14) and 141.3 (C-16), other olefinic carbons at δ_C (ppm) 119.9 (C-13) and 121.2 (C-15), methylene carbons at δ_C

(ppm) 29.9 (C-1), 19.1 (C-2), and 37.9 (C-3), carbonyl carbons at δ_C (ppm) 183.7 (C-11) and 175.8 (C-12), and a quarternary carbon at δ_C (ppm) 34.7 (C-4). These signals indicated the miltiradiene-type nature of AD02's molecule, and a structural resemblance between AD02 and tanshinone IIA. Supported by the observations in its COSY and HSQC spectra, the signal assignment for each of AD02's protons and carbons was conducted. The HMBC spectrum of AD02 yielded the correlations of H-1/C-2, H-2/C-3, H-3/C-4 and C-5, H-18 and H-19/C-4, allowing the determination of dimethylation at C-4 and the ring A of the miltiradiene backbone. Additionally, correlations were observed between H-6/C-5 and C-7, as well as between H-7/C-8 and C-14, indicating the presence of the aromatic B ring of AD02. Together with the correlations of H-16/C-15, H-17/C-13, and C-15, the D ring of AD02's molecule was revealed to exist. With these spectral points, the structural resemblance between AD02 and tanshinone IIA became evident. Compared with the previous publications [9,10], spectral similarities between AD02 and tanshinone IIA were apparent (Table 1). Finally, in the HR-ESI-MS spectrum of AD02, a pseudomolecular ion peak of $[M + H]^+$ was observed at *m/z* 295.1336 (calculated for $C_{19}H_{19}O_3^+$, theoretical value of 295.1334), allowing the structural conclusion for AD02 to be tanshinone IIA (Figure 5).

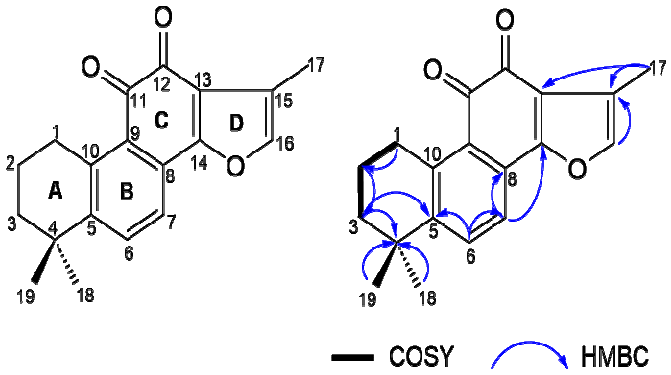

Figure 5. Major COSY, HMBC correlations, and molecular structure of AD02

Table 1. NMR data comparison between AD02 and tanshinone IIA

Position	AD02 ($CDCl_3$)		Tanshinone IIA ($CDCl_3$) [13]	
	δ_H (ppm), *J* (Hz)	δ_C (ppm)	δ_H (ppm), *J* (Hz)	δ_C (ppm)
1	3.18 (2H, t, 6.4)	29.9	3.18 (t, 6.5)	29.9
2	1.80 (2H, m)	19.1	1.80 (m)	19.1
3	1.66 (2H, m)	37.9	1.66 (m)	37.8
4	-	34.7	-	34.7
5	-	144.5	-	144.1
6	7.63 (1H, d, 8.1)	133.5	7.63 (d, 8.0)	133.3
7	7.55 (1H, d, 8.2)	120.2	7.53 (d, 8.0)	120.8
8	-	127.5	-	127.4
9	-	126.5	-	126.5
10	-	150.1	-	150.1
11	-	183.7	-	183.6
12	-	175.8	-	175.7
13	-	119.9	-	119.9
14	-	161.7	-	171.7
15	-	121.2	-	121.4
16	7.22 (1H, q, 1.4)	141.3	7.21 (q, 1.5)	141.1
17	2.26 (3H, d, 1.4)	8.8	2.26 (d, 1.5)	8.7(*)
18	1.31 (3H, s)	31.8	1.31 (s)	31.2
19	1.31 (3H, s)	31.8	1.31 (s)	31.2

Note: (*) Data from Liu et al. (2011) [14]

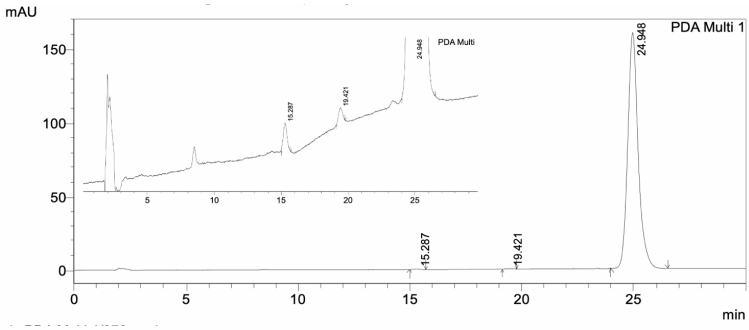

PeakTable @D:\Datalab\tmphuong\2024\Dan sam\15-4\C 0.05.lcd
PDA Ch1 270nm 4nm

Peak#	Ret. Time	Area	Height	Area %	Height %
1	15.287	7431	383	0.143	0.238
2	19.421	3986	201	0.077	0.125
3	24.948	5195774	160019	99.781	99.636
Total		5207191	160603	100.000	100.000

Figure 6. UFLC/PDA analysis result for AD02

Figure 6 shows the UFLC/PDA analysis result of AD02 at 270 nm. In this figure, a single peak at 24.95 min, accounting for 99.781% of the total area, was observed. The PDA purity index (0.999994) exceeded the threshold (0.896635), with no detectable impurities. The spectral homogeneity in the 200 - 400 nm range confirmed that AD02 is a pure in-house reference standard for tanshinone IIA.

3.3. Quantification of TIIA in LC, GL, and LD Danshen roots

3.3.1. Quantification method validation

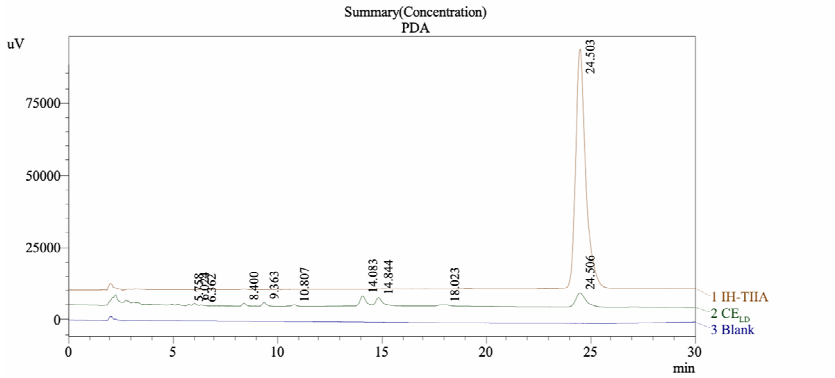

Figure 7. Chromatographic results of the TIIA quantification method validation

Table 2. Validation results of the TIIA quantification method validation

Parameters for validation	Results
System suitability	Retention time (R_t): 24.5248 ± 0.00791 mins
	Peak area: 2199175.500 ± 0.768 (mAU)
	Tailing factor: 1.431 ± 0.444
	Number of plates: 12987.823 ± 0.541
Linearity	R^2= 0.9993; y = 104228669x + 3440.5784
LOD	0.0000528 mg/mL
LOQ	0.000174 mg/mL
Accuracy	98.0–102.0 %
Precision	RSD = 1.154 % (n = 6)

Note: System suitability was evaluated using six injections of a 0.5 mg/mL standard solution; Linearity was established across six calibration levels; LOD and LOQ were calculated using the 3.3σ/S and 10σ/S approaches; Acceptance criteria included: RSD of R_t ≤ 1%, RSD of peak area ≤ 2%, tailing factor 0.8 - 1.5, recovery 98 - 102%, and precision RSD ≤ 2%.

Figure 7 and table 2 show the validation results for the TIIA quantification method. These results indicated that the established method was suitable for quantifying TIIA in Danshen root samples.

3.3.2. Quantification of TIIA in Vietnamese Danshen roots

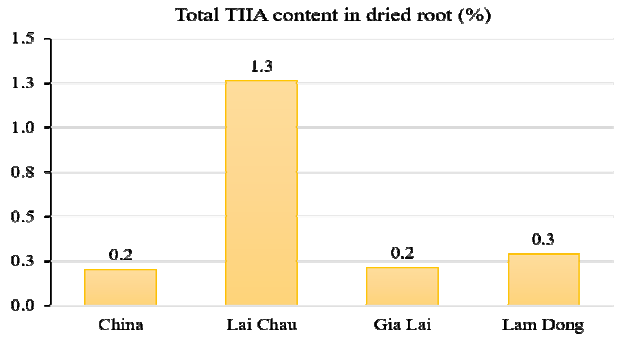

Figure 8. Total TIIA content of Chinese, Lai Chau, Gia Lai, and Lam Dong provinces Danshen roots

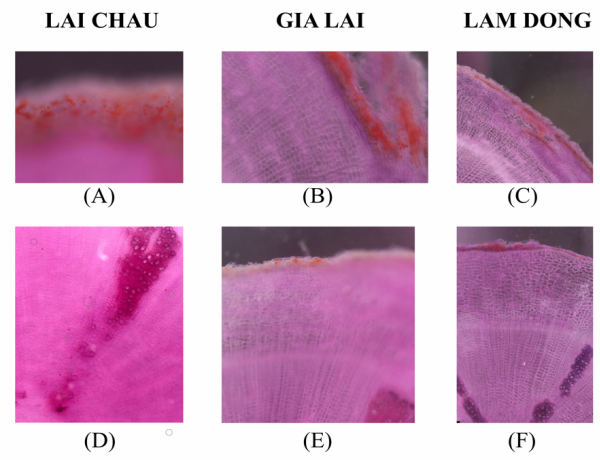

Figure 9. Representative histological sections (10X) of cork (A-C) and parenchyma tissues (D - F) from LC root (A, D), GL root (B, E), and LD root (C, F)

Figure 8 shows the total TIIA content of the Chinese, LC, GL, and LD Danshen roots. This figure shows that the roots from Lai Chau had the highest total TIIA content (1.3%), higher than that of the Chinese roots. Besides, the dense resinous deposits in cork and parenchyma tissues were clearly observed in the histological sections of these samples (Figure 9). These results suggest that the geographical origin of the roots affected both the amount of TIIA and the quality of Danshen. According to the Vietnamese Pharmacopoeia V (2019) [15], Chinese Pharmacopoeia (2020) [16], Japanese Pharmacopoeia XVIII (2021) [17], and Korean Pharmacopoeia XI (2020), *Salvia miltiorrhiza* roots must contain not less than 0.20% of TIIA (HPLC, dry basis). From Figure 8, it was evident that all root samples in this study exceeded this threshold, confirming their compliance with pharmacopoeial standards and their suitability as medicinal raw materials for further pharmaceutical research.

3.4. Establishing a complete protocol for preparing IH-TIIA from Vietnamese Danshen roots

A schematic overview of the preparation workflow is shown in the Scheme 2 and figure S5 of the Supplementary Materials section.

3.4.1. Yield of crude ethanolic extract from Danshen roots

The maceration using ethanol 96% as the extraction solvent was chosen due to the its better scalability. Figure 10 shows the total content of tanshinone IIA, the amount of extracted tanshinone IIA, and the extraction yield (%) of LC, GL, and LD Danshen roots. Observing in this figure that LC roots had the highest tanshinone IIA content (1.2%), but only 0.09% of the compound was extracted. In contrast, the GL roots, which had lower tanshinone IIA content (0.2%), achieved the highest amount of extracted tanshinone IIA (82.1%). The tanshinone IIA chromatographic peak of the samples matched that of IH-TIIA, confirming the component (Figure S6 of the Supplementary Materials section).

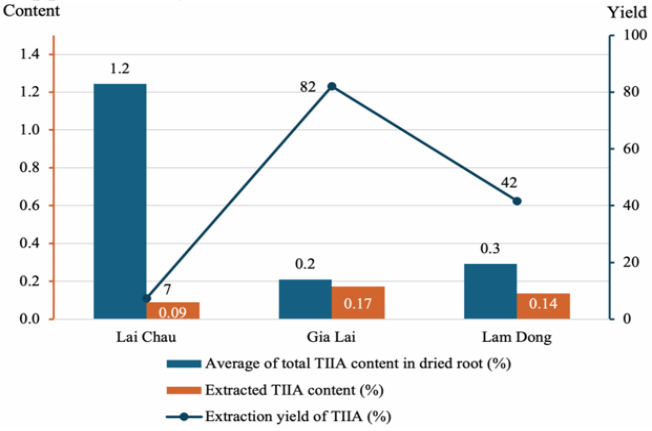

Figure 10. The total content of tanshinone IIA, the amount of extracted tanshinone IIA, and the extraction yield (%) of LC, GL, and LD Danshen roots

3.4.2. Efficiency of tanshinone IIA enrichment for the crude ethanolic extracts

A two-step liquid–liquid extraction procedure, consisting of water/*n*-hexane partition (labelled as Hex1) and then 90% MeOH-H_2O/*n*-hexane partition (labelled as Hex2), was applied for the enrichment of tanshinone IIA for crude ethanolic extracts. Via UFLC/PDA with IH-TIIA as the reference, the amount of enriched tanshinone IIA was determined, and the results are shown in figure 11 and table S1 of the Supplementary Materials section. Observing figure 11 showed that the highest enrichment was obtained from the LD sample (tanshinone IIA content of 16.0%, peak area of 74.0%, and yield of 87.2%), followed by the GL and LC ones.

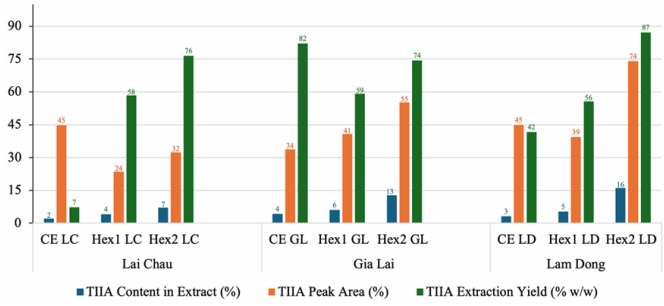

Figure 11. The amount of tanshinone IIA, chromatographic peak area, and extraction yield (%, *w/w*) of the Hex1, Hex2, and crude extracts (CE) of LC, GL, and LD Danshen roots

(n = 3, p < 0.05)

3.4.3. Purification and structural confirmation of isolated tanshinone IIA

The Hex2 extract was eluted by the column chromatography gradient mobile phase of *n*-hexane-ethyl acetate-chloroform. The fractions that had a precipitate were joined, and the precipitate was isolated, crystallized at 0°C in *n*-hexane-chloroform (1.5: 1, *v/v*) to afford a reddish-orange solid. This solid was structurally elucidated and confirmed as tanshinone IIA via UFLC/PDA, NMR, and ESI-MS techniques. Figure 12 is the UFLC results of the tanshinone IIA purification.

Structural confirmation of isolated tanshinone IIA from LC, GL and LD roots was obtained by ^{1}H-, ^{13}C-NMR, and HR-ESI-MS spectra, which showed a full consistency with tanshinone IIA (Table S2 of the Supplementary Materials sections). Specifically, the spectra of all samples exhibited the characteristic aromatic/olefinic proton region (δ_H (ppm) 7.2 - 7.6) and quinoid carbons δ_C (ppm) 183.6 (C-11) and 175.8 (C-12). The $[M]^+$ pseudomolecular ion peak was observed at *m/z* 295.1330 to 295.1335 for all of the samples, in accordance with the molecular formula of tanshinone IIA. The UFLC/PDA analysis confirmed high chromatographic purity for all preparations: 98.68% (GL), 98.76% (LD), and 98.62% (LC) (Figures S7 - S9 of the Supplementary Materials section). These results demonstrated that the tanshinone IIA isolated from LC, GL, and LD Danshen roots totally matches the reference standard grade as the prepared IH-TIIA from Chinese Danshen roots.

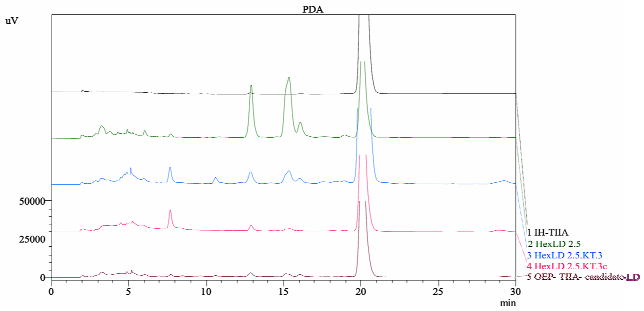

Figure 12. The UFLC results of the purification of tanshinone IIA from LD roots

Stability control for TIIA in root materials and after purification

A single-point comparison between freshly obtained and four-year-stored Chinese Danshen roots (Figure 13) revealed a pronounced decrease in the tanshinone IIA content, from 0.205 2.050 % in the fresh sample to 0.00105 6.62243 % in the stored one. Despite not being a longitudinal study, this substantial reduction aligns with the known instability of diterpenoid quinones in crude botanical matrices, where moisture, enzymatic activity, microbial takes place, and oxidation-accelerated degradation. In contrast, the crystalline form is less susceptible to such matrix-driven loss. These findings underscore the necessity of using freshly prepared IH-TIIA and avoiding prolonged storage of crude root material for accurate quantification and quality control.

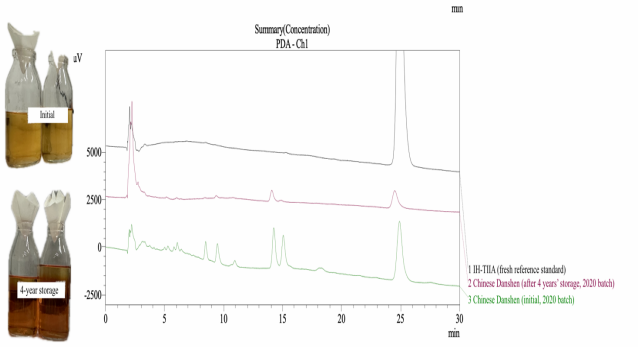

Figure 13. Degradation of Chinese Danshen roots after four years of storage

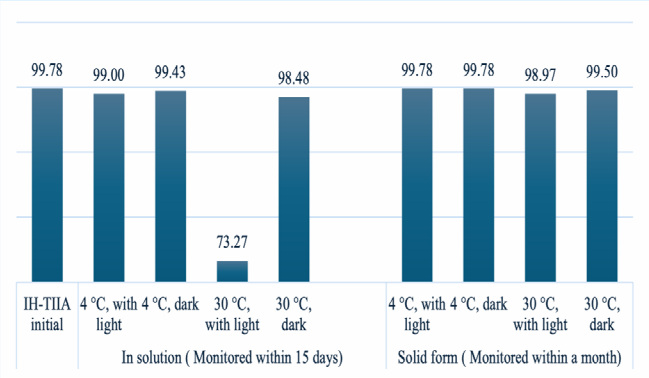

Figure 14. Stability of IH-TIIA in solution and solid forms under different storage conditions

Figure 14 shows the stability of purified IH-TIIA in solution and solid forms under different storage conditions, while Tables S3 and S4 of the Supplementary Materials section summarize the chromatographic purity of IH-TIIA, expressed as the percentage of the tanshinone IIA peak area (mean ± SD, n = 3), under various storage conditions. The initial reference sample exhibited a purity of 99.78167 ± 0.00306%. Stability testing showed that solid IH-TIIA remained essentially unchanged after 1 month, with 99.78% at 4°C and 98.97% at 30°C. In solution, refrigerated samples were well preserved (99.00% under light, 99.43% in the dark), whereas storage at 30°C caused severe photodegradation (73.27% with light) but only minor loss in the dark (98.48%). These results demonstrate that solid-state IH-TIIA is intrinsically stable, while the solution form is susceptible to thermal and photolytic stress. Collectively, the findings underscore that refrigeration and light protection are indispensable for maintaining the integrity of IH-TIIA, reinforcing the need for stringent storage protocols when preparing and handling in-house reference standards.

From the results, it was inferred that IH-TIIA is best preserved in solid form at refrigerated temperatures (equal or below 4°C), ensuring long-term stability and analytical reliability. In contrast, solution samples require strict cold storage to prevent rapid degradation. In solution, IH-TIIA remained highly stable at 4°C (99.00 to 99.43%). At 30°C, however, a strong photodegradation was observed, with purity decreasing to 73.268 ± 0.142% under light, while samples stored in the dark retained 98.4768 ± 0.0213%. In solid form, IH-TIIA exhibited an excellent stability, maintaining approximately 99% purity across all conditions up to six months, including storage at 30°C, with minimal variability. Collectively, the stability profiles demonstrate that solid IH-TIIA is highly suitable for long-term storage across a broad temperature range (4 to 30°C), whereas solution standards require strict control of temperature and light, with refrigeration (≤ 4°C) and light protection being critical to preserving analytical integrity.

4. CONCLUSION

This study established a protocol for isolating tanshinone IIA from Danshen roots collected in Lai Chau, Gia Lai, and Lam Dong provinces, producing an in-house reference standard of (IH-TIIA) with a high purity (> 98.6%) and confirmed structural identity. Using IH-TIIA in a validated UFLC/PDA method, reliable quantification of tanshinone IIA was achieved, from which significant regional variation was indicated. The approach further enabled evaluation of purification efficiency and demonstrated the stability of TIIA under controlled storage (4°C). This work provides a cost-effective, reproducible alternative to imported standards, and delivers a practical framework with direct implications for pharmaceutical standardization and quality control.

ACKNOWLEDGEMENT

This research received support from Institute of Drug Quality Control in Ho Chi Minh city.

REFERENCES

1. Ngoc, N. T., Dung, D. M., Tam, T. T. T., Van, H. T., Dinh, N .L., Tung, N. H., Dinh, T. T. (2021). Simultaneous quantitative analyses of Tanshinone I, Cryptotanshinone, and Tanshinone IIA in Danshen (*Salvia miltiorrhiza* Bunge) cultivated in Vietnam using LC-MS/MS. *Indian Journal of Natural Products and Resources*, 12(1), 74 - 83.

2. Ministry of Science and Technology of Vietnam (2020). Research on the medicinal herb Danshen (*Salvia miltiorrhiza* Bunge) grown in Vietnam: Chemical composition and effects on leukemia cell lines. https://vista.gov.vn/news/ket- qua- nghien- cuu- trien- khai/nghien-cuu-duoc-lieu- dan-sam-salvia-miltiorrhiza-bunge-trong-o-viet-nam-thanh-phan-hoa-hoc-va-tac-dung-tren-cac-dong-te-bao-ung-thu-mau-2652.html. Accessed October 10, 2025.

3. Lv, F. Y. S. L. and B. Lv. (2006). The influence of salvianolic acid B and tanshinone IIA on the nitric oxide and triglyceride in sera of atherosclerosis rabbit. *Journal of Tianjin University of Traditional Chinese Medicine*, 25, 32 - 34.

4. W. Y. Wu and Y. Wang. (2012). Pharmacological actions and therapeutic applications of Salvia miltiorrhiza depside salt and its active components, Acta Pharmacologica Sinica. 33, 1119 - 1130.

5. M. Yang, L.A. Guo, S. S. Song, J. X. Meng, G. D. Deng, X. M. Guo (2006). Characterization of tanshinones in the roots of *Salvia miltiorrhiza* (Danshen) by high-performance liquid chromatography with electrospray ionization tandem mass spectrometry, Rapid Communications in Mass Spectrometry, 20, 1266 - 1280.

6. X. Guan, D. -A. Gao, B. He, H. Chen, S. Sun (2009). Danshen protects kidney grafts from ischemia/reperfusion injury after experimental transplantation, Transplant International, 22, 232 - 241.

7. S. W. S. Leung, D. -Y. Zhou, R. Ma, M. Sun. (2010). Effects of the aqueous extract of *Salvia miltiorrhiza* (danshen) and its magnesium tanshinoate B-enriched form on blood pressure. *Phytotherapy Research*, 24(5), 769 - 774.

8. Xilin Xu, Lv Hang, Xiaodong Li, Hui Su, Xiaofeng Zhang, Jun Yang (2017). Danshen attenuates osteoarthritis-related cartilage degeneration through inhibition of NF-κB signaling pathway *in vivo* and *in vitro*. *Biochemistry and Cell Biology*, 95(6), 644 - 651.

9. Institute of Medicinal Materials. (2004). Medicinal Plants and Animals Used in Vietnam. Science and Technology Publishing House, 732 - 738.

10. Cuong, B. H., Thuan, N. T., Huong, N. L. (2021). Simultaneous quantitative determination of salvianolic acid B and tanshinon IIA in the *Salviae miltiorrhizae* Radix et Rhizoma semisolid extracts by HPLC. *Journal of Scientific and Engineering Research*, 8(5), 36 - 42.

11. Dung, D .M., Ngan, D. T., Hue, N. T., Hung, L. Q., Tung, N. H., Luyen, N. D., Thang, T. D. (2019). Isolation and quantification of tanshinon I, cryptotanshinon, tanshinon IIA from Danshen (*Salvia miltiorrhiza* B.) using UPLC-DAD. *Journal of Science and Technology of the Science and Technology Universities*, 137, 100 - 105.

12. Thuong, P. T., An, N. T. K., Khoi, N. M., Fumiaki, I. (2013). Tanshinones isolated from the acclimatized and cultivated Dashen (*Salvia miltiorrhiza Bunge*) roots. *Journal of Medicine and Pharmacy*, 53(9), 44 - 48.

13. Y. Tezuka, S. Fan, F. Sugiura, S. Arai. (1997). Aldose reductase inhibitory constituents of the root of *Salvia miltiorrhiza* Bunge. *Chemical and Pharmaceutical Bulletin.* 45(8), 1306 - 1311.

14. W. Liu, J. Zhang, G. Gao, Q. Sun, F. Song, J. Hu. (2011). Antiandrogenic, maspin induction and anti-prostate cancer activities of tanshinone IIA and its novel derivatives with modification in ring A. *Journal of Medicinal Chemistry*, 55(2), 201 - 209.

15. The Ministry of Health (2019). *Vietnamese Pharmacopoeia* (5th Ed.). Medical Publishing House, Hanoi.

16. Chinese Food and Drug Administration (2020). *Chinese Pharmacopoeia.* China Medical Science Press, Beijing.

17. The Ministry of Health, Labour, and Welfare (2021). *Japanese Pharmacopoeia* (18th Ed.). Pharmaceuticals and Medical Devices Agency, Tokyo.

OPTIMIZING INORGANIC FERTILIZER APPLICATION FOR OFF-SEASON SAFE TOMATO PRODUCTION IN VAN SON COMMUNE, PHU THO PROVINCE

Nguyen Thi Ngoc Dinh[1], Nguyen Hong Hanh[1,*], Nguyen Thi Ai Nghia[1], Do Thi Huong[1], Nguyen Trong Tuynh[2], Phan Thi Dieu Ninh[3], Pham Thi Bich Phuong[1], Ha Trung Kien[4]

[1]*Faculty of Agronomy, Vietnam National University of Agriculture;*

[2]*Faculty of Accounting and Business Management, Vietnam National University of Agriculture;*

[3]*Vnua Center for Manpower Supply, Vietnam National University of Agriculture;*

[4]*Student of Faculty of Agronomy, Vietnam National University of Agriculture*

[*]*Email: nhhanh@vnua.edu.vn*

ABSTRACT

This study aimed to determine the optimal inorganic fertilizer rate for safe off-season tomato (*Solanum lycopersicum* L.) production under the agroecological conditions of Van Son commune, Phu Tho province - a highland area suitable for temperate vegetable cultivation. A field experiment was conducted using the tomato variety *Savior* under a randomized complete block design (RCBD) with three N, P, K treatments CT1 (120-90-120 kg N-P_2O_5-K_2O ha^{-1}), CT2 (150-110-150 kg ha^{-1}) and CT3 (180-135-180 kg ha^{-1}), following VietGAP production standards. Results showed that CT3 significantly improved plant height, leaf number, fruit number and fruit weight, leading to the highest actual yield of 36.8 t ha^{-1} with 15,2% higher than CT1. Fruit vitamin C content and soluble solids (°Brix) increased under CT3, while nitrate accumulation remained within the safe limit (< 150 mg kg^{-1} fresh weight). Soil pH, organic matter, and heavy metal contents remained stable, indicating no adverse environmental effects. The study suggests that applying 180-135-180 kg N-P_2O_5-K_2O ha^{-1} is optimal for safe off-season tomato production in the Van Son commune highland.

Keywords: *Inorganic fertilizer, off-season cultivation, tomato, VietGAP, Van Son commune highland.*

Received: 20 October 2025, revised: 9 November 2025, accepted: 4 December 2025.

1. INTRODUCTION

Tomato (*Solanum lycopersicum* L.) is a fruit vegetable of high economic and nutritional importance, widely cultivated across diverse ecological zones in Vietnam. Statistical data indicate that the national tomato cultivation area and yield amount to approximately 23 - 25 thousand hectares annually, with production concentrated mainly in the northern delta and midland provinces during the winter-spring season, when temperatures ranging from 18°C to 25°C are favorable for flowering and fruit setting [1]. Nevertheless, due to the short duration of the main cropping season, the supply of fresh tomatoes declines markedly during the summer period, resulting in considerable fluctuations in market prices.

The development of off-season tomato production is regarded as an important strategy to diversify cropping seasons, stabilize market supply and demand, and enhance farmers' economic efficiency. Unlike the main season, off-season tomato cultivation occurs under high-temperature and high-light-intensity conditions that adversely affect plant growth, pest and disease development, fruit setting and product quality [2]. However, this

production system plays a crucial role in ensuring a stable year-round supply of vegetables and increasing farmers' income. Studies conducted in countries with topographical and climatic conditions similar to those of northern mountainous Vietnam have demonstrated that off-season tomato cultivation is both feasible and economically beneficial. Paudel *et al.* (2021) [3] reported that tomatoes can be successfully grown during the summer in hilly regions of Nepal at elevations between 800 and 1,200 m above sea level, where average temperatures range from 20°C to 28°C. These favorable ecological conditions support vigorous growth, high fruit set, and increased yields, while off-season tomatoes fetch market prices two to three times higher than those of the main-season crop. The authors further recommended the use of heat-tolerant varieties, net houses, and appropriate fertilizer management to enhance production efficiency and reduce pest and disease risks. These findings provide valuable insights for Vietnam, particularly for highland areas such as Van Son commune located at an elevation of 600 - 800 m with a cool year-round climate [4]. Such conditions indicate that the Van Son highland possesses significant potential for developing safe off-season tomato production under VietGAP standards, contributing to crop diversification and improved livelihoods for local farmers.

Tomato production under VietGAP standards requires strict adherence to regulations on input use, fertilizer and pesticide management, irrigation water quality and traceability [5]. Inorganic N-P-K fertilizers are key factors affecting yield, fruit quality and nitrate residue. Excessive nitrogen application can delay ripening and increase nitrate accumulation, while nutrient deficiency reduces productivity [6, 7]. Hence, optimizing fertilizer application to enhance nutrient use efficiency and minimize nitrate residues is essential for sustainable agriculture amid climate change [8, 9]. This study, conducted in Van Son commune Phu Tho province, aims to identify the appropriate N-P_2O_5-K_2O rate for the Savior tomato variety grown off-season under VietGAP standards, contributing to safe and sustainable tomato production in northern Vietnam's highlands.

2. MATERIALS AND METHODS

2.1. Materials

The tomato (*Solanum lycopersicum* L.) variety 'Savior' (Syngenta Co., Ltd.) was used in the experiment.

Organic composted cow manure "Thu Hoai 28" (total nitrogen: 1%, moisture content: 30%, organic matter: 22%, C/N ratio: 12, pHH_2O: 5), Song Gianh HC-15 biofertilizer, Ha Bac urea fertilizer (46.3% N), Lam Thao superphosphate (17% P_2O_5) and Ha Anh potassium chloride (60% K_2O) were used.

2.2. Methods

2.2.1. Experimental design and treatments

The experiment was arranged in a randomized complete block design (RCBD) with one factor, three replications, and three fertilizer treatments (T1: 120 kg N + 90 kg P_2O_5 + 120 kg K_2O; T2: 150 kg N + 110 kg P_2O_5 + 150 kg K_2O; T3: 180 kg N + 135 kg P_2O_5 + 180 kg K_2O), corresponding to an N: P: K ratio of 1: 0.75: 1 [10]. Each experimental plot had an area of 50 m^2, with a total of 9 plots and an overall experimental area of 500 m^2 (including buffer zones). The basal dressing consisted of 15 tons of "Thu Hoai" composted organic cow manure and 1,200 kg of Song Gianh HC-15 biofertilizer per hectare. Tomato beds were 1 m wide and 25-day-old seedlings were transplanted at a spacing of 60 cm between rows and 50 cm between plants. Crop management practices followed the Technical Guidelines for Safe Vegetable Production issued by the Hanoi Department of Agriculture and Rural Development under Decision No. 577/QĐ/SNN-TT dated May 10, 2010 [11].

The experiment was conducted during the summer cropping season, from April 14, 2023, to August 2023, at the production site of the Van Son Safe and Organic Vegetable Production

Cooperative Group, Chieng hamlet, Van Son commune, Phu Tho province, which is certified under VietGAP standards (20°33'54.6"N, 105°10'26.0"E).

2.2.2. Measurements and calculations

Growth and development parameters were measured on 10 plants per replication and included: Growth duration (days), plant height (cm), number of leaves per plant, number of flowers in the first five clusters, number of fruits in the first five clusters and fruit set rate (%).

Yield components, yield and quality parameters were measured on five plants per replication and included: Total number of fruits plant-1, average fruit weight (g), individual yield (g plant-1), actual yield (tons hectare-1). Parameters in tomato friuts (each replication analyzed 3 tomato fruits) including: Firmness (kgf) (using Fruit Hardness Tester FHT-1122), Brix content (%) (measured using a Milwaukee 882), NO3- content (10 TCN 457-2001) [12], vitamin C content (TCVN 6427-2:1998) [13], fiber (TCVN 5714:2007) [14], total sugar (TCVN 4594 -88) [15] and heavy metal concentrations of Pb (TCVN 7766:2007) [16] and Cd (TCVN 7768-1:2007) [17].

Water quality parameters included dissolved oxygen (DO) and total dissolved solids (TDS), measured using a HANNA HI 86302 TDS meter, pHKCl, chloride (TCVN 6194:1996) [18], heavy metals such as As, Cd, Cr, Hg, Cu, Pb, and Zn (TCVN 6193:1996) [19], and microbiological indicators including E. coli and coliforms (TCVN 6187-2:1996) [20]. Prior to the experiment, a composite soil sample was collected for baseline analysis, and after the experiment, one soil sample was taken from each replication. In each plot, three subsamples were collected from the 0 - 30 cm cultivation layer and combined to form a composite sample following TCVN 5738-2:2005 and ISO 10381-2:2005 standards [21]. Soil analyses included pHKCl (TCVN 5979:2007) [22], cation exchange capacity (CEC) (TCVN 8568:2010) [23], total organic matter (TCVN 9294:2012) [24], total nitrogen (Nts) (TCVN 6498:1999) [25], total phosphorus (P_2O_5ts) (TCVN 8940:2011) [26], total potassium (K_2Ots) (TCVN 8660:2011) [27] and heavy metals Cd and Pb (TCVN 6496:2009) [28].

Temperature and humidity data at the experimental site were recorded using an ElitechLog V6.4.3 automatic thermo-hygrometer.

2.2.3. Data analysis

Experimental data were processed using the method Analyze variance on statistical software Minitab 16 and compared average values using criteria Tukey standard at 95% confidence level.

3. RESULTS AND DISCUSSION

3.1. Weather conditions and results of water and soil parameters before and after the experiment

Table 1. Temperature and humidity conditions in Van Son commune, (now Van Son commune, Phu Tho province) in 2023

Month	Maximum temperature (°C)	Minimum temperature (°C)	Average temperature (°C)	Maximum humidity (%)	Minimum humidity (%)	Average humidity (%)
4	32.6	16.1	23.8	96.1	61.1	84.5
5	40.7	18.5	26.1	98.8	35.6	78.9
6	40.1	19.8	26.2	100.0	46.2	84.3
7	35.3	19.9	26.3	98.7	49.2	82.4
8	34.2	20.5	25.0	95.4	60.5	86.2

The average temperature during the summer cropping months (April-August) for off-season tomato cultivation ranged from 23.8°C to 26.3°C, while the average humidity fluctuated between 78.9% and 86.2% (Table 1). These results indicate that Van Son commune has favorable climatic

conditions for the production of off-season temperate vegetables, in which the average temperature is suitable for the growth and development of tomato plants [2].

Table 2. Results of water sample analysis before the experiment

Parameter	Unit	Analytical result	Permissible limit
pH		7.36	6 - 8.5
DO	%	61.00	-
Total dissolved solids	mg/l	151.00	-
Chloride (Cl)	mg/l	22.90	≤ 350
Chromium (Cr)	mg/l	0.01	≤ 0.04
Mercury (Hg)	mg/l	KPH	≤ 0.001
Lead (Pb)	mg/l	KPH	≤ 0.005
Cadmium (Cd)	mg/l	KPH	≤ 0.01
Copper (Cu)	mg/l	0.32	≤ 0.5
Zinc (Zn)	mg/l	0.39	≤ 1.5
Arsenic (As)	mg/l	KPH	≤ 0.05
Coliform density	CFU/100 ml	7000 ± 250	≤ 7500
E. coli density	CFU/100 ml	92 ± 50	≤ 100

Note: Permissible limits are compared according to QCVN 08-MT:2015/BTNMT [29].

Water used in the off-season safe vegetable cultivation experiment was suitable for safe vegetable production under the VietGAP standard (Table 2). The water samples collected from the experimental site met the safety requirements of VietGAP production. Parameters such as pH, DO, total dissolved solids, chloride, coliform density and E. coli levels were all within the permissible limits.

Table 3. Soil quality parameters for safe tomato cultivation before and after the experiment

1	pHKcl	-	6.50	6.30	6.60	6.40
2	Cation exchange capacity (CEC)	cmol kg-1	21.50	19.90 (-)	20.1 (-)	20.8 (-)
3	Organic matter	%	2.12	2.13 (+)	1.98 (-)	1.96 (-)
4	Total nitrogen (N)	%	0.22	0.22	0.21 (-)	0.19 (-)
5	Total phosphorus (P_2O_5)	%	0.08	0.08	0.05 (-)	0.07 (-)
6	Total potassium (K_2O)	%	1.10	1.10	1.2 (+)	1.2 (+)
7	Total lead (Pb)	mg kg-1	1.90	2.10 (+)	2.2 (+)	2.2 (+)
8	Total cadmium (Cd)	mg kg-1	0.01	0.02 (+)	0.02 (+)	0.01
9	Electrical conductivity (EC)	mS cm-1	0.21	0.18 (-)	0.22 (+)	0.22 (+)

Note: Pb and Cd indicators were compared according to the National Technical Regulation on allowable limits of heavy metals in agricultural soils [30]; (–) indicates a decrease compared to pre-experiment values; (+) indicates an increase compared to pre-experiment values; CT1: 120 kg N + 90 kg P_2O_5 + 120 kg K_2O; CT2: 150 kg N + 110 kg P_2O_5 + 150 kg K_2O; CT3: 180 kg N + 135 kg P_2O_5 + 180 kg K_2O.

The soil pH in the experimental treatments ranged from 6.3 to 6.6, which is within the optimal range for tomato growth and development. The cation exchange capacity (CEC) values after the experiment decreased in all treatments compared to the initial values, likely due to nutrient uptake by tomato plants and the rapid decomposition of organic matter, leading to reduced soil organic content. The organic matter content increased in treatment 1 but decreased in treatments 2 and 3 compared to before the experiment, which is consistent with the observed reduction in CEC. The

concentrations of Pb and Cd in the soil after the experiment remained within safe limits (Table 3).

3.2. Effects of inorganic fertilizer treatments on the growth and development parameters of off-season safe tomato production

Table 4. Effects of inorganic fertilizer treatments on the growth duration of off-season safe tomato cultivation

Treatment	Days from transplanting to… (days)			
	Flowering	Fruit setting	Fruit ripening	End of harvest
CT1	33	36	75	103
CT2	33	37	76	108
CT3	33	38	78	111
Mean	33	37	76	107

Note: CT1: 120 kg N + 90 kg P_2O_5 + 120 kg K_2O; CT2: 150 kg N + 110 kg P_2O_5 + 150 kg K_2O; CT3: 180 kg N + 135 kg P_2O_5 + 180 kg K_2O.

The period from transplanting to flowering of tomato plants was 33 days across all fertilizer treatments. The time from transplanting to the onset of ripening ranged from 75 to 78 days after transplanting (DAT), with the highest fertilizer rate (CT3) slightly prolonging the ripening period. The total growth duration varied from 103 to 111 DAT, being longest in CT3 and shortest in CT1; however, the difference among treatments was not significant (Table 4).

Table 5. Effect of inorganic fertilizer treatments on plant height of off-season safe tomatoes

Treatment	Plant height (cm)					
	17DAT	24 DAT	31 DAT	38 DAT	45 DAT	52 DAT
CT1	11.9c	21.4a	38.2b	50.3b	66.7b	86.9b
CT2	13.3b	23.9a	42.1a	57.7a	77.0a	94.2a
CT3	14.7a	24.7a	44.2a	59.4a	78.5a	97.3a

Note: Means followed by different letters in the same column are significantly different at $p < 0.05$. CT1: 120 kg N + 90 kg P_2O_5 + 120 kg K_2O; CT2: 150 kg N + 110 kg P_2O_5 + 150 kg K_2O; CT3: 180 kg N + 135 kg P_2O_5 + 180 kg K_2O. DAT: Days after transplanting.

Plant height tended to increase from 17 to 52 days after transplanting (DAT) across all inorganic fertilizer treatments. At all monitoring stages, plant height increased with the fertilizer rate, with CT3 consistently producing the tallest plants. At 17 DAT, plant height ranged from 11.9 to 14.7 cm, with the highest in CT3 and the lowest in CT1. At 24 DAT, plant height ranged from 21.4 cm to 24.7 cm, with no significant differences among treatments. At 31 DAT, height ranged from 38.2 cm to 44.2 cm, highest in CT3, which was not significantly different from CT2 but significantly taller than CT1. At 38 DAT, plant height ranged from 50.3 cm to 59.4 cm, with CT3 significantly taller than CT1. At 45 DAT, height ranged from 66.7 cm to 78.5 cm, highest in CT3, not significantly different from CT2, and lowest in CT1. At 52 DAT, plant height ranged from 86.9 cm to 97.3 cm, highest in CT3, not significantly different from CT2, and lowest in CT1. In summary, increasing the fertilizer rate to CT3 enhanced plant height, although the difference was not significant compared to the medium rate CT2 (Table 5).

Table 6. Effects of inorganic fertilizer treatments on leaf development dynamics of off-season safe tomato plants

Unit: Leaves plant-1

Treatment	17DAT	24 DAT	31 DAT	38 DAT	45 DAT	52 DAT
CT1	5.2b	7.3b	9.3c	12.2c	14.6b	17.1b
CT2	6.2a	8.3a	10.2b	12.8b	15.6a	18.3a
CT3	6.6a	8.9b	10.8b	13.6a	16.2a	19.0a

Note: Means followed by different letters in the same column are significantly different at $p < 0.05$. CT1: 120 kg N + 90 kg P_2O_5 + 120 kg K_2O; CT2: 150 kg N + 110 kg P_2O_5 + 150 kg K_2O; CT3: 180 kg N + 135 kg P_2O_5 + 180 kg K_2O. DAT: Days after transplanting.

At 17 days after transplanting (DAT), the number of leaves ranged from 5.2 to 6.6 per plant across all treatments. The differences among treatments were not statistically significant at the 95% confidence level. Between 17 and 31 DAT, the leaf emergence rate was the highest, as the plants, having established roots and recovered vigor, entered the vegetative stage, rapidly developing leaves. However, significant differences in leaf number were observed among the fertilizer treatments at this stage. Treatment CT3 produced the highest number of leaves, though the difference compared to CT2 was not significant.

From 31 to 45 DAT, leaf emergence slowed to approximately 1.5 - 3 leaves per week, coinciding with the flowering and fruit-setting stage. At 45 DAT, leaf numbers in CT2 and CT3 were not significantly different from each other but were significantly higher than CT1, with CT3 reaching 16.2 leaves per plant. At 52 DAT, CT3 still had the highest leaf number, not significantly different from CT2, while CT1 had the lowest (Table 6).

These results indicate that the highest fertilizer rate, CT3 (180 N : 135 P_2O_5 : 180 K_2O kg ha-1), enhanced plant height, leaf number, and growth rate compared to CT1 and CT2 (Tables 5 and 6). This finding is consistent with previous studies [1], which reported that increasing inorganic fertilizer within an appropriate range promotes vegetative growth and biomass accumulation in high-yielding tomato cultivars. The mechanism is attributed to balanced N and K supply, which stimulates meristem differentiation and carbohydrate accumulation. Other studies have shown that adequate N promotes initial plant height and growth, but excessive N may favor vegetative growth at the expense of flowering, highlighting the need for optimal dosage [6].

Table 7. Effects of inorganic fertilizer treatments on fruit parameters of off-season safe tomato plants

Treatment	Number of flowers in the first five clusters	Number of fruits in the first five clusters	Fruit set rate (%)
CT1	25.5a	19.7a	77.25a
CT2	25.5a	20.4a	80.00a
CT3	28.0a	22.3a	79.64a

Note: Means followed by the same letter in a column are not significantly different at $p < 0.05$. CT1: 120 kg N + 90 kg P_2O_5 + 120 kg K_2O; CT2: 150 kg N + 110 kg P_2O_5 + 150 kg K_2O; CT3: 180 kg N + 135 kg P_2O_5 + 180 kg K_2O.

The total number of flowers on the first five clusters ranged from 25.5 to 28.0 across treatments, indicating that fertilizer rate did not significantly affect flower number on these clusters. Similarly, the number of fruits on the first five clusters showed no significant differences among treatments, ranging from 19.7 fruits to 22.3 fruits. The fruit set rate, calculated as the number of fruits divided by the number of flowers on the same five clusters, also did not differ significantly among treatments, varying from 77.25% to 80.00% (Table 7).

3.3. Effects of inorganic fertilizer treatments on yield components, yield, and quality of off-season safe tomato plants

The highest total number of fruits per plant was recorded in CT3 (33.6 fruits), which was not significantly different from CT2, but was significantly higher than CT1. The highest average fruit weight was observed in CT2 (130.7 g), not significantly different from the higher fertilizer rate in CT3, but significantly higher than CT1. Individual yield was highest in CT3, though not significantly different from CT2, while CT1 had the lowest yield, significantly lower than the other two treatments. Similarly, actual yield was highest in CT3, not significantly different from CT2, and lowest in CT1 (Table 8).

Table 8. Effects of inorganic fertilizer treatments on yield components and yield of off-season safe tomato plants

Treatment	Total fruits plant-1	Average fruit weight (g)	Individual yield (g plant-1)	Actual yield (tons hectare-1)
CT1	29.1b	82.5b	2475.4b	31.2b
CT2	33.3a	130.7a	4219.3a	34.5ab
CT3	33.6a	130.2a	4376.9a	36.8a

Note: Means followed by different letters in the same column are significantly different at $p < 0.05$. CT1: 120 kg N + 90 kg P_2O_5 + 120 kg K_2O; CT2: 150 kg N + 110 kg P_2O_5 + 150 kg K_2O; CT3: 180 kg N + 135 kg P_2O_5 + 180 kg K_2O.

Previous studies optimizing N application [6, 8] have shown that excessive residual N does not always increase yield and may reduce fruit quality; optimal rates can vary depending on soil, cultivar, and season. The increase in fruit number per plant and average fruit weight in CT3 reflects sufficient N supply during flowering, fruit set, and fruit development, while appropriate K application supports fruit size and sugar accumulation. Therefore, a fertilization strategy that balances nutrients for growth and development while minimizing N losses due to leaching during heavy rainfall in highland areas is essential [7]. At the experimental site, CT3 (180-135-180 kg/ha) was found suitable for achieving high yield, although it did not differ significantly from CT2 (150-110-150 kg/ha) (Table 8).

Table 9. Effects of inorganic fertilizer treatments on biochemical quality parameters of off-season safe tomato fruits

Treatment	Fruit firmness (kgf)	Brix (%)	Total solids content (%)	Total sugar (%)	Fiber content (%)	Vitamin C (mg 100g-1)
CT1	4.8a	4.2a	1.2a	2.9a	1.2a	12.8b
CT2	4.1a	4.1b	1.1b	2.8a	1.2a	11.8c
CT3	3.6a	4.0b	1.2a	2.8a	1.1b	13.2a

Note: Means followed by different letters in a column are significantly different at $p < 0.05$. CT1: 120 kg N + 90 kg P_2O_5 + 120 kg K_2O; CT2: 150 kg N + 110 kg P_2O_5 + 150 kg K_2O; CT3: 180 kg N + 135 kg P_2O_5 + 180 kg K_2O.

Tomato firmness ranged from 4.0 kgf to 4.8 kgf and fertilizer rate did not significantly affect fruit firmness. Fruit Brix varied from 4.0 to 4.8, with significant differences among treatments; CT1 had the highest Brix, significantly higher than CT2 and CT3. Total solids content was significantly higher in CT1 and CT3 compared to CT2 (Table 9). Fertilizer treatments did not

significantly influence total sugar content, which ranged from 2.8% to 2.9%. Fiber content varied from 1.1% to 1.2%, with the lowest value observed in CT3. Vitamin C content was highest in CT3, significantly different from the other treatments.

Previous studies have shown that organic amendments or proper N management generally improve quality parameters such as total sugar, vitamin C, and lycopene in tomato fruits, though the extent of improvement depends on the source and timing of fertilizer application [31]. Ronga et al. (2020) [6] also reported that appropriate N rates optimize both yield and biochemical compound accumulation, whereas excessive N may dilute organic compounds in the fruit.

Residual nitrate content in tomato fruits ranged from 100.7 mg/kg to 110.3 mg/kg, which is within the safe limit recommended by the Ministry of Health (maximum limit for tomatoes: 150 mg/kg). Differences in NO_3^- content among the fertilizer treatments were not statistically significant. The levels of Pb and Cd, two heavy metals that must be controlled in safe cultivation under VietGAP standards, were also within safe limits (Table 10).

Table 10. Effects of inorganic fertilizer treatments on food safety quality parameters of off-season tomato fruits

Treatment	NO_3^- content (mg kg-1)	Pb content (mg kg-1)	Cd content (mg kg-1)
CT1	100.7a	0.0422c	0.0122c
CT2	102.7a	0.0560b	0.0225a
CT3	110.3a	0.0647a	0.0175b

Note: Means followed by different letters in the same column are significantly different at $p < 0.05$; CT1: 120 kg N + 90 kg P_2O_5 + 120 kg K_2O; CT2: 150 kg N + 110 kg P_2O_5 + 150 kg K_2O; CT3: 180 kg N + 135 kg P_2O_5 + 180 kg K_2O; Pb and Cd indicators were compared according to the National Technical Regulation on maximum levels of heavy metals contamination in food [32].

Although nitrate content slightly increased with higher N rates, all values remained within the permissible limits. This finding is consistent with previous studies indicating that proper management of fertilizer rates and timing is key to minimizing nitrate residues in produce [7].

4. CONCLUSION

Increasing the inorganic fertilizer rate resulted in the highest growth, development, and physiological parameters at 180 kg N + 135 kg P_2O_5 + 180 kg K_2O (CT3), with significant differences compared to the other treatments. The inorganic fertilizer rate 180 kg N + 135 kg P_2O_5 + 180 kg K_2O also achieved the highest actual yield, although the difference was not significant compared to the lower rate in 150 kg N + 110 kg P_2O_5 + 150 kg K_2O (CT2). Regarding quality parameters, 180 kg N + 135 kg P_2O_5 + 180 kg K_2O produced the highest Brix and total solids content, while nitrate, Pb, and Cd levels remained within the safe limits according to regulations. Notably, vitamin C content was highest in CT3, with significant differences from the other treatments. Therefore, the fertilizer regime of CT3: 180 kg N + 135 kg P_2O_5 + 180 kg K_2O is recommended for off-season cultivation of the Savior tomato variety under safe production standards in Van Son commune, Tan Lac district, Hoa Binh province (now Van Son commune, Phu Tho province).

ACKNOWLEDGMENTS

This research was supported by the project: "Research on the development of some off-season safe and organic vegetables with high economic efficiency in several highland communes of Tan Lac district, Hoa Binh province" The authors sincerely thank the People's Committee of Hoa Binh province and the Department of Science and Technology of Hoa Binh Province for providing the funding that made this study possible.

REFERENCES

1. Nguyen, T. T., Tran, V. Q. & Pham, H. T. (2021). Effects of cropping season and NPK

fertilizer rates on growth and yield of tomato in the Red River Delta, Vietnam. *Vietnam Journal of Agricultural Science*, 19(2), 35 - 42.

2. Zhang, H., Zhang, Z., Xiong, Y., Chen, J. & Zhang, D. (2021). High temperature effects on tomato reproductive growth and fruit set. Journal of Integrative Agriculture, 20(3), 789 - 798. https://doi.org/10.1016/S2095-3119(20)63370-3.

3. Paudel, M. N., Poudel, M. P. & Thapa, R. B. (2021). Constraints and opportunities of off-season tomato production in Nepal. *Journal of Agriculture and Food Research*, 4, 100153. https://doi.org/10.1016/j.jafr.2021.100153.

4. Tan Lac District People's Committee, Hoa Binh province (2020). Land Use Planning Report.

5. Ministry of Agriculture and Rural Development (2017). Good Agricultural Practices (VietGAP) for safe fresh vegetables and fruits. Hanoi, Vietnam.

6. Ronga, D., Zaccardelli, M., Lovelli, S., Perrone, D., Francia, E., Milc, J. A. & Pecchioni, N. (2020). Optimizing nitrogen fertilization to improve yield and quality of tomato. *Scientia Horticulturae*, 261, 108941. https://doi.org/10.1016/j.scienta.2019.108941.

7. Mao, X., Liu, J., Zhang, J., Wang, X. & Zhou, Y. (2024). Yield, quality, and nitrogen leaching of open-field tomato under different nitrogen rates. Plants, 13(3), 541. https://doi.org/10.3390/plants13030541.

8. Cheng, M., Li, T., Chen, J., Chen, Y. & Wang, X. (2021). Effects of nitrogen supply on tomato yield, water use efficiency and fruit quality: A meta-analysis. *Agricultural Water Management*, 250, 106843. https://doi.org/10.1016/j.agwat.2021.106843.

9. Li, C., Zhang, J., Gao, X., Li, Y. & Liu, Z. (2022). Integrated crop-nitrogen management improves tomato yield and reduces residual nitrate. *Agronomy*, 12(3), 521. https://doi.org/10.3390/agronomy12030521.

10. Nguyen Nhu Ha (2010). Fertilizer Textbook. Hanoi: Vietnam National University of Agriculture Publishing House.

11. Hanoi Department of Agriculture and Rural Development (2010). Technical Guidelines for Safe Vegetable Production. Decision No. 577/QĐ/SNN-TT dated May 10, 2010.

12. Sector Standard 10 TCN 452:2001. Plant analysis - Methods for determination of nitrate and nitrite contents.

13. Vietnamese Standard TCVN 6427-2:1998. Fruits and vegetables and their products - Determination of ascorbic acid content - Part 2: Titrimetric method.

14. Ministry of Science and Technology (2007). TCVN 5714:2007: Tea - Determination of crude fiber content. Hanoi: Vietnamese National Standard.

15. Vietnamese Standard TCVN 4594:1988. Sugarcane - Methods for determination of total sugar, reducing sugar, and sucrose content.

16. Vietnamese Standard TCVN 7768-1:2007. Fruits, vegetables and their products - Determination of cadmium content - Part 1: Atomic absorption spectrometric method using graphite furnace.

17. Vietnamese Standard TCVN 7768-1:2007. Fruits, vegetables and their products - Determination of cadmium content - Part 1: Atomic absorption spectrometric method using graphite furnace.

18. Vietnamese Standard TCVN 6194:1996. Water quality - Determination of chloride - Silver nitrate titration with chromate indicator (Mohr's method).

19. Vietnamese Standard TCVN: 6193: 1996. Water quality - Determination of cobalt nickel, copper, zinc, cadmium, and lead Flame atomic absorption spectrometric methods.

20. Vietnamese Standard TCVN 6187-2:1996. Water quality - Detection and enumeration of organisms thermotolerant coliform organisms and presumptive Escherichia coli. Part 2: Multiple tube (most probable number) method.

21. Vietnamese Standard TCVN 5738-2:2005 (ISO 10381-2:2002). Soil quality - Sampling - Part 2: Guidance on sampling techniques.

22. Vietnamese National Standard TCVN 5979:2007 (ISO 10390:2005). Soil quality - Determination of pH.

23. Vietnamese Standard TCVN 8568:2010. Soil quality- Method for determination of cation exchange capacity (CEC) by ammonium acetate method

24. Vietnamese National Standard TCVN 9294:2012. Fertilizers - Determination of total organic carbon by the Walkley-Black method.

25. Vietnamese Standard TCVN 6498:1999 (ISO 11261:1995). Soil quality - Determination of total nitrogen - Modified Kjeldahl method.

26. Vietnamese National Standard TCVN 8940:2011. Soil quality - Determination of total phosphorus - Colorimetric method.

27. Vietnamese National Standard TCVN 8660:2011. Soil quality - Determination of total potassium.

28. Vietnamese National Standard TCVN 6496:2009 (ISO 11047:1998). Soil quality - Determination of cadmium, chromium, cobalt, lead, copper, nickel, manganese, and zinc in soil extracts - Flame and electrothermal atomic absorption spectrometric methods.

29. Ministry of Natural Resources and Environment (2015). QCVN 08-MT:2015/BTNMT. National technical regulation on surface water quality.

30. Ministry of Natural Resources and Environment (2015). QCVN 03-MT:2015/BTNMT. National technical regulation on permissible limits of heavy metals in soil.

31. Gao, F., Li, H., Mu, X., Gao, H., Zhang, Y., Li, R., Cao, K. & Ye, L. (2023). Effects of organic fertilizer application on tomato yield and quality: A meta-analysis. *Applied Sciences*, 13(4), 2184. https://doi.org/10.3390/app13042184.

32. Ministry of Health (2011). QCVN 8-2:2011/BYT. National technical regulation on maximum levels of heavy metal contamination in food.

RESULTS OF AN UNDERPLANTING TRIAL WITH TWO NATIVE TREE SPECIES *T. javanica* AND *E. fordii* IN *Acacia* hybrid PROTECTION PLANTATIONS IN QUANG TRI PROVINCE

Truong Quang Tri[1,*], Ha Van Nam[1], Ta Van Han[1], Nguyen Van Khanh[2]

[1]*Research Institute for Forest Ecology and Environment, Vietnamese Academy of Forest Sciences*

[2]*Quang Trach Protection Forest Management Board*

** Email: quangtri1vfu@gmail.com*

ABSTRACT

This study was conducted to assess the growth of two native tree species planted under the canopy of *Acacia* hybrid plantations in Quang Tri province and Hue city. It provides the basic for selecting appropriate species to establish a model of converting monoculture *Acacia* hybrid plantation forest into mixed native forest in Quang Tri province. The ealier survey had identified eleven native tree species planted under the canopy of plantation forest within the study area. Among these, two species (*E. fordii* and *T. javanica* Blume) were selected for underplanting experiment in *Acacia* hybrid canopies at two different canopy closure levels (0.3 - 0.4 and 0.5 - 0.6, respectively). After 2 years of planting, *E. fordii* demonstrated a survival rate of 90.4 - 92.3%, while *T. javanica* showed a lower, rate of 88.0 - 91.3%. Both species showed greater diameter at ground level (D_{00}) and total height (Hvn) growth under the 0.3 - 0.4 canopy closure compared with the 0.5 - 0.6 canopy level. Within the 0.3 - 0.4 canopy condition, *E. fordii* achieved the average D_{00} of 1.55 cm and Hvn of 1.35 m, whereas *T. javanica* recorded as of 1.45 cm 1.25 m, respectively. The chlorophyll *a/b* ratio < 2.3 indicated that both species exhibit shade tolerance during the early growth stages, with *E. fordii* showing a higher degree of shade tolerance than that of *T. javanica*. The findings suggested that maintaining a closure level of 0.3 - 0.4 in the second year would be an appropriate silvicultural measure, facilitating optimal growth of underplanted native species in the process of converting *Acacia* hybrid plantations into mixed native forests.

Keywords: *Plantation forest, native trees, canopy closure, chlorophyll, Quang Tri province, underplanting.*

Received: 12 August 2025; revised: 16 October 2025; accepted: 3 December 2025.

1. INTRODUCTION

The North Central and South-Central Coastal regions of Vietnam together cover an area of 5,649,651 ha of forest, including 3,778,853 ha of natural forests and 1,870,798 ha of plantations, with forest cover reaching 54.23% [1]. Although forest areas and cover have increased markedly in recent years, the overall forest quality remains low: Much of the natural forest area is degraded, valuable timber species are scarce, natural regeneration is weak, and growth rate is slow.

Protection forests play a particularly important role in the North Central region by protecting watershed, reducing erosion, regulating water and conserving biodiversity. However, for many years, protection forests have been established predominantly as monoculture plantation forests - particularly *Acacia* hybrid and *Pinus massoniana* and *Pinus latteri*, which has revealed several limitations.

Monoculture Acacia plantations are easy to establish and fast - growing, but their single - layered canopies have low ecological resilience. Understory vegetation and biodiversity are poor, soil - erosion protection is suboptimal and the ecosystem is prone to degradation. Pest and

disease outbreaks are more likely, particularly under increasingly extreme weather. In some areas, serious diseases have been widespread, e.g., *Phanerochaete* sp. and heart rot in Acacia, reducing timber value and increasing fallen risk.

These issues degrade both productivity and protective function and lead to economic losses from premature stand failure. Sustainable forest development is therefore essential to conserve biodiversity, stabilize the environment, and enhance the protective functions of forests. Compared to monoculture forest, underplanting broadleaved native species under plantation forest canopy can reduce fire and pest outbreak risk, improve stand structural complexity and plant - community composition and enhance protective and carbon-sequestration functions. This approach can also mitigate erosion and landslides and increase resistance to windstorms and climate change, thereby pushing the forest ecosystem toward conditions approaching natural tropical forests and providing a foundation for sustainable forestry.

In recent years, some localities in the Central region have developed native tree planting under the canopy of monoculture Acacia and Pine plantations, with initial remarkable results. According to data from the Hue Forest Protection Department, the area of native tree planted under the Acacia and Pine forests was 586.22 ha; in which Quang Tri accounts for 3,082.04 ha, respectively with popular species including *E. fordii, Hopea odorata, Dipterocarpus alatus, Parashorea chinensis*, etc. Although underplanting under Acacia has been implemented, there has been little systematic research to identify which native species are suitable to local's specific site conditions, canopy - closure levels and planting methods. As a result, scaling up underplanting under monoculture Acacia forests remains challenging and lacks a firm scientific basis.

Moreover, native species differ in their adaptability and growth rate across sites, as well as in their tolerance capable of adverse environmental conditions and their growth dynamics change across space and time. Therefore, study on the growth of native tree species on different types of sites and specific planting techniques is necessary, providing a scientific basis for selecting appropriate tree species and planting techniques on each site condition, contributing to accelerating forest development towards sustainable development, meeting economic, environmental and social requirements in the North Central region.

2. STUDY MATERIAL AND METHODOLOGY

2.1. Study materials, timeframe and sites

2.1.1. Study materials

Native tree species underplanted in *Acacia* hybrid and *Pinus massoniana* plantations.

2.1.2. Study timeframe and sites

- Growth performance of native species underplanted in selected plantations has been monitored since 2023 in the North Central region, particularly in Trung Thuan commune and Dong Son ward, Quang Tri province; Chan May - Lang Co commune and Thuy Bang ward, Hue city.

- Research on the cultivation of two native tree species models, *E. fordii* and *T. javanica*, was conducted in Trung Thuan commune, Quang Tri province during the period of 2023 - 2025.

2.2. Study content and methodology

2.2.1. Study content

- Evaluation of growth of two selected native species underplanted in plantations some North Central provinces.

- Species selection and research on techniques for planting native tree species under the canopy of monoculture protection forests of *Acacia* hybrid in Quang Tri province.

2.2.2. Methodology

- Evaluate growth of selected native species underplanted in plantations:

+ Data collection: Data and information on site characteristics, afforestation and forest protection programs and projects in Quang Tri province and Hue city, forest status maps, forest planting design maps, etc, were collected from trustful sources.

+ Field survey: Sample plots were established to measure and monitor growth rates of native tree species planted in the study area.

Survey was conducted on native tree planted under pine and acacia forest canopy in Quang Tri province and Hue city to select points for establishing sample plots (OTC). The area of each OTC was from 500 - 1,000 m^2 (25 m x 20 m or 50 m x 20 m), ensuring that each OTC had a large sample capacity ($n \geq 30$ native trees/OTC). In total, 12 OTCs were surveyed in the 2 provinces. In each OTC, the following indicators were measured:

* Canopy closure, elevation, slope, species, year of planting, initial density (if known), current density, and survival rate.

* Diameter at breast height ($D_{1.3}$) or stump diameter (D_{00} - for small trees), Total height (H_{vn}) and height to crown base (H_{dc}), crown diameter (Dt).

+ Soil characteristics of the planting sites: On each OTC, one soil profile was excavated at the OTC center to describe soil depth, color, rock fragments, compaction and mechanical component.

- Species selection and research on techniques for planting native species under *Acacia* hybrid plantations in Quang Tri province:

Species selection: From the survey results, growth, survival rate and adaptability were assesed to select suitable native tree species for planting under plantation canopy in Quang Tri province and Hue city. From the list of selected tree species, 2 species with the best growth and adaptability, *T. javanica* Blume and *E. fordii* were chosen to develope a model of planting under the canopy of monoculture *Acacia* hybrid protection forests in Quang Tri province, with an experiment of 2 treatmentss on different canopy closure levels, including:

+ Treatment 1 (TN1): Canopy closure of 0.3 - 0.4.

+ Treatment 2 (TN2): Canopy closure of 0.5 - 0.6.

Each experimental area covered an area of 0.5 ha, with a density of 832 trees/ha, including 4 replications. *E. fordii* was planted alternately with *T. javanica* in each replication. To ensure that the canopy coverage was achieved according to the teatment and maintained throughout the monitoring period, Acacia trees were selectively thinned over the entire area before planting and after one year of planting. The canopy closure after thinning was checked through taking foliage photos.

Growth data (D_{00}, H_{vn}) were collected annually in the first 2 years. Shade tolerance was assessed in the second year through leaf chlorophyll content analysis according to the Grodzinxki method (1981), leaf samples were taken from the middle layer of the canopy in 4 directions East - West - South - North, 12 - 15 leaves/sample, 1 sample/tree x 3 trees/species x 2 species x 2 experiments = 12 samples.

2.2.3. Data analysis

Excel statistical processing software was used according to the instructions of Nguyen Hai Tuat *et al.* (2002) [2].

Student's t-test was used to compare D_{00} and Hvn of the two species across treatments on SPSS statistical software. Effect Size was calculated using Cohen's d coefficient to evaluate the level and practical significance of the observed difference between the two treatments.

3. RESULTS AND DISCUSSION

3.1. Evaluate growth of several native species planted under plantation forest canopies in some North Central provinces

3.1.1. Climatic characteristics of the study site

Table 1. Climatic characteristics of the area where native trees are grown under plantation forest canopy in the study area

No.	Indicator	Quang Tri province		Hue city	
		Trung Thuan	Dong Son	Thuy Bang	Chan May – Lang Co
1	Temperature (T)				
	Mean T (°C)	25	24.4	25.1	24.5
	Maximum T (°C)	40	40.6	41.3	41

	Minimum T (°C)	10	7.8	7.7	9
2	Rainfall (P)				
	Mean annual rainfall (mm/year)	2,100 - 2,500	2,100 - 2,600	2,500 - 2,800	2,400 - 2,900
	Months with rainfall ≥ 100 mm	3 - 6	3 - 6	4 - 6	4 - 7
3	Mean annual relative humidity (W; %)	80 - 84	83 - 86	82 - 85	80 - 90

Source: Data reported by local Protection Forest Management Boards

Table 1 showed that: In Trung Thuan commune Dong Son ward, the average annual temperature (T) was from 24.4 - 25^{0}C, the average annual humidity (W) was from 80 - 86%, the average annual rainfall (P) was from 2,100 - 2,600 mm/year, the number of months with rainfall ≥ 100 mm was from 3 - 6 months/year. Meanwhile, in Chan May - Lang Co commune, Thuy Bang ward, Hue city, T from 24.5 - 25.1^{0}C, W from 80 - 90%, P from 2,400 - 2,900 mm/year, the number of months with rainfall ≥ 100 mm was from 4 - 7 months/year. Thus, in all areas, the average T was from 24.4 - 25.1^{0}C, W was from 80 - 90% and rainfall was 2,100 - 2,900 mm/year, the number of months with rainfall ≥ 100 mm was from 3 to 7 months in a year.

Thus, at 4 survey positions, the climatic conditions were quite similar, with average temperature, rainfall and high annual air humidity suitable for the biological characteristics of many native tropical plants.

3.1.2. Terrain and soil characteristics

Table 2. Terrain and soil characteristics of the area where native trees are grown under plantation forest canopy in the study area

Forest type	Sample	Absolute height (m)	Soil profile thickness (cm)	Mixed rock ratio (%)	Compactness	Mechanical composition	Color by depth layer (cm)		
							0 - 20	21 - 40	41 - 70
Acacia hybrid	QT-1	102	68	31	Tight	Loam	Yellowish brown	Yellow	Yellow
	QT-2	110	72	35	Tight	Loam	Light brown	Yellow	Yellow
	QT-3	115	65	37	Tight	Loam	Yellowish brown	Yellow	Yellow
Pinus masso-niana	QT-4	131	56	38	Tight	Silt loam	Brown	Brown	Yellow
	QT-5	135	62	43	Tight	Silt loam	Yellowish brown	Yellow	Yellow
	QT-6	125	65	38	Tight	Silt loam	Yellow	Yellow	Yellow
Pinus latteri	H-1	75	55	46	Tight	Loam	Yellowish red	Yellow	Yellow
	H-2	60	60	50	Tight	Loam	Yellowish red	Yellow	Yellow
	H-3	58	58	43	Tight	Loam	Yellowish red	Light yellow	Yellow
Acacia hybrid	H-4	145	63	40	Tight	Loam	Yellowish brown	Gray	Yellow
	H-5	155	70	32	Tight	Loam	Yellowish brown	Yellow	Yellow
	H-6	150	73	30	Tight	Loam	Brown	Yellowish brown	Light yellow

Note: QT - Quang Tri; H - Hue.

Table 2 reflected the clear differences in site quality among the plantation models. In general, soil under Acacia canopy had more favorable conditions for the development of native trees thanks to its relatively thick profile, low rock content and suitable mechanical composition,

which helps retain moisture and create better root development space. In contrast, soil under Pine canopy showed typical limitations of feralit soil group on acid rocks: thinner soil profile, high rock content and low moisture and nutrient retention capacity, reducing the suitability for growing native trees.

The characteristic of soil color gradually changing from yellowish-brown to yellow in deep layers showed the strong weathering and leaching of materials common in humid tropical climates, contributing to the reduction of natural soil fertility.

Compared with the site suitability classification of Ngo Dinh Que (2015) [3], the models under the canopy of Acacia generally belong to the very suitable group (S1) thanks to favorable site conditions. On the contrary, the models under the canopy of *Pinus massoniana* were at less favorable level due to thin soil profile and high rock content, while the models under the canopy of *Pinus latteri* were mostly unfavorable because of dry soil, limited soil profile and high rock content.

3.1.3. Growth characteristics of the upper tree layer

Table 3. Growth characteristics of upper tree layer where native trees are grown under the plantation forest canopy in the study area

Loca-tion	Forest type	OTC	Current density (trees /ha)	Age	$D_{1.3}$ (cm)		Hvn (m)		Canopy closure
					Xtb	S%	Xtb	S%	
Quang Tri province	*Acacia* hybrid	QT-1	820	6	17.6	16.0	14	8.4	0.65
		QT-2	825	8	18.0	14.3	13.9	8.1	0.72
		QT-3	815	8	18.2	14.9	13.9	8.3	0.60
	Pinus masso-niana	QT-4	515	26	36.0	5.3	18.2	3.4	0.58
		QT-5	525	26	36.6	5.0	18.3	3.8	0.62
		QT-6	521	26	36.5	5.1	18.3	3.8	0.60
Hue city	*Pinus latteri*	H-1	750	39	30.8	7.8	19.8	4.0	0.50
		H-2	748	39	30.8	7.1	19.9	3.7	0.56
		H-3	760	39	31.3	7.4	19.6	3.5	0.48
	Acacia hybrid	H-4	1890	12	24.8	16.6	16.4	4.7	0.65
		H-5	475	19	25.3	4.1	18.1	5.9	0.60
		H-6	460	19	25.5	4.1	18.2	6.0	0.58

Survey results showed that in Quang Tri province, Pine and Acacia species grew at an medium rate. Acacia density ranged from 815 to 825 trees/ha while Pine from 515 - 521 trees/ha. After 6 - 8 years, Acacia reached the following growth indicators: average $D_{1.3}$ 36.0 - 36.6 cm, Hvn 18.2 - 18.3 m. After 26 years of growth, *Pine* reached: average $D_{1.3}$ from 17.6 - 18.2 cm, Hvn 13.9 - 14 m. The fluctuations in diameter, height and canopy diameter of both Acacia and Pine were low to medium.

In Hue, the density of Pine was 748 - 760 trees/ha, after 39 years the growth indicators were as follows: $D_{1.3}$ ranged from 30.8 - 31.3 cm, Hvn from 19.6 - 19.9 m. As for Acacia, the density had a clear difference between the two age groups: Age

12 had a density of 1,890 trees/ha while at age 19 the remaining density reached 460 - 475 trees/ha. However, the growth of 12 and 19-years old Acacia trees in Hue city showed no difference: Average diameter 24.8 - 25.5 cm, Hvn 16.4 - 18.2 m.

In general, the tree species were growing and developing as normal, the coefficients of variation of diameter, height and canopy diameter remained relatively stable, in addition to the site factor in the growing areas of Acacia and Pine, it depended heavily on the application planting and tending techniques, particularly Acacia trees in these two areas.

The canopy closure of Acacia in the two provinces reached from 0.58 - 0.72, remaining at a higher level compared to that of Pine which ranged 0.48 - 0.62.

The remaining tree density and canopy closure of plantation forests posed a great impact on the growth and development of native tree species planted under the canopy.

3.1.4. Growth characteristics of the native tree species

The results of growth assessment of native tree species under plantations in the study sites were summarized in table 4.

Table 4. Growth characteristics of native tree species planted under forest canopy in the study area

Loca-tion	Forest type	OTC	Spe-cies	Age	Planting density (trees /ha)	Current density (trees /ha)	Sur-vival rate	$D_{1.3}$ (cm)			Hvn (m)			Dt (m)	
								Xtb	$\Delta D_{1.3}$ (cm/ year)	S%	Xtb	ΔHvn (m/ year)	S%	Xtb	S%
Quang Tri province	*Acacia* hybrid	QT-1	Ef	6	500	460	92.0	6.5	1.1	16.8	7.4	1.2	24.7	3.1	24.4
		QT-2	Ef	8	550	515	93.6	6.2	0.8	23.5	7.5	0.9	23.8	3.0	28.5
		QT-3	Tj	6	550	472	85.8	9.6	1.6	16.7	5.6	0.9	17.9	3.2	15.5
	Pinus masso-niana	QT-4	Ef	6	500	442	88.4	8.5	1.4	12.9	3.9	0.7	3.5	2.8	6.5
		QT-5	Ef	6	500	460	92.0	8.2	1.4	12.8	3.8	0.6	3.5	2.7	7.0
		QT-6	Ef	6	500	455	91.0	8.0	1.3	13.2	3.6	0.6	3.6	2.7	7.8
Hue city	*Pinus latteri*	H-1	Lf	7	100	85	84.0	9.4	1.4	7.8	8.4	1.2	2.5	3.6	2.0
			Tj	7	100	80	80.0	6.8	1.0	3.8	5.9	0.8	3.3	2.9	2.6
			Pp	7	100	78	78.0	5.6	0.8	15.4	4.8	0.7	12.9	1.9	10.2
		H-2	Mm	7	100	76	76.0	7.4	1.1	5.6	6.5	0.9	7.2	2.2	3.0
			Sz	7	100	86	86.0	10.5	1.5	3.7	11.3	1.6	1.6	3.3	3.8
			Ef	7	100	82	82.0	5.9	0.8	8.1	5.1	0.7	4.9	2.1	12.2
		H-3	Cb	7	100	84	84.0	10.7	1.5	2.8	8.4	1.2	2.1	3.8	5.1
			Vk	7	100	70	70.0	4.6	0.7	4.1	6.3	0.9	11.6	1.8	9.3
			Pa	7	100	86	86.0	6.3	0.9	4.3	3.8	0.5	10.9	3.5	5.5
	Acacia hybrid	H-4	Ef	8	700	620	88.5	9.3	1.2	30.9	6.8	0.9	7.8	2.8	18.7
			Ho	8	700	612	87.4	6.2	0.8	14.3	5.6	0.7	5.0	2.4	8.8
		H-5	Ef	8	266	242	93.0	6.9	0.9	30.4	5.5	0.7	13.6	2.0	31.6
			Ct	8	266	236	90.0	6.2	0.8	8.4	5.3	0.7	2.6	1.8	5.5
			Tj	8	266	238	91.5	17.4	2.2	8.8	11.6	1.5	5.3	5.1	9.9
		H-6	Ef	8	266	235	90.4	6.8	0.8	29.2	5.5	0.7	13.9	2	29.7
			Ct	8	266	218	83.8	6.5	0.8	8.3	5.3	0.7	2.4	1.7	7.2
			Tj	8	266	220	84.6	17.0	2.1	9.4	11.4	1.4	6.7	5	10.6

Note: Ef: E. fordii; Tj: T. javanica Blume; Mm; Michelia mediocris Dandy; Vk: Vatica tonkinensis A. Chev.; Ho: Hopea odorata; Cb: Cinnamomum bejolghota; Lf: Lithocarpus fissus Champ ex Benth; Pp: Peltophorum pterocarpum; Sz: Syzygium zeylanicum (L.) DC.; Pa: Prunus arborea; Ct: Chukrasia tabularis A. Juss.

** In Quang Tri province*

The survival rate of the species was fairly high, ranging from 85.8 - 93.6%. Of which, 6-year-old *E. fordii* planted under Acacia forest canopy achieved the highest rate of 93.6%

The growth of *E. fordii* under Acacia forest canopy was surveyed at QT-1, QT-2 at age 6: $D_{1.3}$ from 6.2 - 6.5 cm, Hvn from 7.4 - 7.5 m, Dt from 3.0 - 3.1 m. The growth of 6-year-old *T. javanica* under Acacia forest canopy was evaluated at QT-3: $D_{1.3}$ reached 5.6 cm, Hvn 7.9 m, Dt 3.2 m. It can be seen that the growth of these two species was relatively good, the fluctuations of the indicators were at medium level.

The growth of *E. fordii* under pine forest canopy was observed at QT-4, QT-5 and QT-6 at the age 6. The growth indicators were specifically evaluated as follows: $D_{1.3}$ from 8.0 - 8.5 cm, Hvn from 3.6 - 3.9 m, Dt reached 2.7 - 2.8 m. The growth of the species under pine forest canopy

was quite good, but the height was lower than that of planted trees at the same age under the Acacia forest canopy.

** In Hue city*

Native trees planted under the canopy of monoculture pine and Acacia protection forests were diverse and showed positive results. Popular planted native trees under the canopy included: *Lithocarpus fissus*, *Peltophorum pterocarpum*, *Tarrietia javanica*, *E. fordii*, *Michelia mediocris*, *Vatica tonkinensis*, *Hopea odorata, Cinnamomum bejolghota*, *Syzygium zeylanicum*, *Prunus arborea*, *Chukrasia tabularis*.

The survival rate of native tree species ranged from 70.0 - 93.0%. In which, the highest survival rate belonged to 8-year-old *E. fordii* planted under Acacia forest canopy and the lowest was 7-year-old *Vatica tonkinensis* planted under pine forest canopy.

The growth of some species planted under the canopy of Acacia forest was surveyed at H-4, H-5 and H-6 at age 8 as follows:

- *E. fordii*: $D_{1.3}$ from 6.8 - 9.3 cm, Hvn 5.5 - 6.8 m, Dt 2.0 - 2.8 m. The growth of the species after 8 years of planting was quite good. The fluctuation of the indexes was at average level.

- *Chukrasia tabularis*: $D_{1.3}$ at 6.2 - 6.5 cm, Hvn at 5.1 - 5.3 m, Dt 1.7 - 1.8 m. The growth of the species after 8 years of planting was quite good. The fluctuation of the growth indexes was at a low level, showing high growth uniformity.

- *Hopea odorata*: $D_{1.3}$ at 6.2 cm, Hvn 5.6 m, Dt 2.4 m. The growth of this species after 8 years of planting was quite good. The fluctuation index of the indexes is at an average level.

- *Tarrietia javanica*: $D_{1.3}$ at 17.0 - 17.4 cm, Hvn 11.4 -11.6 m, Dt 5.0 - 5.1 m. After 8 years of planting the species grew very well. Some indicators such as diameter and height were almost double that of the two species *Chukrasia tabularis* and *E. fordii*. Showing the suitability and development of *T. javanica* here, it was tending to rise to the upper layer to replace a part of the Acacia trees that had past maturity and were drying out or dying.

Growth of some 7-year-old native tree species planted under the canopy of pine forest: *Michelia mediocris*, *Syzygium zeylanicum*, *E. fordii*, *Cinnamomum bejolghota*, *Vatica tonkinensis*, *Prunus arborea, Tarrietia javanica, Lithocarpus fissus* were as follows: $D_{1.3}$ of the species was from 4.6 - 10.7 cm in which *Cinnamomum bejolghota* had the largest figure while *Vatica tonkinensis* had the lowest one; Hvn was from 3.8 - 11.3 m in which the highest was found in *Syzygium zeylanicum*, the lowest was in *Prunus arborea*; Dt was from 1.8 - 3.8 m in which the largest was *Cinnamomum bejolghota*, the smallest was *Vatica tonkinensis*.

In 11 native tree species investigated and evaluated. Native trees planted under the canopy of Acacia forest: 8-year-old *E. fordii* in Quang Tri province and 8-year-old *T. javanica* in Hue city had the highest survival rate of 91.5 - 93.6%, besides, the growth of the latter in Hue was also superior compared to other tree species in the same conditions (1.5 - 2 times higher). For native tree species planted under the canopy of Pine forest: *E. fordii* in Quang Tri province; *Prunus arborea*, *Cinnamomum bejolghota* and *Syzygium zeylanicum* in Hue city were the 3 species with the highest survival rate of 85 - 86%. According to the general assessment of growth indicators of diameter and height, the 2 species with the ability to develop outstandingly were *Cinnamomum bejolghota* and *Syzygium zeylanicum*.

3.2. Species selection and research results on techniques for planting native tree species under the canopy of monoculture protection forests of *Acacia* hybrid in Quang Tri province

3.2.1. Species selection for developing forest conversion model

Through the results of growth assessment and site conditions in content 3.1, it could be seen that:

Among the 11 species of trees surveyed, 5 tree species with the best survival and growth rates, adapting to different canopy levels are: *E. fordii*, *Tarrietia javanica*, *Prunus arborea*, *Cinnamomum bejolghota*, *Syzygium zeylanicum*

Among the 5 identified tree species, 2 with the widest adaptability to site conditions in the 2 provinces, *E. fordii* and *Tarrietia javanica*, were selected to establish a model of planting under the canopy of Acacia forest in Quang Tri province for futher asessement.

3.2.2. Results of establishing a model to convert monoculture plantation forests to mixed forests of native trees after 2 years in Quang Tri province

Table 5. Growth of *E. fordii* and *T. javanica* planted under Acacia forest canopy in Quang Tri province

Species	Canopy closure	1 year after planting					2 years after planting				
		Survival rate (%)	D_{00} (cm)		Hvn (m)		Survival rate (%)	D_{00} (cm)		Hvn (m)	
			Xtb	ΔD_{00} (cm/year)	Xtb	ΔHvn (m/year)		Xtb	ΔD_{00} (cm/year)	Xtb	ΔHvn (m/year)
E. fordii	0.3 - 0.4	93.3	0.99	0.28	0.76	0.31	92.3	1.65	0.67	1.36	0.59
	0.5 - 0.6	92.8	0.97	0.24	0.73	0.27	90.4	1.51	0.55	1.25	0.52
P-value			0.36		0.007			0.007		<0.001	
Effect size			0.09		0.27			0.56		0.48	
Tarrietia javanica	0.3 - 0.4	92.3	0.88	0.22	0.65	0.24	91.3	1.50	0.62	1.20	0.55
	0.5 - 0.6	90.4	0.86	0.23	0.62	0.21	88.0	1.40	0.54	1.06	0.45
P-value			0.20		0.03			<0.001		<0.001	
Effect size			0.13		0.22			0.63		0.98	

The results of the growth measurement of 2-year-old *E. fordii* and *T. javanica* planted under the canopy of Acacia protection forests at different canopy levels of 0.3 - 0.4 and 0.5 - 0.6 in Quang Tri province were summarized in table 5.

After 2 years, the two species planted under monoculture Acacia protection forest canopy with 2 canopy levels of 0.3 - 0.4 and 0.5 - 0.6 showed differences in some growth indicators and characteristics, as follows:

3.2.2.1. E. fordii

Under canopy closure of 0.3 - 0.4: After 1 year of planting, the survival rate was 93.3%, slightly decreased in the second year but maintained a very high level of 92.3%.

After 1st year, D_{00} reached 0.98 cm corresponding to a diameter growth of 0.28 cm/year, the average Hvn reached 0.76 m corresponding to a height growth of 0.31 m/year

After 2nd year, the average D_{00} reached 1.65 cm corresponding to a diameter growth of 0.67 cm/year, the average Hvn reached 1.35 m or a growth rate of 0.59 m/year.

Under canopy closure of 0.5 - 0.6: After year 1st, the survival rate was 92.8%, slightly decreased in the second year but still at a very high level of 90.4%.

At the same time, the average D_{00} reached 0.96 cm (diameter growth of 0.24 cm/year), the average Hvn reached 0.73 m, corresponding to a height growth of 0.27 m/year.

After 2 years, the average D_{00} reached 1.51 cm, corresponding to a diameter growth of 0.55 cm/year; the average Hvn reached 1.25 m (growth rate of 0.52 m/year). The t-test results (Student) showed that after one year of planting, the D_{00} growth of *E. fordii* was not statistically difference ($p > 0.05$); while Hvn, on the contrary, had a difference ($p < 0.05$). However, the average difference between the two treatments was only 0.03 m (0.73 m and 0.76 m), a small value with no biological meaning. This difference was within the range of natural fluctuations, reflected in a small statistical effect (Cohen's d = 0.27). However, after two years, the difference in D_{00} and Hvn between the two treatments was significant ($p < 0.05$), the

effect size was high (Cohen's d = 0.48 - 0.56) showing a difference with biological and practical significance, in which the growth of trees at a canopy closure of 0.3 - 0.4 was higher than at a canopy closure of 0.5 - 0.6. It can be seen that *E. fordii* planted in Quang Tri showed great potential with stable growth and development indexes. This indicated the suitability of this species to the site conditions. According to initial assessment, after 2 years of planting, the species had better growth and development under canopy closure of 0.3 - 0.4 than 0.5 - 0.6.

3.2.2.2. Tarrietia javanica

Under canopy closure of 0.3 - 0.4: After 1 year of planting, the survival rate of the species was 92.3%. In the second year, it decreased slightly to 91.3%.

At 1st year, the average D_{00} reached 0.88 cm (diameter growth of 0.22 cm/year), the average Hvn reached 0.65 m, corresponding to a height growth of 0.24 m/year.

After 2nd year, D_{00} reached 1.50 cm, corresponding to a diameter growth of 0.62 cm/year, Hvn reached 1.20 m, or a growth rate of 0.55 m/year.

Under canopy closure of 0.5 - 0.6: After 1st year, the survival rate of the species was 90.4% then decreased slightly to 88.0% after the 2nd year.

At year 1, D_{00} reached 0.86 cm, corresponding to a diameter growth of 0.23 cm/year, the average Hvn reached 0.61 m (height growth of 0.21 m/year).

After 2 years, the average D_{00} reached 1.40 cm, corresponding to a diameter growth of 0.54 cm/year, Hvn reached 1.06 m (growth rate of 0.45 m/year). This result was in-line with the the result published by Pham Xuan Dinh (2022) [4], *T. javanica* was the native tree species that had been planted widely in the Central Central region, especially in Quang Tri province, with Hvn growth from 0.6 - 0.9 m/year, $D_{1.3}$ from 0.7 - 1.0 cm/year, in which planting on bare land had the lowest growth rate, mixed planting and under poor forest canopy had better growth.

Figure 1. 2-year-old green *E. fordii* under canopy closure of 0.3 - 0.4

Figure 2. 2-year-old green *T. javanica* under canopy closure of 0.3 - 0.4

The t-test (Student) result showed that after one year, there was no statistically significant difference in D_{00} growth ($p > 0.05$). For Hvn, the difference was significant ($p < 0.05$); however, the average difference was only 0.03 m (0.65 m and 0.62 m), this small value has no biological significance, as shown by the low effect size (Cohen's d = 0.22). After two years, the difference in D_{00} and Hvn between the two treatments was clearly evident and had both statistical and biological significance ($p < 0.05$). Notably, the level of growth difference was large, as shown by the

high effect size (Cohen's d = 0.63 - 0.98). Tree growth at canopy closure 0.3 - 0.4 was superior to that at of 0.5 - 0.6.

General assessment of *E. fordii* and *T. javanica* showed that in the first year of planting, there was no difference or the difference was relatively small and had little biological significance in D_{00} and Hvn growth at 2 different canopy closure levels. However, in the second year, the effect of canopy closure became more evident when both species grew better at canopy level 0.3 - 0.4 compared to 0.5 - 0.6. This showed that in the second year, reasonable thinning techniques should be applied to the upper tree layer to adjust the canopy closure appropriately to ensure favorable light conditions for better tree growth.

3.2.3. Results of determining chlorophyll content of E. fordii and T. javanica

Leaves were very important part of plants where photosynthesis, water and gas exchange took place. In addition, leaves were also an indicator to determine the nutritional status as well as the suitability of plants to the external environment.

Chlorophyll a and b were pigments that play an important role in the photosynthesis process of vascular plants. However, chlorophyll content was an easily fluctuating index, depending on internal and external conditions, especially lighting regime. Chlorophyll content and chlorophyll a/b ratio indicated whether the plant was light-tolerant or shade-tolerant. The chlorophyll a/b ratio most clearly reflects the light-tolerant or shade-tolerant nature of the plant. According to the color comparison method of Lichtenthaler and Wellburn. (1983) [5], it was believed that light - tolerant plants had a chlorophyll a/b ratio greater than 3; neutral plants had a chlorophyll a/b ratio of about 2.3 - 3 and shade - tolerant plants had a chlorophyll a/b ratio less than 2.3.

The results of the analysis of chlorophyll a and b content in the leaves of *E. fordii* and *T. javanica* after two years of planting under the canopy of *Acacia* hybrid forest showed that the content of Chlorophyll a in the former ranged from 2.520 - 2.565 mg/g, Chlorophyll b from 4.212 - 4.591 mg/g, while in the latter it was 1.460 - 1.525 mg/g and 0.890 - 1.102 mg/g, respectively. Thus, the total chlorophyll content (TChl) of *E. fordii* (6.732 - 7.156 mg/g) was significantly higher than that of *T. javanica* (2.350 - 2.627 mg/g).

Table 6. Results of analysis of chlorophyll a, b content in *E. fordii* and *T. javanica* leaves in Quang Tri province after 2 years of planting

Species	Canopy closure	Chlorophyll content (mg/g)			a/b ratio
		Chl.a (mg/g)	Chl.b (mg/g)	Total a+b	
E. fordii	0.3 - 0.4	2.520	4.212	6.732	0.598
	0.5 - 0.6	2.565	4.591	7.156	0.559
T. javanica	0.3 - 0.4	1.460	0.890	2.350	1.640
	0.5 - 0.6	1.525	1.102	2.627	1.383

The a/b ratio of both species was < 2.3 (*E. fordii* 0.559 - 0.598; *T. javanica* 1.383 - 1.640), showing that both species belong to the group of shade-tolerant trees in the early stages, suitable for planting under the forest canopy at a certain shade level. The total chlorophyll content of *E. fordii* increased slightly when the shade level increased from 0.3 - 0.4 to 0.5 - 0.6, demonstrating the ability to adapt to low light conditions. This was also a physiological characteristic of shade -

tolerant species when increasing the total chlorophyll content to increase the ability to absorb low light. However, the growth results (Table 5) show that D_{00} and Hvn of this species at canopy closure of 0.3 - 0.4 were higher than at 0.5 - 0.6, demonstrating that although high canopy closure stimulated chlorophyll synthesis, it still limits actual photosynthesis due to reduced light intensity, reducing growth rate.

For *T. javanica*, the total chlorophyll content was lower but the a/b ratio was still < 2.3, showing that this species had a certain shade tolerance level but lower than *E. fordii*. The slight increase in Total a+b content when the canopy closure increased reflected an adaptive physiological response, but the amplitude of change was small, showing that the light demand of this species was higher.

The results showed that *E. fordii* was a shade-tolerant species at early stage, after 2 years there was no need to adjust the canopy closure in case the upper layer cannot be thinned. However, if conditions permit, adjusting the canopy closure to 0.3 - 0.4 would be optimal. *T. javanica* was moderately shade - tolerant, after 2 years it was recommended to reduce the canopy closure from 0.5 - 0.6 to about 0.3 - 0.4 to ensure the best growth of the tree. In the mixed planting model with both species, maintaining a uniform canopy closure at 0.3 - 0.4 after two years would be appropriate, meeting the ecological requirements of both species and improving the efficiency of converting *Acacia* hybrid forests into mixed forests of native trees.

4. CONCLUSION

Initial research results show that planting native trees *E. fordii* and *T. javanica* under *Acacia* hybrid forest canopy in Quang Tri province was feasible and had high prospects. These two tree species had a high survival rate (over 85%), grew stably in the site conditions in Quang Tri province, especially at a canopy of 0.3 - 0.4.

Both species showed shade-tolerant ability in the early stages, adapt well under the canopy of *Acacia* hybrid forest, with a fairly high growth rate. After two years, *E. fordii* reached an average diameter at ground level of 1.65 cm, height of 1.35 m; while these figures for *T. javanica* was 1.55 cm and 1.20 m, respectively. High total chlorophyll content, a/b ratio < 2.3 proved their shade-tolerant characteristics, suitable for intercropping or converting monoculture plantation forest to mixed forests.

The combined planting of *E. fordii* and *T. javanica* under Acacia forest canopy helped increase biodiversity, improved the structure and protection capacity of the forestand at the same time contributed to the restoration of the natural forest ecosystem. In particular, *T. javanica* was a fast - growing species with good coverage ability, while *E. fordii* developed stably and sustainably, creating a long-term foundation for mixed forests.

The research results were important scientific basis for selecting suitable native tree species and building mixed-species models, converting monoculture Acacia plantation forest in Quang Tri province in particular and the North Central region in general, towards the goal of sustainable forest development, enhancing ecological and economic values.

REFERENCE

1. Ministry of Agriculture and Environment (2025). *Decision No. 561/QD-BNNMT dated March 31, 2025 on the announcement of the national forest status in 2024.*

2. Nguyen Hai Tuat, Vu Tien Hinh, Ngo Kim Khoi (2002). *Instructions for using Excel software to process statistical data in forestry research.* Agriculture Publishing House, Ha Noi.

3. Ngo Dinh Que (2015). *Zoning of suitable site conditions for production forest planting (comprehensive research content).* Vietnamese Academy of Forest Sciences, Ha Noi.

4. Pham Xuan Dinh (2022). *Research on selecting varieties and techniques for intensive forest planting of T. javanica Blume to provide large timber in the North Central and South Central regions.* Summary report of the Ministry-level project, Forestry Science Center for North Central Vietnam.

5. Lichtenthaler, H. K., & Wellburn, A. R. (1983). *Determinations of total carotenoids and chlorophylls a and b of leaf extracts in different solvents. Biochemical Society Transactions,* 11(5), 591 - 592.

EFFECTS OF WATER TEMPERATURE AND FEEDING RATE ON BARRAMUNDI (*Lates calcarifer*) JUVENILE

Le Minh Hoang[1,*], Pham Phuong Linh[1],
Ngo Van Manh[1], Pham Duc Hung[1], Pham Quoc Hung[1]
[1]*Institute of Aquaculture, Nha Trang University*
[*]*Email: hoanglm@ntu.edu.vn*

ABSTRACT

The present study examined how temperature and feeding rate interact to influence survival rate, growth performance, respiration, and feeding ability in juvenile Barramundi (*Lates calcarifer*). Twenty-day-old fish were cultured for 28 days under three temperatures (30, 32 or 34˚C) combined with three feeding rates (50%, 75% or 100% of the recommended ration), followed by another 28 days of post-experimental recovery at 30˚C with a full feeding rate (100%). During the experimental stage, the survival rate varied between 69.0% and 94.0%, reaching its maximum at 30˚C with a full feeding rate (100%) and declining to the lowest value at 34˚C under the 50% feeding rate. Growth performance was significantly affected by the combined effects of temperature and feeding rate ($P < 0.0001$). The greatest final length (1.50 ± 0.12 cm) and weight (0.05 ± 0.012 g) occurred at 30˚C and 100% feeding, corresponding to SGR_L = 2.10 ± 0.26% day^{-1} and SGR_W = 5.72 ± 0.80% day^{-1}, whereas the lowest growth (0.88 ± 0.04 cm; 0.01 ± 0.001 g) was recorded at 34˚C and 50% feeding. Respiratory activity increased with temperature: gill cover movements rose from 142.00 ± 6.26 times min^{-1} (30˚C) to 162.78 ± 3.41 times min^{-1} (34˚C), while oxygen consumption ranged between 0.08 ± 0.01 and 0.81 ± 0.14 ppm 5 min^{-1}. Feeding ability varied slightly among treatments (12.5 - 18.3 Artemia 5 min^{-1}). During the 28-day recovery stage, survival reached 100% in all treatments, and fish previously exposed to 34˚C exhibited significant compensatory growth, attaining 2.67 ± 0.07 cm and 0.25 ± 0.037 g at 100% feeding. These findings indicate that optimal growth and physiological efficiency of *L. calcarifer* juveniles occur at 30˚C with full ration, while elevated temperature and feed restriction impair growth and metabolism but do not compromise recovery potential.

Keywords: *Barramundi, Lates calcarifer, temperature, feeding rate, survival, growth, respiration, feeding ability.*

Received: 18 September 2025; revised: 6 November 2025; accepted: 10 December 2025.

1. INTRODUCTION

Barramundi or Asian seabass (*Lates calcarifer*) is a euryhaline, fast-growing species that supports important capture fisheries and a rapidly expanding aquaculture industry across the Indo-Pacific region. During the past twenty years, global farming of barramundi (*Lates calcarifer*) has expanded rapidly, and the species is now viewed as a principal contributor to satisfying future demand for premium aquatic protein [1, 2]. Because of its tolerance to varying salinities, excellent meat texture, and proven suitability for high-density culture, Barramundi plays an increasingly important role in advancing aquaculture across tropical and subtropical regions [1].

Fish growth and physiology are highly sensitive to water temperature, which regulates metabolic rate, enzyme activity, and feeding intensity [3 - 5]. For Barramundi, optimal growth is generally achieved within the range of 30 - 32˚C, whereas performance drops markedly when

temperatures exceed 35°C [6 - 8]. Exposure to extreme temperatures narrows aerobic scope, raises metabolic energy costs, and reduces feed conversion efficiency [9 - 11]. With global warming expected to increase both the frequency and duration of heat waves, oxygen availability in aquatic environments is predicted to decline while oxygen demand in ectothermic species such as barramundi will rise [1, 12]. Understanding how juvenile *Lates calcarifer* respond to moderate but ecologically realistic conditions is essential for improving nursery management under future climate scenarios.

In addition to temperature, feeding management plays a crucial role in determining fish growth and survival in culture systems. Both underfeeding and overfeeding can compromise performance limited feeding constrains nutrient availability, while excess feed contributes to waste buildup and degraded water conditions [1]. Experiments with *L. calcarifer* and other tropical fish species, research has shown that optimal growth and feed efficiency occur at intermediate to full ration levels [13, 14]. Temperature further mediates these effects; elevated temperatures heighten metabolic maintenance demands, redirecting energy away from somatic growth [3, 9].

Despite advances in the biological knowledge of Barramundi, interactions between temperature and feeding rate have rarely been investigated, particularly in early juvenile performances. Most available studies have tended to single-factor effects, such as temperature-related to growth performance, protein synthesis, or oxygen consumption patterns [6 - 8]. Only a few studies have explored how different feed levels, when combined with temperature variation, shape immediate performance and recovery capacity, including compensatory growth under optimal rearing conditions [5, 15 - 17]. Understanding these combined effects is important for optimizing aquaculture management under dynamic environmental regimes.

Physiological and behavioral parameters such as respiration, oxygen consumption, and feeding ability provide useful information about how fish respond to changing environmental and nutritional conditions. As water temperature rises, fish generally elevate both oxygen demand and gill ventilation, reflecting higher metabolic activity and reduced energy availability for growth [18, 19]. Feeding ability also varies with water temperature, physiological conditions, and satiety level [11, 20]. Nevertheless, the combined effects of feeding levels and temperature on the physiological and behavioral activities of juvenile *Lates calcarifer* remain underexplored. The present study therefore aimed to evaluate how these two factors to influence on growth, respiration, and feeding ability in juvenile Barramundi *L. calcarifer*.

2. MATERIALS AND METHODS

2.1. Fish and experimental design

Juvenile Asian seabass were obtained from a commercial hatchery (Hoang Phat, Vietnam) at 20 days post-hatch, when they were actively feeding on *Artemia* nauplii. The average initial total length and body weight (mean ± SD) were 0.786 ± 0.077 cm and 0.009 ± 0.002 g, respectively. Upon arrival at the Aquaculture Research Station (Nha Trang University, Vietnam), the fry were held in aerated tanks at ~30°C and 30‰ salinity for 3 days to acclimate and recover from transport stress.

The experiment was set up in a controlled laboratory system with 200-L water baths as temperature-controlled environments. There were two phases of the experiment.

Phase 1: We used a factorial design with three water temperature levels (30°C, 32°C, 34°C) and three feeding levels (50%, 75%, 100% of satiation), making nine treatment combinations. Each treatment was replicated in five independent rearing units (n = 5). The experimental unit was a 1-L plastic cup containing 10 fish (density 10 fish L^{-1}) in the water bath. The experiment was performed using forty-five individual rearing cups, each placed within aerated water baths to ensure uniform environmental control. Water temperature was held at the designated levels (± 0.5°C) with aquarium heaters and thermostats and verified daily using a calibrated thermometer. Salinity was adjusted to 30 ppt by mixing filtered seawater with

freshwater. To maintain water quality, a biological filtration system was employed, and approximately 50% of the water was renewed weekly, during which organic debris was carefully removed. Throughout the experimental period, dissolved oxygen remained more than 6 mg L^{-1}, and ammonia-N concentrations were maintained below 0.5 mg L^{-1}.

Prior to the 28-day exposure experiment, a preliminary feeding assessment was carried out to determine the satiation level for juveniles at each temperature. Groups of fish were supplied with *Artemia* nauplii to apparent satiation, and total consumption within a 24 hours period was calculated. A known *Artemia* density was proposed, and uneaten *Artemia* were calculated after 15, 45, and 90 minutes, and irregularly up to 24 hours. The total number of *Artemia* consumed per fish in 24 hours was reflected in the 100% ration for that temperature, from which 75% and 50% rations were regularly received. This procedure confirmed that the full-feeding level perfectly considered near-satiation intake while accounting for thermal differences in appetite. On average, fish at higher temperatures used slightly more *Artemia*, although differences among treatments were minor and rations were regulated relative to body weight and temperature. Following the feeding ration calibration, the main experimental phase (thermal exposure, Phase 1) commenced. Fish were randomly placed in treatments and gently transferred to 1-L rearing cups at a density of ten individuals per cup. For groups exposed to 32˚C and 34˚C, the temperature was gradually increased by approximately 1˚C per day from ambient levels until the desired treatment temperature was reached within 2 - 3 days. During the 28 days exposure phase, fish were fed their assigned ration three times per day (07:00, 15:00, 23:00). The feed consisted of freshly hatched *Artemia* nauplii, distributed evenly to each cup. In 100% ration treatments, excess nauplii were provided to ensure satiety, whereas in 50% and 75% ration treatments the allotted quantity (previously determined) was provided and typically consumed within a short time. Any residual *Artemia* were siphoned out after each feeding to prevent water fouling. Rearing conditions (temperature, salinity, aeration) were kept constant throughout the experiment. Fish behavior and health were observed multiple times daily. Mortality was recorded immediately and dead individuals (if any) were removed promptly.

Phase 2 (recovery phase) began immediately after the 4 weeks exposure. At the end of Phase 1, all surviving fish from all treatments were transferred to recovery conditions to assess delayed effects. Recovery conditions were chosen to be optimal for Barramundi growth: temperature ~30˚C (close to ambient "room" temperature and within the optimal range) and 30‰ salinity for all fish. All groups were henceforth maintained under an identical environment, effectively removing the temperature and feeding differences. During recovery, all fish were fed to apparent satiation (ad libitum *Artemia* nauplii offered in excess) three times daily. Fish from different initial treatments were kept separate in labeled containers (maintaining the replicate units) to track their performance. Recovery was continued for an additional 4 weeks (28 days). This duration was expected to be sufficient for compensatory growth if it were to occur, given the small size and high growth potential of the juveniles.

2.2. Data collection

2.2.1. Survival rate

Fish survival was monitored daily. Survival rate (%) for each replicate was calculated at the end of Phase 1 and Phase 2 as 100 * (number of fish alive/initial number stocked). Any mortalities were noted with date and treatment.

2.2.2. Growth measurements

Fish were sampled at the start, end of Phase 1, and end of Phase 2 to assess fish growth in length and weight. At stocking (day 0), a subsample of 30 fry was lightly anesthetized (in 50 mg L^{-1} MS-222) and measured for initial length and weight (these initial values were given above). At the end of the 4 weeks exposure, all fish from each replicate were counted and a subset of ~5 fish per replicate were anesthetized for individual measurements of total

length (to nearest 0.01 mm) and wet weight (to 0.1 mg). The remaining fish were returned to their cups for the recovery phase. Similarly, at the end of the 4 weeks recovery, fish were counted and ~5 individuals per replicate were measured. Specific growth rate (SGR, % per day) in terms of weight and in terms of length was calculated for each replicate over each phase: SGR = 100 * (ln(final) - ln(initial))/days. We report SGR in weight (SGR-W) and SGR in length (SGR-L). Condition factor or other growth indices could also be computed, but given the small size, we focused on SGR and absolute gains.

2.2.3. Respiration rate

The oxygen consumption of fish was used as an indicator of metabolic rate under the different treatments. At the end of Phase 1, we measured the routine metabolic rate of fish from each treatment using a closed respirometry method. In brief, one fish from each replicate (randomly netted) was placed in a sealed glass chamber (volume ~100 mL) filled with well-aerated seawater. A fiber-optic oxygen probe (FireStingO_2 system, PyroScience, Germany) continuously recorded the dissolved oxygen (DO) level in the chamber for 5 minutes. A parallel control chamber without fish was run to account for background oxygen change. The test was conducted at the fish's rearing temperature to reflect the in-treatment metabolic rate. The oxygen consumption rate was calculated as the decline in DO over 5 minutes, corrected by subtracting the DO change in the control (blank) and expressed as mg O_2 consumed per fish per hour. This was further normalized to the fish's body weight (mg O_2 per gram fish per hour) for comparison between size groups. Opercular ventilation (gill beat) frequency was also noted during the test by visual observation (beats per minute), as an ancillary measure of respiratory response. We term this breathing rate.

At the end of Phase 2 (after recovery), respiration measurements were repeated to assess any persistent differences. Fish had been in a common temperature (30°C) for 4 weeks, so any differences in metabolism would reflect the lasting effects of their prior treatments and/or size differences. One fish per replicate was tested at 30°C following the same protocol. DO consumption in 5 minutes was measured (at 30°C for all fish) and gill beat frequency was recorded. These post-recovery metabolic rates thus allow comparison of fish that had different histories (prior temprature/feeding) but are now in the same environment.

2.2.4. Feeding rate/appetite

We assessed feeding ability and appetite after the recovery phase as a measure of the delayed effect on feeding behavior. At the end of Phase 2, fish from each replicate were subjected to a short-term feeding assay. Each group of fish (still in their 1-L cup at 30°C) was offered a known number of *Artemia* nauplii (considerably in excess, e.g. 30 nauplii per fish) after 24 hours of fasting. The number of prey consumed within 5 minutes was quantified for each replicate by counting remaining prey. This feeding rate (prey intake rate) in 5 minutes served as an index of appetite or feeding motivation. Differences between treatments would indicate if fish that were previously underfed or overheated exhibit higher appetite (compensatory feeding) compared to fish that were well-fed or kept at normal temperature. Prey consumption was expressed as the number of *Artemia* eaten per fish in 5 min.

2.3. Statistical analysis

All data are presented as mean ± standard deviation (SD) of five replicate units per treatment. Two-way analysis of variance (ANOVA) was used to test the effects of temperature, feeding rate, and their interaction on growth performance (SGR-W, SGR-L), survival, respiration rate, and feeding intake, separately for Phase 1 (immediate effects) and Phase 2 (delayed effects). Homogeneity of variances was confirmed with Levene's test, and data were log-transformed where necessary to meet ANOVA assumptions. When a significant factor effect was found ($p<0.05$), Tukey's HSD post-hoc test was applied to compare means among levels. For the recovery phase data, the initial treatment groups were the factors in the ANOVA (using the original temperature and feed

assignments as factors even though all fish were in common conditions during recovery). Statistical analyses were performed using SPSS 22.0 (IBM Corp.). A significance level of $\alpha = 0.05$ was applied for all tests.

3. RESULTS

3.1. Survival rate

The survival rate of *Lates calcarifer* juveniles varied markedly among treatments depending on both temperature and feeding rate (Figure 1). At 30˚C, fish survival rose with higher feeding rates, starting at around 73% under the lowest ration and peaking near 94% with full feeding. When temperature increased to 32˚C, survival dropped slightly, reaching 78%, 81%, and 85% for the three feeding levels. The lowest results occurred at 34˚C, where survival ranged between 69% and 80%. These results show that juveniles grew best at 30 ˚C with full feeding level, while both higher temperature and decreased feeding level clearly lowered survival. Heat stress was shown to worsen the negative effects of feed restriction under culture conditions.

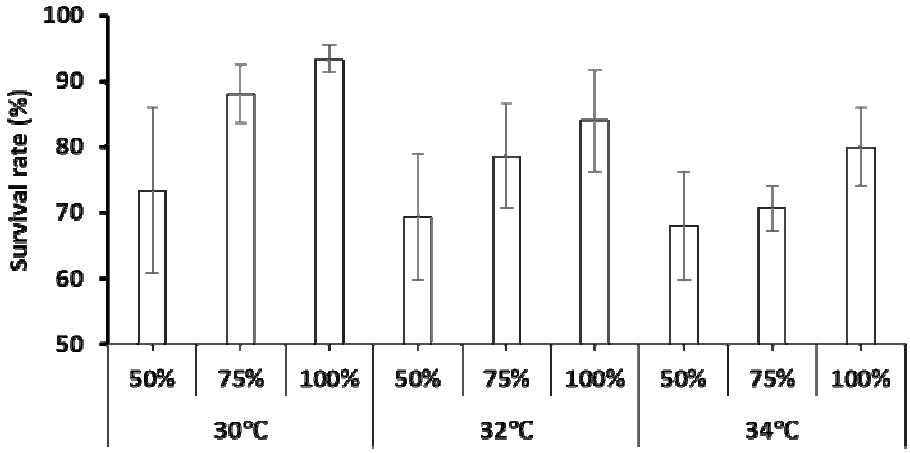

Figure 1. Effect of temperature and feeding rate on the survival rate of juvenile Barramundi during the experimental rearing stage

Table 1 indicates that all juvenile *Lates calcarifer* survived during the post-experimental period, regardless of temperature (30 - 34 ˚C) or feeding level (50 - 100 %). No mortality occurred, demonstrating complete recovery after the stress phase. Following 28 days of rearing at 30˚C with 100% feeding level, every fish survived, suggesting that once favorable conditions were restored, the juveniles quickly recovered stability. This finding highlights the remarkable tolerance and adaptability of juvenile Barramundi under varying environmental conditions.

Table 1. Survival rate of juvenile Barramundi under different temperature and feeding rates during the post-experimental phase

Temperature	30˚C			32˚C			34˚C		
Feeding rate (%)	50	75	100	50	75	100	50	75	100
Survival rate (%)	100	100	100	100	100	100	100	100	100

3.2. Growth performance

As shown in Table 2, temperature and feeding rate both had a strong effect on the growth performance of juvenile Barramundi during the experiment. The initial fish length and weight in all treatments did not differ among treatments ($P > 0.05$). Final fish length and weight were significantly affected by temperature ($P < 0.001$) and feeding level ($P < 0.001$), with a significant interaction between the two factors for final length ($P < 0.05$). The best growth occurred at 30˚C under 100% feeding rate, where fish attained a mean final length of 1.50 ± 0.12 cm and a final weight of 0.05 ± 0.012 g. Specific growth rates in both length (SGR_L) and weight (SGR_W) also indicate significant variation among treatments (P

< 0.001 for both). The maximum SGR_L (2.10 ± 0.26% day^{-1}) and SGR_W (5.72 ± 0.80% day^{-1}) occurred at 30°C and 100% feeding, whereas the lowest values were found at 34°C and 50% feeding (SGR_L = 0.37 ± 0.16% day^{-1}; SGR_W = 1.46 ± 0.30% day^{-1}). These results indicate that moderate temperature (30°C) combined with adequate feeding (100%) provides optimal conditions for growth, while higher temperature (≥ 34°C) and feed restriction significantly depress the growth of Barramundi juveniles.

Table 2. Effect of temperature and feeding rate on the growth of Barramundi during the experimental rearing stage

Temperature	30°C			32°C			34°C			P value		
Feeding rate (%)	50	75	100	50	75	100	50	75	100	Temp.	Feed.	Temp.×Feed.
Initial length	0.786± 0.077	0.786± 0.077	0.786± 0.077	0.786± 0.077	0.786± 0.077	0.786± 0.077	0.786± 0.077	0.786± 0.077	0.786± 0.077	-	-	-
Initial weight	0.009± 0.002	0.009± 0.002	0.009± 0.002	0.009± 0.002	0.009± 0.002	0.009± 0.002	0.009± 0.002	0.009± 0.002	0.009± 0.002	-	-	-
Final length	1.13± 0.042	1.18± 0.040	1.50± 0.124	1.07± 0.061	0.95± 0.022	1.10± 0.037	0.88± 0.040	1.03± 0.033	1.15± 0.081	<0.001	<0.001	0.046
Final weight	0.02± 0.003	0.03± 0.004	0.05± 0.012	0.02± 0.001	0.02± 0.003	0.02± 0.004	0.01± 0.001	0.02± 0.003	0.03± 0.004	<0.001	<0.001	0.120
SGR_L	1.21± 0.122	1.36± 0.112	2.10± 0.264	0.99± 0.187	0.63± 0.079	1.11± 0.111	0.37± 0.162	0.90± 0.110	1.23± 0.225	<0.001	<0.001	0.040
SGR_W	3.33± 0.431	4.19± 0.420	5.72± 0.802	2.17± 0.193	3.23± 0.384	3.18± 0.516	1.46± 0.303	2.98± 0.405	3.81± 0.401	<0.001	<0.001	0.368

Table 3. Effect of temperature and feeding ration on the growth of Barramundi during the post-experimental stage

Temperature	30°C			32°C			34°C			P value		
Feeding rate (%)	50	75	100	50	75	100	50	75	100	Temp.	Feed.	Temp.×Feed.
Initial length	1.13± 0.042	1.18± 0.040	1.50± 0.124	1.07± 0.061	0.95± 0.022	1.10± 0.037	0.88± 0.040	1.03± 0.033	1.15± 0.081	-	-	-
Initial weight	0.02± 0.003	0.03± 0.004	0.05± 0.012	0.02± 0.001	0.02± 0.003	0.02± 0.004	0.01± 0.001	0.02± 0.003	0.03± 0.004	-	-	-
Final length	1.70± 0.100	1.80± 0.100	2.00± 0.058	1.77± 0.120	1.80± 0.058	2.30± 0.153	1.73± 0.033	1.87± 0.067	2.67± 0.067	0.011	<0.0001	0.018
Final weight	0.09± 0.011	0.10± 0.011	0.14± 0.004	0.12± 0.023	0.11± 0.005	0.26± 0.049	0.10± 0.004	0.12± 0.019	0.25± 0.037	0.030	<0.0001	0.145
SGR_L	0.02± 0.003	0.02± 0.003	0.01± 0.001	0.02± 0.003	0.03± 0.002	0.03± 0.003	0.03± 0.001	0.03± 0.002	0.04± 0.001	<0.0001	0.054	0.002
SGR_W	0.06± 0.005	0.06± 0.005	0.05± 0.001	0.09± 0.009	0.08± 0.004	0.11± 0.009	0.10± 0.002	0.08± 0.007	0.10± 0.008	<0.0001	0.042	0.037

The growth performance of *Lates calcarifer* juveniles during the post-experimental stage was significantly affected by temperature and feeding ration (Table 3). Initial body length and weight did not differ among treatments (P > 0.05), confirming that fish were homogeneous at the start of the recovery phase. Final length and final weight were significantly influenced by both temperature (P < 0.05 and P < 0.05, respectively) and feeding ration (P < 0.001 for both). The interaction between temperature and feeding ration was also significant for final length (P = 0.05). The highest growth was observed at 34°C and 100% feeding, with a final length of 2.67 ± 0.07 cm and final weight of 0.25 ± 0.037 g, while the lowest values occurred at 30°C and 50% feeding (final length 1.70 ± 0.10 cm; final weight 0.09 ± 0.011 g). Both length- and weight-specific growth rates (SGR_L and SGR_W) varied notably among treatments. Temperature strongly affected both indices (P < 0.001), while feeding level had a smaller but detectable influence (P = 0.054 for SGR_L; P < 0.05 for SGR_W). A significant temperature-by-feeding interaction was found for SGRi (P < 0.01) and

SGR*w* ($P < 0.05$). The fastest weight-specific growth (0.10 ± 0.008 % day^{-1}) occurred in fish reared at 34 ˚C under full feeding. This outcome suggests that adequate feeding at higher temperatures facilitated compensatory growth following earlier stress. Altogether, juveniles of L. calcarifer recovered well, showing optimal growth and metabolic restoration at 34˚C with unrestricted feeding.

3.3. Respiration and metabolic response

As shown in table 4, temperature had a dominant effect on the respiration response of juvenile Barramundi, while feeding rate contributed only slightly. The number of gill cover beats increased with temperature, ranging from about 142 beats min^{-1} at 30˚C (100 % ratio) to 163 beats min^{-1} at 34˚C (50% ratio). Statistical analysis showed a clear temperature effect ($P < 0.005$), but no significant influence of feeding rate ($P > 0.05$) or their interaction ($P > 0.05$). Likewise, oxygen consumption indicated a strong dependence on temperature ($P < 0.001$) and a smaller yet significant effect of feeding level ($P < 0.05$). The highest oxygen uptake was measured at 32˚C and 50% feeding (0.81 ± 0.14 ppm/5 min), while the lowest was at 30˚C with 100% feeding (0.08 ± 0.01 ppm/5 min). When adjusted for body weight, oxygen consumption also increased significantly with temperature ($P < 0.001$) and feeding rate ($P < 0.005$). The highest mass-specific oxygen consumption was found at 34˚C and 50% feeding (57.50 ± 5.95 ppm/5 min/W), whereas the lowest value was observed at 30˚C and 100% feeding (2.01 ± 0.75 ppm/5 min/W). Overall, higher temperatures led to noticeably stronger respiration activity, consistent with an increase in metabolic demand. Fish provided with 100% feeding rations showed more balanced oxygen consumption. The lack of a significant temperature and feeding rate interaction ($P > 0.05$) suggests that these two factors influenced respiration independently.

Table 4. Effect of temperature and feeding rate on the respiration of Barramundi during the experimental rearing stage

Temperature	30°C			32°C			34°C			P value		
Feeding rate (%)	50	75	100	50	75	100	50	75	100	Temp.	Feed.	Temp.×Feed.
Length (cm)	1.13± 0.042	1.18± 0.040	1.50± 0.124	1.07± 0.061	0.95± 0.022	1.10± 0.037	0.88± 0.040	1.03± 0.033	1.15± 0.081	-	-	-
Weight (g)	0.02± 0.003	0.03± 0.004	0.05± 0.012	0.02± 0.001	0.02± 0.003	0.02± 0.004	0.01± 0.001	0.02± 0.003	0.03± 0.004	-	-	-
Gill cover movement rate (times/min)	149.00± 4.61	143.56± 5.87	142.00± 6.26	159.56± 3.88	155.33± 5.16	151.28± 2.36	162.78± 3.41	154.78± 2.06	154.67± 3.33	0.002	0.083	0.990
Oxygen consumption (ppm/5 min)	0.40± 0.19	0.20± 0.01	0.08± 0.01	0.81± 0.14	0.70± 0.13	0.51± 0.09	0.79± 0.10	0.66± 0.15	0.57± 0.12	<0.0001	0.022	0.987
Oxygen consumption (ppm/5 min/W)	16.38± 7.62	6.90± 0.87	2.01± 0.75	39.06± 8.91	43.82± 9.27	23.81± 5.49	57.50± 5.95	37.01± 12.17	23.41± 6.49	<0.0001	0.004	0.384

The respiratory responses of *Lates calcarifer* juveniles during the post-experimental stage were significantly affected by temperature and feeding rate (Table 5). The gill cover movement rate increased with temperature, ranging from 125.11 ± 4.15 times/min at 30˚C and 100% feeding to 161.33 ± 4.67 times/min at 34˚C and 50% feeding. Temperature significantly affected the respiration of *L. calcarifer* juveniles ($P < 0.05$), while feeding rate and its interaction with temperature were not statistically significant ($P > 0.05$). Oxygen consumption (ppm/5 min) increased with both higher temperature and restricted feeding, reaching 0.48 ± 0.10 at 34˚C and 50% feeding, compared with only 0.04 ± 0.01 at 30˚C and 100% feeding. Both factors significantly influenced oxygen uptake ($P < 0.001$ and $P < 0.05$), and their interaction was also significant ($P < 0.05$). When adjusted for body weight, oxygen consumption rose markedly under high temperature and limited

feeding 1.54 ± 0.27 ppm/5 min/W at 34˚C and 50% feeding versus 0.10 ± 0.02 ppm/5 min/W at 30˚C and full feeding. Overall, these findings indicate that elevated temperature and lower ratios heightened metabolic activity and oxygen demand, while optimal conditions maintained efficient respiration and physiological stability.

Table 5. Effect of temperature and feeding rate on the respiration of Barramundi during the post-experimental stage

Temperature	30°C			32°C			34°C			P value		
Feeding rate (%)	50	75	100	50	75	100	50	75	100	Temp.	Feed.	Temp.× Feed.
Length (cm)	1.13± 0.042	1.18± 0.040	1.50± 0.124	1.07± 0.061	0.95± 0.022	1.10± 0.037	0.88± 0.040	1.03± 0.033	1.15± 0.081	-	-	-
Weight (g)	0.02± 0.003	0.03± 0.004	0.05± 0.012	0.02± 0.001	0.02± 0.003	0.02± 0.004	0.01± 0.001	0.02± 0.003	0.03± 0.004	-	-	-
Gill cover movement rate (times/min)	137.33± 8.35	125.44± 17.88	125.11± 4.15	147.33± 7.69	144.44± 8.75	132.22± 16.59	161.33± 4.67	154.22± 6.19	153.33± 8.74	0.017	0.387	0.972
Oxygen consumption (ppm/5 min)	0.08± 0.04	0.05± 0.01	0.04± 0.01	0.16± 0.02	0.11± 0.07	0.09± 0.03	0.48± 0.10	0.25± 0.04	0.13± 0.02	<0.0001	0.004	0.032
Oxygen consumption (ppm/5 min/W)	0.30± 0.16	0.18± 0.03	0.10± 0.02	0.46± 0.04	0.33± 0.20	0.11± 0.03	1.54± 0.27	0.71± 0.01	0.17± 0.01	<0.0001	<0.0001	0.002

3.4. Feeding ability

As shown in table 5, temperature and feeding level had little effect on the feeding behavior of juvenile *Lates calcarifer*. The number of *Artemia* consumed in 5 minutes did not vary significantly across treatments ($P > 0.05$ for temperature, feeding rate, and their interaction). Even so, a minor reduction in feeding activity was noted at higher temperatures and lower rations. Fish at 30˚C displayed the greatest feeding rate (18.33 ± 1.12 *Artemia*/5 min, 50% ration), followed by those at 32˚C (17.67 ± 1.56 *Artemia*/5 min, 50% ration), whereas feeding performance was lowest at 34˚C with full feeding (12.50 ± 2.13 *Artemia*/5 min).

Overall, the results suggest that *L. calcarifer* juveniles maintain relatively stable feeding performance within the temperature range tested, but higher temperatures (≥ 34˚C) may slightly reduce feeding motivation and prey capture efficiency.

Table 6. Effect of temperature and feeding rate on the feeding ability of Barramundi during the experimental rearing stage

Temperature	30°C			32°C			34°C			P value		
Feeding rate (%)	50	75	100	50	75	100	50	75	100	Temperature	Feeding rate	Temp. x Feed.
Feeding ability (Artemia/5 min)	18.33 ± 1.12	15.33 ± 1.43	15.00 ± 2.00	17.67 ± 1.56	16.17 ± 1.35	15.83 ± 2.18	16.50 ± 2.01	14.17 ± 2.21	12.50 ± 2.13	0.301	0.113	0.975

The feeding ability of *Lates calcarifer* juveniles during the post-experimental stage was slightly affected by feeding rate but not by temperature (Table 7). Statistical analysis showed that temperature had no significant effect ($P > 0.05$), while feeding rate had a significant influence ($P < 0.01$) on feeding ability. The interaction between temperature and feeding rate was non-significant ($P > 0.05$). Although temperature effects were relatively small, fish tended to feed more actively at 32˚C, reaching 26.33 ± 0.67 *Artemia*/5 min at 50% feeding. Feeding performance decreased at both 30˚C and 34˚C, especially when fish were applied the full ration, averaging 17.33 ± 3.18 and 19.67 ± 0.88 *Artemia*/5 min, respectively. In general, the feeding level seemed to be the key factor shaping feeding ability after the experiment. Moderate rations promoted stronger prey capture, while overfeeding appeared to suppress inspiration, probably because the fish were already satiated.

Table 7. Effect of temperature and feeding rate on the feeding ability of Barramundi during the post-experimental stage

Temperature	30°C			32°C			34°C			P		
Feeding rate (%)	50	75	100	50	75	100	50	75	100	Temp.	Feed.	Temp.× Feed.
Feeding ability (Artemia/5 min)	25.00± 0.58	20.33± 2.91	17.33± 3.18	26.33± 0.67	23.00± 1.53	19.00± 3.21	23.00± 3.51	22.33± 1.45	19.67± 0.88	0.606	0.0015	0.853

4. DISCUSSION

This study provides novel insights into how elevated temperature and limited feeding rate interact to affect Barramundi juveniles, and how these fish recover once favorable conditions are restored. The findings largely support our hypotheses: High water temperature (34°C) and feed restriction (50% satiation) each imposed clear stress on barramundi fry, evidenced by suppressed growth and heightened metabolic rates, and their combination had compounding negative effects. However, upon returning to optimal environmental conditions (30°C, full feeding), the fish demonstrated a strong capacity for compensatory growth and feeding, though some effects of the prior stress (particularly elevated metabolic rate) persisted. These results are discussed in light of the known physiology of barramundi and comparable tropical species (e.g., cobia), and they carry important implications for aquaculture under climate change scenarios.

4.1. Survival rate

Juvenile *Lates calcarifer* tolerated all experimental conditions without mortality, indicating a high capacity to withstand short-term exposure to thermal and nutritional stress (Section 3.1). Survival ranged from 69% to 94% during the 28-day trial, with the highest rates recorded at 30°C and full feeding. Elevated temperature (34°C) and restricted rations (50 - 75%) reduced survival moderately, reflecting the combined physiological burden of heat and limited energy intake. This pattern is consistent with the general understanding that thermal stress raises maintenance energy costs and reduces the energy available for physiological functions including immunity and survival [3, 5]. The interaction between temperature and feeding rate implies that under higher thermal load, fish are less tolerant of feed restriction: those under - fed are further compromised. Interestingly, during the post-experimental recovery phase all treatments achieved 100% survival, indicating that once favourable conditions (temperature, feeding) were restored the fish were able to fully recover, a measure of strong resilience. This resilience aligns with the eurythermal capacity reported for barramundi [7, 8, 21] which found that juveniles maintain high survival and growth across a relatively wide temperature range.

4.2. Growth performance

The growth results (Section 3.2) demonstrated significant effects of both temperature and feeding rate, and an interaction between them. The optimal growth (final length and weight, SGR) was seen at 30°C with 100% feeding. Growth was considerably suppressed at 34°C and 50% feeding. The literature on juvenile barramundi supports the notion that optimal growth occurs around ~30 - 32°C, with feed intake and growth efficiency dropping at higher temperatures. Earlier work by Katersky and Carter [7, 8] showed that Barramundi grow best around 31 - 32°C, with feed intake and growth dropping once the water gets warmer. Our findings mirror this trend and point to a typical metabolic response: As temperature increases, the cost of maintaining basic physiological functions rises faster than the fish's ability to use food for growth [5]. Feed limitation exacerbates this imbalance, producing an additive or even synergistic reduction in growth. Similar temperature-ratio interactions have been described in cobia and turbot [16, 17, 22]. In our study, fish subjected to both high temperature and feed restriction gained minimal weight, suggesting

most ingested energy was expended on maintenance. During the recovery phase, full survival and rapid compensatory growth confirmed that juvenile barramundi can partially recover from prior stress. The greatest rebound occurred in fish previously held at 34˚C and refed at 100%, indicating that once optimal conditions return, this species can restore growth potential effectively. However, complete compensation was not achieved within 28 days, suggesting that extended recovery may be required to eliminate residual size disparities.

4.3. Respiration and metabolic response

According to the respiration results (Section 3.3), Temperature had a dominant influence on respiration. Gill cover movements and oxygen consumption increased markedly at 34˚C, following the expected Q_{10}-type response typical of ectothermic species. The rise in metabolic rate reflects the higher energetic cost of homeostasis and oxygen delivery under heat stress. Feeding level exerted a smaller, yet detectable, effect: mass-specific oxygen consumption tended to be higher in restricted-fed fish, likely due to their smaller body size and increased activity when searching for food. When temperature and feeding stress coincided, oxygen consumption reached its highest levels, implying that the energy budget was largely allocated to maintenance rather than growth. These findings are consistent with reports for cobia and salmonids, where elevated temperatures increase basal metabolism and reduce feed efficiency [3, 23]. Even after returning to 30˚C, oxygen uptake remained slightly elevated in fish previously exposed to 34˚C, suggesting a persistent elevation in metabolic demand, possibly a carry-over effect of prior stress on gill morphology or mitochondrial activity. Moreover, previous work in barramundi has highlighted that growth efficiency is maintained across a moderate temperature range due to efficient nutrient utilisation, but declines sharply when metabolic cost becomes excessive. Our results therefore support the conclusion that under high temperature or feed limitation, the fish shift energy away from growth towards maintenance (respiration), which leads to lower growth and survival.

4.4. Feeding ability

Regarding feeding ability (Sections 3.4), during the experimental stage the number of *Artemia* consumed per 5 minutes was not significantly affected by either temperature ($P > 0.05$) or feeding rate ($P > 0.05$). However, during the post-experimental recovery stage feeding rate became significant ($P < 0.05$) while the temperature remained non-significant ($P > 0.05$). This suggests that under the acute experimental treatments the prey-capture behaviour of juveniles may be less sensitive to temperature *per se*, but during recovery the nutritional status (feeding level) becomes more influential in determining prey intake. The literature reports that while appetite and feed intake can increase with temperature to a point, above the optimal range feed intake declines (e.g., Bermudes *et al.* (2010) [6] reported declines above 38˚C in barramundi). Our less-pronounced effect may be due to the narrower temperature range (30 - 34˚C) and possibly acclimation. Nevertheless, the finding indicates that feeding strategy is crucial for restoring feeding ability in the recovery phase, and that under adequate feeding juvenile Barramundi can rapidly regain feeding capacity irrespective of moderate temperature differences.

4.5. Practical implications

From a practical perspective, these findings carry important implications for Barramundi culture in tropical environments increasingly affected by climate warming. Maintaining routine feeding regimes during high-temperature events may not sustain growth, as metabolic costs rise sharply above 32˚C. Conversely, feed restriction often applied to limit water quality deterioration can compound growth losses under thermal stress. Farmers should consider adaptive feeding strategies, such as smaller but more frequent meals, energy-dense diets, or antioxidant supplementation to help fish cope with elevated metabolic demands. Temperature control measures, including shading, aeration, or

recirculating cooling systems, could further mitigate performance declines. The strong compensatory growth observed after stress periods indicates that barramundi can recover substantially if optimal conditions are restored promptly; however, recovery may require increased feeding input to offset prior energy deficits. Overall, maintaining juveniles near 30°C with adequate feeding appears essential for maximizing growth efficiency and ensuring stable production under variable climatic conditions.

4.6. Study Limitations and Further Work

The present study was limited by both its short duration and narrow thermal range, which may not fully capture the long-term physiological adjustments of juvenile *Lates calcarifer*. Extended experiments covering wider temperature and feeding gradients are necessary to determine precise tolerance thresholds and the duration required for complete compensatory recovery. Incorporating finer physiological indicators, such as nitrogen excretion and protein synthesis would provide deeper insight into nutrient use under combined temperature and feeding challenges [6 - 8, 21]. Future work should also include additional physiological and biochemical indicators, such as nitrogen excretion, protein turnover, and hormonal markers of appetite regulation, to better understand how energy and nutrients are partitioned under concurrent heat and feed stress. Furthermore, examining the combined effects of temperature with other environmental factors, such as dissolved oxygen, salinity, and feed formulation would provide a more realistic representation of aquaculture conditions. These investigations will contribute to refining feeding management strategies and improving resilience models for Barramundi culture in the context of climate variability.

5. CONCLUSION

Temperature and feeding rate jointly affected juvenile Lates calcarifer. The best growth (SGRt = 5.72 ± 0.80% day^{-1}) and survival (94%) occurred at 30°C and 100% feeding. Both heat stress (34°C) and feed restriction impaired performance but triggered compensatory growth once fish returned to favorable conditions. Full recovery (100% survival) and strong compensatory responses confirm that maintaining 30°C with sufficient feed optimizes growth and highlights the species' resilience to temporary thermal and nutritional stress.

ACKNOWLEDGEMENTS

The authors wish to thank the technical staff at the Institute of Aquaculture, Nha Trang University, for their valuable assistance and support throughout the experiments. This research is funded by Vietnam National Foundation for Science and Technology Development (NAFOSTED) under grant number 106.05-2023.79.

REFERENCES

1. Glencross, B. (2006). The nutritional management of barramundi, *Lates calcarifer*–a review. *Aquaculture Nutrition*, 12(4), 291 - 309.

2. Schipp, G., Bosmans, J., & Humphrey, J. (2007). Barramundi farming handbook. *Department of Primary Industry, Fisheries and Mines, Northern Territory Government*, 1-81.

3. Brett, J. & Groves, T. (1979). Physiological energetics. In *Fish physiology* (Vol. 8, pp. 279 - 352). Elsevier.

4. Deslauriers, D., Chipps, S. R., Breck, J. E., Rice, J. A., & Madenjian, C. P. (2017). Fish bioenergetics 4.0: An R-based modeling application. *Fisheries*, 42(11), 586 - 596.

5. Jobling, M. (1993). Bioenergetics: Feed intake and energy partitioning. In *Fish ecophysiology* (pp. 1 - 44). Springer.

6. Bermudes, M., Glencross, B., Austen, K., & Hawkins, W. (2010). The effects of temperature and size on the growth, energy budget and waste outputs of barramundi (Lates calcarifer). *Aquaculture*, 306(1 - 4), 160 - 166.

7. Katersky, R. S. & Carter, C. G. (2007). High growth efficiency occurs over a wide temperature range for juvenile barramundi *Lates calcarifer* fed a balanced diet. *Aquaculture*, 272(1 - 4), 444 - 450.

8. Katersky, R. S. & Carter, C. G. (2007). A preliminary study on growth and protein synthesis

of juvenile barramundi, *Lates calcarifer* at different temperatures. *Aquaculture*, 267(1 - 4), 157 - 164.

9. Clark, T. D., Sandblom, E. & Jutfelt, F. (2013). Aerobic scope measurements of fishes in an era of climate change: respirometry, relevance and recommendations. *Journal of Experimental Biology*, 216(15), 2771 - 2782.

10. Noyes, P. D., McElwee, M. K., Miller, H. D., Clark, B. W., Van Tiem, L. A., Walcott, K. C., Erwin, K. N. & Levin, E. D. (2009). The toxicology of climate change: environmental contaminants in a warming world. *Environment international*, 35(6), 971 - 986.

11. Pörtner, H. O. & Farrell, A. P. (2008). Physiology and climate change. *Science*, 322(5902), 690 - 692.

12. Islam, M. J., Kunzmann, A. & Slater, M. J. (2022). Responses of aquaculture fish to climate change-induced extreme temperatures: A review. *Journal of the World Aquaculture Society*, 53(2), 314 - 366.

13. Ganzon-Naret, E. S. (2013). Effects of feeding frequency on growth, survival rate and body composition in sea bass (*Lates calcarifer*) juveniles fed a commercial diet under laboratory condition. *Animal Biology & Animal Husbandry*, 5(2), 175 - 176.

14. Katersky, R. S. & Carter, C. G. (2010). The effect of temperature on post-prandial protein synthesis in juvenile barramundi, *Lates calcarifer*. *Comparative Biochemistry and Physiology Part A: Molecular & Integrative Physiology*, 156(4), 529 - 536.

15. Ali, M., Nicieza, A. & Wootton, R. J. (2003). Compensatory growth in fishes: a response to growth depression. *Fish and fisheries*, 4(2), 147 - 190.

16. Le, M.-H., Espe, M., Conceição, L. E., Nguyen, M. V., Yúfera, M., Engrola, S., Jordal, A.-E. O., Pham, H. Q. & Rønnestad, I. (2024). Impact of feed availability on growth performance and amino acid utilization of cobia (*Rachycentron canadum*) at elevated temperature. *Frontiers in Aquaculture*, 3, 1476881.

17. Sun, L. & Chen, H. (2009). Effects of ration and temperature on growth, fecal production, nitrogenous excretion and energy budget of juvenile cobia (*Rachycentron canadum*). *Aquaculture*, 292(3 - 4), 197 - 206.

18. Chabot, D., Steffensen, J. & Farrell, A. (2016). The determination of standard metabolic rate in fishes. *Journal of Fish Biology*, 88(1), 81 - 121.

19. Norin, T. & Metcalfe, N. B. (2019). Ecological and evolutionary consequences of metabolic rate plasticity in response to environmental change. *Philosophical Transactions of the Royal Society B*, 374(1768), 20180180.

20. Schulte, P. M. (2015). The effects of temperature on aerobic metabolism: towards a mechanistic understanding of the responses of ectotherms to a changing environment. *The Journal of experimental biology*, 218(12), 1856 - 1866.

21. Katersky, R. S. & Carter, C. G. (2005). Growth efficiency of juvenile barramundi, Lates calcarifer, at high temperatures. *Aquaculture*, 250(3 - 4), 775 - 780.

22. Van Ham, E. H., Berntssen, M. H., Imsland, A. K., Parpoura, A. C., Bonga, S. E. W. & Stefansson, S. O. (2003). The influence of temperature and ration on growth, feed conversion, body composition and nutrient retention of juvenile turbot (*Scophthalmus maximus*). *Aquaculture*, 217(1 - 4), 547 - 558.

23. Volkoff, H. & Rønnestad, I. (2020). Effects of temperature on feeding and digestive processes in fish *Temperature*, 7(4), 307 - 320.

A REVIEW OF POTENTIAL IMPACT OF TOTAL SUSPENDED SOLIDS ON SURFACE WATER QUALITY AND WATER USES IN THE VIETNAMESE MEKONG DELTA

Ha Thao Nguyen[1, 2], Nguyen Thanh Giao[1, *]

[1] *College of Environment and Natural Resources, Can Tho University*

[2] *Master student in Enivronment and Natural Resources Management, College of Environment and Natural Resources, Can Tho University*

[*] *Email: ntgiao@ctu.edu.vn*

ABSTRACT

The Vietnamese Mekong Delta (VMD) is an internationally significant region for agricultural production and biodiversity, yet it faces escalating challenges to its water resources. Total Suspended Solids (TSS) represent a critical water quality parameter within this complex deltaic system, with profound implications for its ecological integrity and socio-economic activities. TSS in the VMD originate from a combination of natural processes, such as riverbank erosion and sediment resuspension and increasingly dominant anthropogenic activities, including intensive agriculture, aquaculture, urban and industrial wastewater discharge, upstream hydropower dam development leading to sediment trapping and localized sand mining. Elevated TSS concentrations and alterations in sediment composition directly degrade water quality by increasing turbidity, reducing light penetration essential for aquatic photosynthesis and acting as a transport mechanism for nutrients and various contaminants, including heavy metals and pesticides. These TSS-induced changes in water quality have substantial adverse consequences for key water uses. Agricultural productivity is affected through impacts on irrigation infrastructure and alterations to soil fertility due to reduced beneficial sediment deposition. Aquaculture operations face challenges related to fish and shrimp health, pond management and overall productivity. The suitability of surface water for domestic supply is compromised, necessitating more complex and costly treatment processes and posing potential health risks. Furthermore, TSS contributes to the degradation of aquatic ecosystem health by altering habitats, affecting biodiversity and disrupting fundamental ecological processes. The cumulative effect of these impacts, particularly the long-term reduction in sediment delivery to the delta, also threatens the VMD's geomorphological stability in the face of land subsidence and sea-level rise. Understanding and effectively managing TSS loads and their sources are therefore paramount for the sustainable development and environmental protection of the VMD.

Keywords: *Total Suspended Solids, Vietnamese Mekong Delta, water quality, water uses, environmental impact.*

Received: 2 June 2025; revised: 19 August 2025; accepted: 2 December 2025.

1. INTRODUCTION

The Vietnamese Mekong Delta (VMD), a vast and fertile plain at the terminus of the Mekong river, stands as a region of profound socio-economic and ecological importance. It is a global breadbasket, critical for Vietnam's food security through extensive rice cultivation and a burgeoning aquaculture industry, simultaneously harbors unique biodiversity within its intricate network of rivers, canals and estuaries [1 - 3]. The

delta's productivity and ecological character are intrinsically linked to the seasonal pulses of water and sediment delivered by the Mekong river. However, these vital resources are under mounting pressure from a confluence of factors, including rapid population growth, the intensification of agricultural and industrial activities, the far-reaching impacts of upstream hydropower development, the pervasive threats of climate change, notably sea-level rise and increased frequency of saltwater intrusion [4 - 7]. These stressors collectively jeopardize the quality of the VMD's water resources and consequently, the livelihoods of millions who depend upon them. The historical development trajectory within the VMD, particularly the widespread construction of dike systems to facilitate rice intensification and flood control since the early 1990s and more significantly after the major floods in 2000, has fundamentally altered local hydrological regimes and sediment dynamics [8, 9]. While these engineering interventions have supported agricultural expansion, they have also inadvertently modified how water and sediment are distributed and retained within the delta, potentially increasing the system's vulnerability to changes in upstream sediment inputs and contributing to the local generation and accumulation of suspended solids in certain areas [9]. This human-modified landscape now interacts with larger-scale pressures, creating a complex environmental scenario where water quality is a concern.

Within this context, Total Suspended Solids (TSS) emerge as a pivotal water quality parameter. TSS refers to the diverse array of particulate matter, both organic and inorganic, held in suspension within the water column. In natural deltaic environments, suspended sediments play a crucial constructive role, contributing essential nutrients to floodplain soils, facilitating land accretion that counteracts subsidence, and creating diverse habitats that support rich aquatic ecosystems [3, 10]. However, significant deviations in the quantity, composition, or timing of TSS delivery, largely driven by intensifying anthropogenic activities across the Mekong basin and within the delta itself, can transform these solids from a vital resource into a significant environmental stressor. There is growing scientific evidence and mounting concern regarding persistently elevated TSS levels and profoundly altered sediment regimes within the VMD [2, 11, 12]. These changes are increasingly linked to observable degradation in surface water quality and are exerting tangible negative impacts on the region's primary water-dependent sectors and overall ecological balance. The situation in the VMD reflects a broader global pattern where large river deltas are experiencing significant alterations to their sediment loads due to extensive damming, intensified land use and the effects of climate change, making the VMD a critical case study with implications for other similarly vulnerable systems worldwide [10].

The primary purpose of this review is to synthesize and critically evaluate the existing body of published scientific knowledge concerning the multifaceted impacts of TSS on water quality and its subsequent effects on key water uses-specifically agriculture, aquaculture, domestic water supply and the health of aquatic ecosystems-within the VMD.

2. RESEARCH METHODOLOGY

A systematic literature search was conducted using the Web of Science, Scopus, PubMed and Google Scholar databases for publications up to May 2025. Search terms were combined using keyword categories related to: (1) suspended solids (e.g., "TSS," "suspended sediment," "turbidity"); (2) geography (e.g., "VMD," "Can Tho"); (3) specific water uses (e.g., "agriculture," "aquaculture," "domestic water supply") and (4) impact drivers (e.g., "dam impacts," "sand mining," "climate change"). Stringent inclusion criteria were applied to select scientific sources. The primary criteria required that studies: (1) possess a Digital Object Identifier (DOI) for verification; (2) directly address the sources, concentrations, or impacts of TSS (or closely related parameters) on water quality or water uses within the VMD; (3) be published as a peer-

reviewed journal article (presenting original research, modeling, or reviews) or a high-quality, citable report (e.g., Mekong River Commission). An analysis was performed on the selected references. Data pertaining to TSS sources, characteristics, and its consequences - including effects on physicochemical parameters, agriculture, aquaculture, domestic water supply and ecosystem health - were systematically extracted and collated. This synthesis aimed to identify recurrent themes, cause-effect relationships and knowledge gaps, integrating findings from diverse methodologies (e.g., field monitoring, modeling, impact assessments) into a cohesive analytical narrative.

3. RESULTS AND DISCUSSION

3.1 Characteristics and sources of total suspended solids in the Vietnamese Mekong Delta

TSS concentrations in the surface waters of the VMD exhibit significant spatial and temporal variability, frequently surpassing national water quality standards and posing considerable environmental concern. Studies have reported TSS values reaching as high as around 146 mg/L in certain areas [13], with average concentrations in major rivers like the Tien river fluctuating seasonally, for instance, around 30 mg/L in the dry season and increasing to about 48 mg/L in the rainy season, often exceeding permissible limits for various water uses [11, 12]. In some coastal provinces, measured TSS values have been found to exceed allowable thresholds by around 1.05 to 6.52 times, underscoring the severity of the issue [14]. This variability is influenced by a complex interplay of factors including hydrological conditions, land use patterns and specific pollution sources. For example, urban areas and regions with intensive dike systems, which alter local hydrology, often exhibit higher pollution levels, including elevated TSS or turbidity [9, 13]. Seasonality plays a crucial role, with many studies indicating higher TSS concentrations during the rainy season due to increased surface runoff, soil erosion and the flushing of pollutants from terrestrial sources into water bodies [11, 12, 15, 16]. Conversely, in some confined canal systems or during periods of low flow, resuspension of settled materials can lead to elevated TSS even in the dry season [14]. The fundamental nature of TSS in the VMD is also undergoing a significant transformation; there is a discernible shift from a system historically dominated by natural fluvial sediments to one increasingly influenced by locally generated, often finer, and more organically enriched or polluted suspended particles due to reduced upstream sediment influx and increased local anthropogenic inputs [2, 3, 5, 10, 13, 17 - 22].

The sources of TSS in the VMD are diverse, stemming from both natural processes and a wide range of anthropogenic activities. Natural sources include the erosion of riverbanks and channel beds, a process that can be significantly exacerbated by altered hydrological regimes and a deficit in the natural sediment load arriving from upstream [10, 18]. The reduction in sediment supply from upstream, primarily due to sediment trapping by hydropower dams, increases the erosive power of the river water downstream leading to enhanced scour of riverbeds and banks within the delta itself [3]. This internally generated sediment then contributes to local TSS concentrations, creating a feedback mechanism where an upstream anthropogenic intervention (dam construction) amplifies a natural process (erosion) within the delta, thereby compounding the TSS problem. Resuspension of bottom sediments due to tidal currents, wind-induced wave action, navigation, particularly in shallow canals and estuarine areas, also contributes to natural TSS levels [23, 24].

Anthropogenic activities, however, are increasingly dominant contributors to the TSS load in the VMD. Intensive agricultural practices, especially rice cultivation, which covers vast areas of the delta, lead to significant soil erosion and the discharge of particulate organic and inorganic matter into adjacent waterways during irrigation and rainfall events [2, 9, 13]. Effluents from the rapidly expanding aquaculture sector, including shrimp and catfish farming, release substantial quantities of TSS in the form of uneaten feed, fecal matter and eroded pond sediment [2, 12, 25].

Urban and industrial wastewater, often discharged with inadequate or no treatment from densely populated areas and industrial zones, introduces high concentrations of suspended solids and organic pollutants into the river and canal network [2, 12, 13]. Furthermore, the construction of extensive high-dike systems for flood control and agricultural intensification, while beneficial for crop production, has altered local hydrodynamics. These systems can trap finer sediments and associated pollutants within canal networks, particularly during periods of low flow or specific sluice gate operations, leading to chronic localized high TSS levels and degraded water quality [8, 9]. This represents a more diffuse and less immediately obvious source of TSS compared to direct point source discharges. A major driver of altered sediment regimes at the delta scale is the construction of numerous hydropower dams in the upper Mekong basin. These dams trap enormous quantities of sediment, drastically reducing the natural sediment flux to the VMD [3, 5, 10, 17, 22, 26]. Estimates suggest that full hydropower development could trap as much as around 94 - 96% of the river's sediment load, with significant reductions already observed at downstream monitoring stations [5, 10]. This sediment starvation not only impacts TSS levels directly but also contributes to increased coastal and riverbank erosion. Concurrently, in-stream sand mining activities within the delta directly extract vast quantities of riverbed material and cause significant resuspension of fine sediments, further elevating local TSS concentrations and altering channel morphology [18, 20].

3.2. Impacts of total suspended solids on water quality in the Vietnamese Mekong Delta

The presence of TSS in the waters of the VMD exerts multitude impacts on their physical, chemical and biological characteristics, often leading to significant degradation of overall water quality. Physically, the most direct and observable impact of elevated TSS is increased turbidity and reduced water clarity [9, 14, 27]. This reduction in clarity significantly limits light penetration into the water column, which has profound implications for aquatic ecosystems by inhibiting the photosynthetic activity of submerged aquatic vegetation and phytoplankton, the primary producers at the base of the aquatic food web [27]. While less commonly highlighted, very high TSS concentrations may also cause minor alterations in water temperature profiles due to increased absorption of solar radiation, although this effect is generally secondary to other factors. The diminished clarity also negatively affects the aesthetic quality of water, which have a concern for domestic users and potential recreational activities.

Chemically, TSS plays a crucial role as both a carrier and a reactor for various substances in the aquatic environment. The nature of the suspended particles, whether they are predominantly inorganic clays, silts, or organic detritus, dictates their chemical reactivity and their capacity to adsorb or desorb nutrients and contaminants. Fine-grained inorganic particles, such as clays, possess large surface areas that readily adsorb nutrients like phosphorus and nitrogen compounds, as well as various pollutants [10, 16, 23]. Organic components of TSS also bind pollutants and serve as a substrate for microbial activity. Consequently, TSS significantly influences nutrient dynamics; it can transport essential nutrients vital for fisheries and agriculture, but excessive loads or altered sediment types can also contribute to nutrient imbalances, potentially leading to eutrophication in receiving waters or, conversely, nutrient depletion in areas starved of natural sediment input [10, 13]. Suspended particles are well-documented vectors for a range of contaminants, including heavy metals such as arsenic, iron and others, as well as pesticides originating from agricultural runoff [2, 4, 12, 28]. The association of these pollutants with TSS facilitates their dispersal throughout the delta's waterways and eventual deposition into bed sediments. This transport mechanism influences the bioavailability, persistence and potential toxicity of these contaminants. For instance, contaminants adsorbed to TSS can settle and accumulate in sediments, creating a long-term

reservoir of pollution. Subsequent resuspension events, triggered by high flows, dredging, or boat traffic, can reintroduce these contaminants into the water column, leading to secondary pollution episodes even if the primary sources have been curtailed [8, 27]. This creates an effect where past pollution associated with TSS continues to impair water quality over extended periods. Furthermore, TSS interacts with salinity in estuarine environments, where changes in ionic strength can induce flocculation of fine particles, altering settling velocities and patterns of deposition [23, 24].

Biologically, high concentrations of TSS, particularly those rich in organic matter, can lead to a significant depletion of dissolved oxygen (DO) in the water column as microorganisms decompose the organic material [2, 11, 13, 16, 29]. This oxygen depletion can create hypoxic or even anoxic conditions, which are detrimental to most aquatic organisms. The reduction in light penetration due to high turbidity, as previously mentioned, directly curtails primary production by phytoplankton and submerged macrophytes. This not only reduces the autochthonous food supply at the base of the aquatic food web but also diminishes an important source of dissolved oxygen generated through photosynthesis during daylight hours. This creates a detrimental synergy that reduced oxygen production combined with increased oxygen consumption from organic TSS decomposition significantly elevates the risk of low DO conditions. The physical abrasion by suspended particles can also directly harm aquatic organisms, for example, by clogging fish gills and filter-feeding apparatus of invertebrates. Finally, the settling of suspended solids can lead to habitat alteration by smothering benthic environments, covering spawning grounds, and changing the substrate composition, thereby affecting the communities of organisms that inhabit the river and canal beds [10].

3.3. Consequences of altered water quality due to total suspended solids for water uses in the Vietnamese Mekong Delta

The degradation of water quality stemming from elevated and altered TSS regimes in the VMD has far-reaching consequences for essential human water uses and the overall health and stability of the delta's ecosystems. These impacts are often interconnected, creating a cascade of challenges for the region's inhabitants and its natural environment. For instance, water quality deterioration driven by agricultural runoff with high TSS loads can subsequently impair downstream aquaculture operations, affect the suitability of water for domestic abstraction and degrade the general ecological condition of receiving waters, underscoring the need for integrated management approaches that recognize these linkages [2, 4].

In the agricultural sector, high TSS levels in irrigation water can lead to the clogging of irrigation canals, intake structures and pumping equipment, thereby reducing the efficiency of water delivery systems and incurring increased operational and maintenance costs [4]. While direct evidence on canal clogging specific to the VMD was not prominent in the selected literature, the principle is well-established for sediment-laden irrigation waters and the mention of silt and suspended solids complicating water treatment processes implies broader usability issues [4]. Perhaps more critically, the long-term reduction in the deposition of nutrient-rich natural sediments on floodplains, a consequence of upstream dam construction trapping a significant portion of the Mekong rivers sediment load (of which TSS is a component), is leading to a decline in inherent soil fertility [3, 10]. This necessitates increased reliance on synthetic chemical fertilizers by farmers to maintain crop yields, which in turn can contribute to further water pollution through runoff if not managed properly, potentially creating a maladaptive cycle. Poor water quality, including the presence of contaminants adsorbed to TSS or conditions of low dissolved oxygen in irrigation water, can also negatively affect crop productivity and health. Furthermore, delta subsidence, partly linked to sediment starvation, exacerbates saline intrusion, which severely

impacts rice farming and other agricultural activities [4, 15].

Aquaculture, a cornerstone of the VMD's economy, is particularly vulnerable to TSS-related water quality issues. High concentrations of suspended solids in source water or within culture ponds can directly harm farmed species such us fish and shrimp by abrading and clogging gills, reducing feeding efficiency and inducing physiological stress, thereby increasing their susceptibility to diseases [2, 25]. The management of pond water quality becomes more complex and costly when source water has high TSS levels, as this can lead to increased turbidity within ponds, limit natural primary productivity which can be a food source and elevate oxygen demand from the decomposition of organic particulate matter [2]. Ultimately, degraded water quality attributable to TSS and associated pollutants can lead to reduced growth rates, lower survival, and diminished overall productivity and economic viability of aquaculture enterprises [2, 10].

The provision of safe domestic water supply is also significantly challenged by high TSS. Elevated levels of suspended solids in raw water sources necessitate more sophisticated and expensive treatment processes, typically involving enhanced coagulation, flocculation, sedimentation and filtration stages to achieve acceptable clarity and remove particulate-bound contaminants [4, 15]. Turbid water is aesthetically unappealing to consumers and can harbor microorganisms. More importantly, various contaminants, including pathogens, heavy metals and pesticides, can be adsorbed onto suspended particles. If these are not effectively removed during water treatment, they can pose significant health risks to the population relying on these water sources for drinking and other domestic purposes [4, 12]. The economic burden of these impacts, such as increased costs for canal dredging, water treatment, reduced agricultural and aquacultural outputs and potential health expenditures, often disproportionately affects the rural and economically vulnerable populations of the VMD.

Finally, the impacts of TSS on ecosystem health are pervasive. Changes in water clarity, dissolved oxygen levels, nutrient balances and the physical structure of aquatic habitats, all influenced by TSS, can lead to shifts in aquatic species composition, reductions in biodiversity and the overall degradation of ecosystem integrity [3, 10, 13]. The smothering of benthic habitats by excessive sedimentation can destroy critical spawning and nursery grounds for fish and invertebrates, while reduced light penetration due to persistent turbidity negatively affects submerged macrophytes, which provide food and shelter for many aquatic organisms [6, 13]. These alterations disrupt fundamental ecological processes, including nutrient cycling and food web dynamics. On a larger and longer timescale, the significant reduction in the total sediment supply to the delta, a phenomenon in which TSS dynamics play a part, is a critical factor contributing to coastal erosion, land subsidence and increased vulnerability to sea-level rise. These geomorphological changes fundamentally threaten the physical existence and ecological functioning of the entire delta ecosystem, highlighting the profound and existential threat posed by altered sediment regimes [3, 5, 10, 17, 18, 20, 22, 30].

4. CONCLUSIONS

This review confirms that TSS represent a critical water quality concern in the VMD, with profound environmental and socio-economic consequences. TSS concentrations frequently exceed standards, driven largely by anthropogenic pressures. These include sediment trapping by upstream hydropower dams, intensive local agriculture and aquaculture, widespread sand mining and inadequately treated wastewater discharges. The impacts are multifaceted. Elevated TSS increases turbidity, reducing light penetration and suppressing primary productivity. Suspended particles also act as vectors for contaminants (e.g., heavy metals, pesticides) and contribute to dissolved oxygen depletion. These water quality deteriorations adversely affect key sectors such as agriculture faces irrigation challenges and reduced soil fertility; aquaculture

contends with compromised aquatic health and lower yields and domestic water supplies require more complex, costly treatment. Critically, the systemic reduction in sediment delivery exacerbates land subsidence and coastal erosion, threatening the VMD's long-term geomorphological stability, particularly in the context of climate change. Significant knowledge gaps persist regarding the synergistic impacts of TSS with climate change and the full socio-economic costs of this degradation. Future research should prioritize integrated monitoring, predictive modeling under future scenarios, and assessing the efficacy of mitigation measures. The findings indicate the VMD is approaching a critical environmental threshold. Addressing these interconnected challenges demands holistic, adaptive and transboundary management strategies to ensure the region's sustainable development.

REFERENCES

1. Berg, H., Lan, T. H. P., Da, C. T. & Tam, N. T. (2023). Stakeholders assessment of status and trends of ecosystem services in the Mekong Delta for improved management of multifunctional wetlands. *Journal of Environmental Management*, 338, 117807.

2. Hong, T. T. K. & Giao, N. T. (2022). Analysis of surface water quality in upstream province of Vietnamese Mekong Delta using multivariate statistics. *Water*, 14(12), 1975.

3. Kondolf, G. M., Rubin, Z. K. & Minear, J. T. (2014). Dams on the Mekong: Cumulative sediment starvation. *Water Resources Research*, 50(6), 5158 - 5169.

4. Tuan, D. D. A., Loc, N. T, Phuong., N. T. N. & Trung, N. H. (2020). Assessing existing surface water supply sources in the Vietnamese Mekong Delta: Case study of Can Tho, Soc Trang and Hau Giang provinces. *Vietnam Journal of Science, Technology and Engineering*, 62(4), 65 - 70.

5. Pokhrel, Y., Burbano, M., Roush, J., Kang, H., Sridhar, V. & Hyndman, D. W. (2018). A review of the integrated effects of changing climate, land use and dams on Mekong river hydrology. *Water*, 10(3), 266.

6. Nguyen, B. T., Nguyen, V. N., Truong, H. T. T., Do, D. D., Nguyen, T. X., Nguyen, D. T. P., Nguyen, M. H., Dong, H. P., Le, A. H. & Bach, Q. V. (2020). Assessment and source quantification of heavy metal(loid)s in surface water using multivariate analyses from the Saigon river, Vietnam. *Environmental Science and Pollution Research*, 27(16), 19383 - 19397.

7. Whitehead, P. G., Jin, L., Bussi, G., Voepel, H. E., Darby, S. E., Vasilopoulos, G., Manley, R., Rodda, H., Hutton, C., Hackney, C., Tri, V. P. D. & Hung, N. N. (2019). Water quality modelling of the Mekong river basin: Climate change and socioeconomics drive flow and nutrient flux changes to the Mekong Delta. *Science of The Total Environment*, 673, 218 - 229.

8. Hung, N. N., Delgado, J. M., Güntner, A., Merz, B., Bárdossy, A. & Apel, H. (2014). Sedimentation in the floodplains of the Mekong Delta, Vietnam. Part I: Suspended sediment dynamics. *Hydrological Processes*, 28(7), 3132 - 3144.

9. Minh, H. V. T., Kurasaki, M., Ty, T. V., Tran, D. Q., Le, K. N., Avtar, R., Rahman, M. M. & Osaki, M. (2019). Effects of multi-dike protection systems on surface water quality in the Vietnamese Mekong Delta. *Water*, 11(5), 1010.

10. Allison, M. A., Nittrouer, C. A., Ogston, A. S., Mullarney, J. C. & Nguyen, T. T. (2017). Sedimentation and survival of the Mekong Delta: A case study of decreased sediment supply and accelerating rates of relative sea level rise. *Oceanography,* 30(3), 98 - 109.

11. Giao, N. T. & Minh, V. Q. (2021). Evaluating surface water quality and water monitoring parameters in the Tien river, Vietnamese Mekong Delta. *Jurnal Teknologi (Sciences & Engineering)*, 83(3), 29 - 36.

12. Giao, N. T., Phan, K. A. & Huynh, T. H. N. (2022). Major concerns of surface water quality in South - West coastal regions of Vietnamese Mekong Delta. *Sustainable Environment Research*, 32(1), 46.

13. Wehrheim, C., Lübken, M., Stolpe, H. & Wichern, M. (2023). Identifying key influences on surface water quality in freshwater areas of the Vietnamese Mekong Delta from 2018 to 2020. *Water*, 15(7), 1295.

14. Giao, N. T. & Ly, N. H. T. (2023). Evaluating surface water quality in a coastal province of Vietnamese Mekong Delta using water quality index and statistical methods. *Polish Journal of Environmental Studies*, 32(3), 2113 - 2124.

15. Tran, Q. N., Thi Vo, N. N., Pham, T. T. & Lam, H. S. T (2024). Hydrate technology for water desalination in the Mekong Delta, Vietnam. *Heliyon*, 10(19), e38974 .

16. Tran, T. T., Liem, N. D., Hieu, H. H., Tam, H. T., Mong, N. V., Yen, N. T. M., Yen, T. T. H., Quang, N. X. & Luu, P. T. (2023). Assessment of long-term surface water quality in Mekong river estuaries using a comprehensive water pollution. *Environment and Natural Resources Journal*, 21(6), 524 - 533.

17. Ang, W. J., Park, E., Pokhrel, Y., Tran, D. D. & Loc, H. H. (2024). Dams in the Mekong: A comprehensive database, spatiotemporal distribution and hydropower potentials. *Earth Syst Sci Data*, 16(3), 1209 - 1228.

18. Binh, D. V., Kantoush, S. & Sumi, T. (2020). Changes to long-term discharge and sediment loads in the Vietnamese Mekong Delta caused by upstream dams. *Geomorphology*, 353, 107011.

19. Loisel, H., Mangin, A., Vantrepotte, V., Dessailly, D., Dinh, D. N, Garnesson, P., Ouillon, S., Lefebvre, J. -P., Mériaux, X. & Minh, T P. (2014). Variability of suspended particulate matter concentration in coastal waters under the Mekong's influence from ocean color (MERIS) remote sensing over the last decade. *Remote Sensing of Environment*, 150, 218 - 230.

20. Nittrouer, C. A., Mullarney, J. C., Allison, M. A. & Ogston, A. S. (2017). From the guest editors introduction to the special issue on sedimentary processes building a tropical delta yesterday, today and tomorrow: The Mekong system. *Oceanography*, 30(3), 10 - 21.

21. Ha, N. T. T., Yu-Li, W., Van, B. D. & and Dang, T. D (2025). Hydrological alterations and sediment changes caused by dams in the Mekong river basin. *Hydrological Sciences Journal*, 70(10), 1744 - 1760.

22. Triet, N. V. K., Dung, N. V., Hoang, L. P., Duy, N. L., Tran, D. D., Anh, T. T., Kummu, M., Merz, B. & Apel, H. (2020). Future projections of flood dynamics in the Vietnamese Mekong Delta. *Science of The Total Environment*, 742, 140596.

23. Gratiot, N., Bildstein, A., Anh, T. T., Thoss, H., Denis, H., Michallet, H. & Apel, H. (2017). Sediment flocculation in the Mekong river estuary, Vietnam, an important driver of geomorphological changes. *Géoscience*, 349(6 - 7), 260 - 268.

24. Hung, N. N., Delgado, J. M., Güntner, A., Merz, B., Bárdossy, A. & Apel, H. (2014). Sedimentation in the floodplains of the Mekong delta, Vietnam Part II: Deposition and erosion. *Hydrological Processes*, 28(7), 3145 - 3160.

25. Tran, V. L. T., Barnes, A. C., Samsing, F., Vu, U. N. & Wiley, K. (2025). Striped catfish (*Pangasianodon hypophthalmus*) farmers' perspectives on challenges and health management practices in the Mekong delta, Vietnam: A qualitative study. *Preventive Veterinary Medicine*, 239, 106527.

26. Mekong River Commission (MRC) (2022). Sustainable hydropower development strategy: A basin-wide strategy for a changing Mekong river basin. Vientiane: MRC Secretariat.

27. Nguyen, T. H. D., Phan, K. D., Nguyen, H. T. T., Tran, S. N., Tran, T. G., Tran, B. L. & Doan, T. N. (2020). Total suspended solid distribution in Hau river using sentinel 2a satellite imagery. *ISPRS Ann Photogramm Remote Sens Spatial Inf Sci*, VI-3/W1-2020, 91 - 97.

28. World Bank & ICEM (2022). Climate resilient rural water supply in the Mekong delta, Vietnam. Volume I: Situation analysis and vulnerability assessment. World Bank.

29. World Bank & ICEM (2022). Climate resilient rural water supply in the Mekong delta, Vietnam. Volume II: Tools for building resilience of centralized rural domestic water supply systems. World Bank.

30. Thanh, V. Q., Roelvink, D., van der Wegen, M., Reyns, J., van der Spek, A., Van Vinh, G., Phuong Linh, V. T., Tu, L. X. & Trung, N. H. (2025). A numerical investigation on the suspended sediment dynamics and sediment budget in the Mekong delta. *Continental Shelf Research*, 286, 105427.

MULTIVARIATE STATISTICAL ANALYSIS OF CONTINUOUS AUTOMATIC SURFACE WATER QUALITY DATA AT BA LANG AND CAI CON STATIONS IN CAN THO CITY

Nguyen Thanh Giao[1], Ly Quoc Su[2], Le Duc Thua[2], Nguyen Thi Mong Tuyen[2]

[1]College of Environment and Natural Resources, Can Tho University

[2]Center for Natural Resources and Environment Monitoring, Department of Agriculture and Environment

[*]Email: ntgiao@ctu.edu.vn

ABSTRACT

The study utilized multivariate statistics to analyze water quality data continuously measured at two monitoring stations in Can Tho City, Vietnam. Surface water quality is assessed using national technical regulations on surface water (QCVN 08:2023/BTNMT). The water quality difference between two monitoring stations and between months in 2023 was analyzed using the Independent-Sample Test and One-way ANOVA. The relationship between water quality indicators is analyzed using the Pearson correlation. Cluster analysis (CA) is used to group water quality over time and suggest monitoring frequency, while principal component analysis (PCA) is used to identify the number of main sources affecting the water quality monitoring parameters. Surface water quality classification results show that pH and NH_4^+-N are in level A while TSS is in level B, DO is in level D, COD is in level C - D. Water quality is site and time dependent. Cluster analysis results show that water quality fluctuates greatly over time and the months to be monitored are January, March, May, July, September, November. PCA identified 2 - 3 main sources that have a significant impact on the parameters of salinity, pH, DO, COD, TSS, NH_4^+-N. The current study results contribute to providing important information for designing the frequency of monitoring surface water quality in Can Tho city. Subsequent studies need to identify monitoring indicators to continue perfecting the monitoring network in the study area.

Keywords: *Multivariate statistics, water quality, continuous monitoring, Ba Lang, Cai Con, Can Tho city.*

Received: 9 Stember 2025; revised: 12 November 2025; accepted: 4 December 2025.

1. INTRODUCTION

Water quality monitoring is fundamental for forecasting environmental status, evaluating the effectiveness of environmental protection regulations, and assessing sustainable development progress [1 - 4]. In Vietnam, surface water monitoring networks regarding ponds, lakes, and rivers are established based on national technical regulations [2, 5, 6]. The selection of sampling locations typically focuses on control areas or zones impacted by agriculture, industry, urbanization and monitoring frequency is heavily dictated by budgetary allocations and the nature of specific pollution sources [2, 5, 6]. Consequently, the design of these monitoring systems often lacks a rigorous scientific basis for optimization, relying instead on financial constraints [2].

To address such inefficiencies, multivariate statistical techniques, including correlation analysis, analysis of variance (ANOVA), cluster analysis (CA), and principal component analysis (PCA), have been widely adopted globally to

optimize monitoring networks [7 - 12]. Correlation analysis evaluates relationships between indicators to identify and remove redundant parameters [13-14], while ANOVA assesses spatial variation to support decision-making regarding monitoring locations [4, 15 - 18]. Furthermore, CA is utilized to group water quality data based on spatiotemporal similarities, providing a basis for rationalizing sampling frequency [7 - 9, 12, 19]. However, effective CA application requires robust, multi-temporal datasets [9, 10, 19 - 22]. Complementary to this, PCA serves to identify key loading factors determining which indicators require continuous monitoring and to apportion the primary sources influencing water quality [7 - 10, 19].

Despite the proven utility of these statistical methods, the design of surface water quality monitoring systems in Vietnam remains predominantly based on impact sources and funding, with limited application of multivariate analysis for network optimization [2]. Therefore, this study aims to analyze continuous automatic surface water quality monitoring data in Can Tho City using multivariate statistics. The findings provide a comprehensive assessment of current water quality and pollution sources, serving as a scientific basis to propose a redesigned, cost-effective monitoring frequency that contributes to perfecting the surface water monitoring network in the study area.

2. MATERIALS AND METHODS

Table 1. Summary of the amount of data collected from continuous automatic monitoring stations

Parameters	pH	Salinity	DO	TSS	COD	NH_4^+-N
Ba Lang station						
Number of full data	96,192	96,192	96,192	96,192	96,192	96,192
The number of received data	90,720	91,296	90,432	91,584	89,568	80,064
The number of valid data	82,080	81,216	73,728	77,184	79,200	71,424
Cai Con station						
Number of full data	96,192	96,192	96,192	96,192	96,192	96,192
The number of received data	86,400	91,296	78,048	80,640	80,352	34,848
The number of valid data	77,760	82,080	69,408	69,120	68,832	17,568

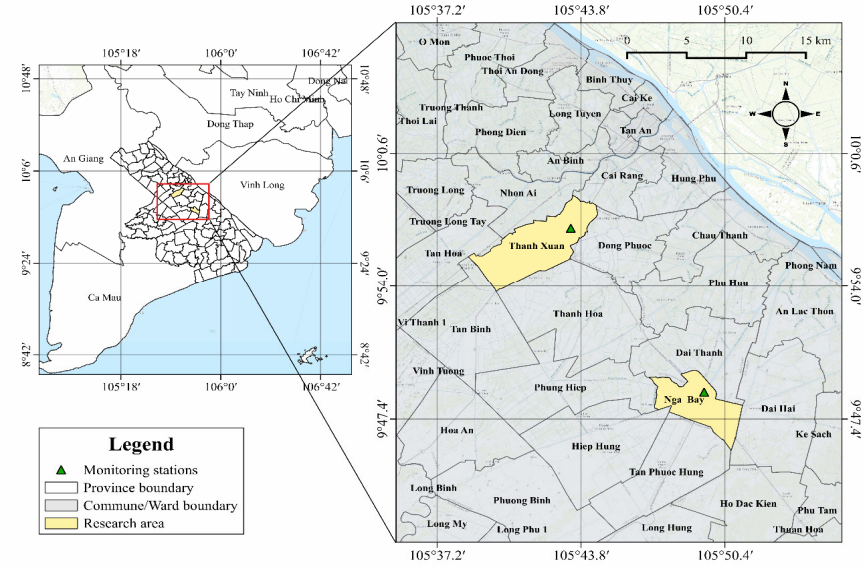

Figure 1. Map of Ba Lang and Cai Con surface water quality monitoring stations

The study was conducted at two automatic monitoring stations in Can Tho city: Ba Lang, representing industrial impacts, and Cai Con, representing urban impacts [23]. Surface water quality data, including pH, salinity, DO, TSS, COD, and NH_4^+-N, were collected daily from January to November 2023 [23]. Analytical instruments included Datalink (France) sensors for salinity,

TSS, and DO, and LAR (Germany) analyzers for COD and NH_4^+-N.

Water quality was assessed according to the national technical regulation QCVN 08:2023/BTNMT [6]. Statistical analyses employed Pearson correlation to examine relationships between parameters, while Independent-Sample T-Test and One-way ANOVA evaluated spatiotemporal variations. Multivariate techniques, specifically Cluster Analysis (CA) and Principal Component Analysis (PCA), were utilized to group water quality temporal fluctuations and identify potential pollution sources. All statistical data processing was performed using SPSS (Version 20) [24] and Primer (Version 5) [25].

3. RESULTS AND DISCUSSION

3.1. Evaluating surface water quality

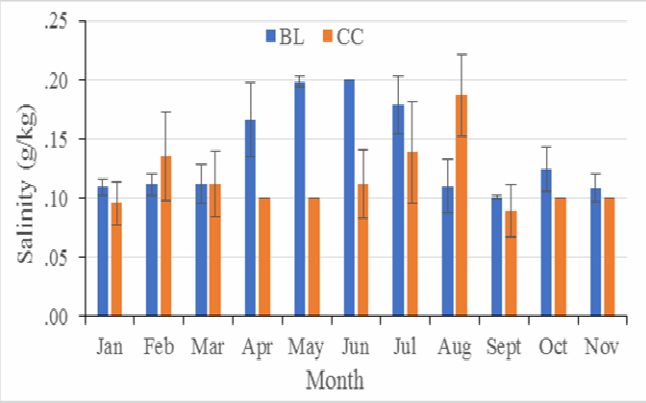

Figure 2. Salinity changes in the study area

Salinity concentrations at Ba Lang and Cai Con stations ranged from 0.10 - 0.20 g/kg and 0.09 - 0.19 g/kg, respectively. Peak values occurred from April to July at Ba Lang, and in February, July, and August at Cai Con. Statistical analysis revealed Ba Lang had significantly higher salinity during April–July ($p < 0.05$), whereas Cai Con was higher in February and August. Generally, salinity levels remained low and posed no significant impact on aquatic life [5, 6].

The pH at Ba Lang ranged from 6.83 ± 0.04 to 7.61 ± 0.34 (slightly acidic to neutral), while Cai Con varied from neutral to slightly alkaline. Temporal analysis indicated lowest values in January for both stations, with peaks occurring in July/October at Ba Lang and October/November at Cai Con. All recorded values fell within the QCVN 08:2023/BTNMT [6] allowable limits (Level A), suitable for aquatic development. These results align with previous findings of neutral pH ranges in the Mekong Delta [16, 26 - 30].

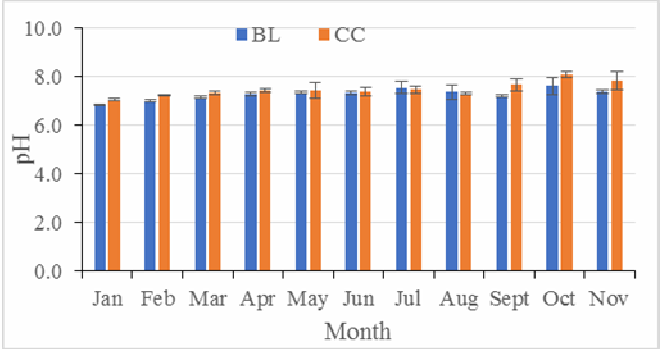

Figure 3. pH changes in the study area

TSS concentrations at Ba Lang (23 ± 9.2 - 40.2 ± 19.3 mg/L) and Cai Con (22.6 ± 7.2 - 38.8 ± 19.3 mg/L) consistently exceeded QCVN 08:2023/BTNMT limits by 1 - 1.6 times, classifying water quality as Level B [6]. Temporal peaks occurred in June and November at Ba Lang, and January and August at Cai Con. Spatially, Ba Lang exhibited significantly higher TSS ($p < 0.05$) in June, October, and November, whereas Cai Con was higher in January, July, and September. These elevated values, consistent with previous studies [15, 26, 31 - 35], are attributed to erosion, runoff, and phytoplankton [7, 26, 31, 35 - 37], negatively impacting aquatic ecosystems and treatment efficiency [26, 31, 37].

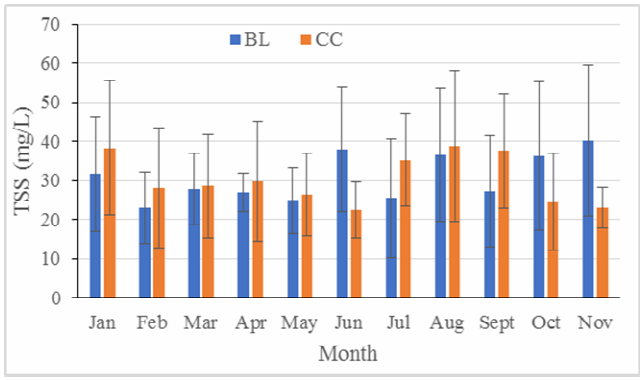

Figure 4. TSS changes in the study area

Dissolved oxygen (DO) concentrations at Ba Lang (1.4 ± 0.4 - 2.2 ± 0.3 mg/L) were significantly lower than at Cai Con (2.3 ± 0.3 - 3.2 ± 0.4 mg/L). Despite this spatial variation, both stations were classified as Level D2. These values are notably

lower than previous regional findings in An Giang [33], Can Tho [17], Ca Mau [30], and the Tien and Hau Rivers [27, 32], confirming a widespread trend of DO deficiency in the Mekong Delta. Low DO levels are attributed to organic loading [21, 31], hydrological disturbances [7], phytoplankton dynamics [35], and biological respiration [5]. Consequently, the observed hypoxia restricts water utility primarily to navigation purposes and poses significant risks to aquatic ecosystems.

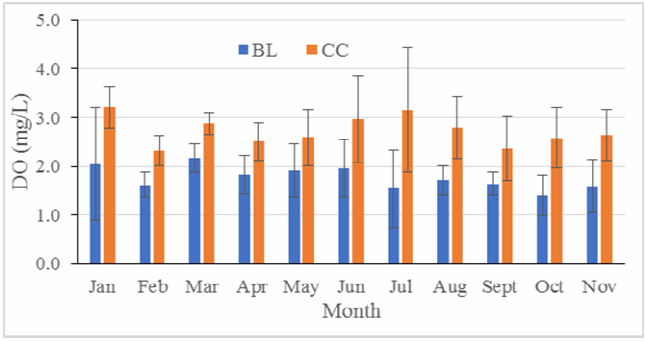

Figure 5. DO changes in the study areas

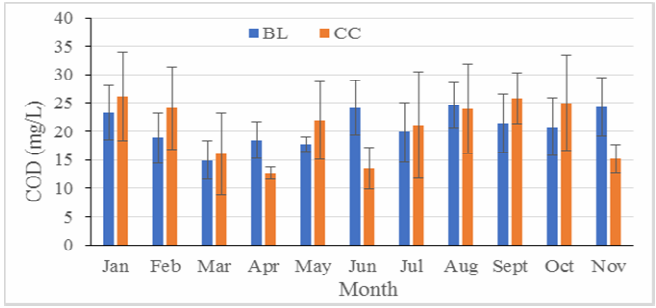

Figure 6. COD changes in the study areas

Organic matter concentrations (COD) at Ba Lang (14.9 ± 3.3 - 24.6 ± 4 mg/L) and Cai Con (12.6 ± 1.1 - 26.2 ± 7.8 mg/L) frequently exceeded the QCVN 08:2023/BTNMT Level C limit (20 mg/L), ranking water quality from poor (Level C) to very poor (Level D). Spatial variations were observed, with Cai Con generally exhibiting higher peaks during early months (January-February), while Ba Lang showed elevated levels in transition periods. These findings corroborate previous reports of widespread organic pollution across the Mekong Delta [17, 30, 32, 34]. Such contamination poses serious public health risks due to the potential formation of harmful disinfection by-products during water treatment.

NH_4^+-N concentrations at Ba Lang and Cai Con stations ranged from 0.02 ± 0.02 - 0.12 ± 0.06 mg/L and 0.12 ± 0.01 - 0.17 ± 0.01 mg/L, respectively (Figure 7). NH_4^+-N concentrations at both monitoring stations tend to be higher in the dry season (Jan - Apr). The measurement results of NH_4^+-N values at Cai Con station in February, March, April were significantly higher than the NH_4^+-N values at Ba Lang station. All NH_4^+-N values measured at two stations, Ba Lang and Cai Con are within the allowable limit of QCVN 08:2023/BTNMT [6] (0.3 mg/L) for human health. Previous studies also showed that the NH_4^+-N value in water sometimes exceeds the allowable limit [16, 26, 37]. The origin of NH_4^+-N in water is due to the influence of wastewater (domestic and industrial), the use of fertilizers in agricultural cultivation, and the process of decomposition of organic matter [7 - 9].

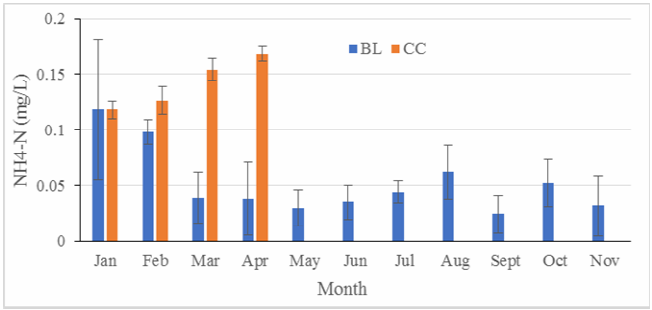

Figure 7. NH_4^+-N changes in the study area

3.2. Correlation among surface water parameters

The correlation between water quality assessment indicators during the period from January to November of 2023 at Ba Lang station is presented in Table 2. Research results show that salinity has a positive correlation at an average level with pH. Salinity has a weak negative correlation with NH_4^+-N. Salinity, COD, TSS and DO were not correlated (Table 2). The pH has a moderate negative correlation with NH_4^+-N and a weak negative correlation with dissolved oxygen. Previous research also found a negative correlation between pH and NH_4^+-N because an increase in NH_4^+-N concentration leads to a decrease in pH value [13]. The conversion of NH_4^+-N into nitrate also consumes oxygen, making NH_4^+-N and DO negatively correlate [8, 9, 13, 21]. NH_4^+-N has a very weak correlation with COD. Analysis results show a weak correlation of COD with TSS (r=0.207) and with DO (-0.241) (Table 2). Overall, the research

results show that the correlation between observed indicators is only weak to moderate. Previous research showed that surface water quality indicators had weak correlations except for ions dissolved in water [13, 20].

Table 2. Relationship between observed water quality parameters at the Ba Lang station

Parameter		Sal	pH	NH_4^+-N	COD	TSS	DO
Sal	r	1	0.317**	-0.244**	-0.078	0.010	-0.003
	Sig		0.000	0.000	0.178	0.874	0.957
	N	316	302	252	300	238	251
pH	r	0.317**	1	-0.410**	0.061	0.006	-0.233**
	Sig	0.000		0.000	0.287	0.925	0.000
	N	302	313	258	310	247	262
NH_4^+-N	r	-0.244**	-0.410**	1	0.134*	-0.018	0.018
	Sig	0.000	0.000		0.032	0.803	0.792
	N	252	258	258	255	202	223
COD	r	-0.078	0.061	0.134*	1	0.207**	-0.241**
	Sig	0.178	0.287	0.032		0.001	0.000
	N	300	310	255	311	245	259
TSS	r	0.010	0.006	-0.018	0.207**	1	-0.068
	Sig	0.874	0.925	0.803	0.001		0.327
	N	238	247	202	245	249	208
DO	r	-0.003	-0.233**	0.018	-0.241**	-0.068	1
	Sig	0.957	0.000	0.792	0.000	0.327	
	N	251	262	223	259	208	262

***. Correlation is significant at the 0.01 level (2-tailed).*

**. Correlation is significant at the 0.05 level (2-tailed).*

Correlation analysis at Cai Con (Table 3) revealed distinct patterns compared to Ba Lang. While salinity showed weak associations with other parameters, pH exhibited a strong positive correlation with NH_4^+-N. Notably, NH_4^+-N displayed a significant negative correlation with COD (r = -0.611), a sharp contrast to the negligible relationship observed at Ba Lang. Other interactions, such as COD vs. TSS, remained weak. These inconsistent correlations align with previous findings [13, 20], suggesting that site-specific environmental drivers heavily influence hydro-chemical dynamics, thereby limiting the predictive power of simple correlation matrices in complex surface water systems.

Table 3. Relationship between observed water quality parameters at the Ba Lang station

Parameter		Sal	pH	NH_4^+-N	COD	TSS	DO
Sal	r	1	-0.190**	-0.076	0.236**	0.123	-0.152*
	Sig		0.002	0.409	0.000	0.051	0.020
	N	301	267	120	250	253	234
pH	r	-0.190**	1	0.837**	-0.036	-0.180**	-0.048
	Sig	0.002		0.000	0.557	0.004	0.444
	N	267	300	108	269	258	252
NH_4^+-N	r	-0.076	0.837**	1	-0.611**	-0.267**	-0.204*
	Sig	0.409	0.000		0.000	0.004	0.037
	N	120	108	120	114	114	104
COD	r	0.236**	-0.036	-0.611**	1	0.203**	-0.108

	Sig	0.000	0.557	0.000		0.001	0.098
	N	250	269	114	279	246	234
TSS	r	0.123	-0.180**	-0.267**	0.203**	1	-0.046
	Sig	0.051	0.004	0.004	0.001		0.476
	N	253	258	114	246	276	238
DO	r	-0.152*	-0.048	-0.204*	-0.108	-0.046	1
	Sig	0.020	0.444	0.037	0.098	0.476	
	N	234	252	104	234	238	265

***. Correlation is significant at the 0.01 level (2-tailed).*

**. Correlation is significant at the 0.05 level (2-tailed).*

3.3. Analysis of temporal variation of surface water quality

Cluster analysis of monthly mean values at Ba Lang station revealed significant temporal fluctuations, categorizing parameters into 2 to 3 distinct groups (Table 4). These clusters reflect specific hydrological regimes, such as salinity intrusion periods and varying concentration gradients for pH, NH_4^+-N, COD, TSS and DO. For instance, salinity groupings clearly differentiated between intrusion and non-intrusion months. The formation of distinct temporal clusters confirms that surface water quality in the study area is highly dynamic and time-dependent. These results align with previous findings on the temporal variability of surface water environments [8, 9, 13, 21, 27, 28, 33].

Table 4. Temporal variation of water quality parameters at Ba Lang station

Parameters	Number of clusters	Cluster 1	Cluster 2	Cluster 3
Sal	2	Jan, Feb, Mar, Aug, Sept, Oct, Nov	Apr, May, Jun, Jul	None
pH	3	Jan, Feb	Jul, Oct	Mar, Apr, May, Jun, Aug, Sept, Nov
NH_4^+-N	3	Jan, Feb	Aug, Oct	Mar, Apr, May, Jun, Jul, Sept, Nov
COD	3	Mar	Jan, Jun, Aug, Nov	Feb, Apr, May, Jul, Sept, Oct
TSS	3	Feb, Mar, Apr, May, Jul, Sept	Jan	Jun, Aug, Oct, Nov
DO	3	Jan, Mar, May, Jun	Oct	Feb, Apr, Jul, Aug, Sept, Nov

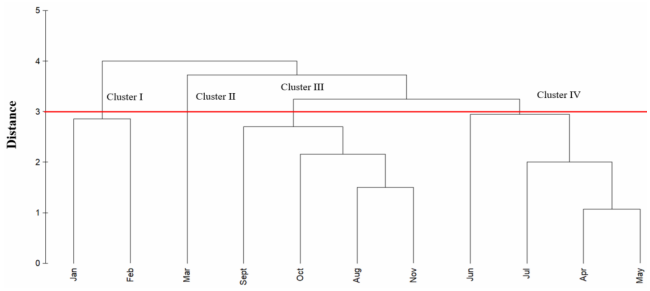

Figure 8. Clustering surface water quality at the Ba Lang station

Cluster Analysis (CA) categorized the 11 monitoring months at Ba Lang into four distinct temporal groups (Figure 8), reflecting seasonal water quality variations. Applying the principle of reducing sampling redundancy within similar clusters, specific representative months were selected: January, March, May, July, September, and November. Consequently, the monitoring frequency can be scientifically reduced from 11 to 6 times per year. This optimization maintains data representativeness while offering a significant solution for environmental monitoring in Vietnam under budgetary constraints.

Variations over time in the average (monthly) values of water quality indicators at Cai Con station are presented in Table 5. Variations over time of each indicator are classified into 2 to 4 groups in period from January to November. Salinity is classified into 3 groups, in which the highest salinity

value is found in group 1, the lowest value is found in group 3, while group 2 has an intermediate value between group 1 and group 3 (Table 5). pH values are classified into 4 groups in ascending order: Group 3 < group 4 < group 2 < group 1. COD is divided into 2 groups in which group 1 includes months with higher COD values than COD during the months in group 2. TSS has increasing values in the groups in the order group 3 < group 2 < group 1. DO fluctuates greatly and is divided into 4 groups with the order group 1 < group 2 < group 4 < group 3. Thus, water quality indicators at Cai Con station, especially pH and DO, are subject to greater fluctuations over time than indicators at Ba Lang station. The research results show that water quality indicators at Cai Con station also fluctuate over time and this is also consistent with the results of previous studies in the Mekong Delta region [27, 35].

Table 5. Temporal variation of water quality parameters at Cai Con station

Parameters	Number of clusters	Cluster 1	Cluster 2	Cluster 3	Cluster 4
Sal	3	Aug	Feb, Jul	Jan, Mar, Apr, May, Jun, Sept, Oct, Nov	None
pH	4	Oct	Sept, Nov	Jan	Feb, Mar, Apr, May, Jun, Jul, Aug
COD	2	Jan, Feb, May, Jul, Aug, Sept, Oct	Mar, Apr, Jun, Nov	None	None
TSS	3	Jan, Jul, Aug, Sept	Jun, Oct, Nov	Feb, Mar, Apr, May	None
DO	4	Feb, Sept	Apr, May, Oct, Nov	Jan, Jul	Mar, Jun, Aug

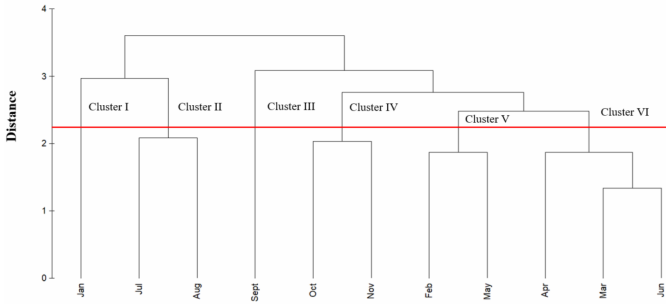

Figure 9. Clustering surface water quality at the Ba Lang station

Cluster analysis classified the Cai Con dataset into six distinct temporal groups (Figure 9). By selecting one representative month per cluster to minimize redundancy, the optimal monitoring schedule was identified as January, March, May, July, September, and November. This temporal pattern mirrors the results obtained for Ba Lang station. Consequently, the study proposes a unified monitoring frequency of six times per year for both stations. This optimized schedule maintains data representativeness regarding seasonal fluctuations while significantly reducing sampling efforts compared to the original monthly regime.

3.4. Potential polluting sources and key variables

Principal Component Analysis (PCA) at Ba Lang extracted three primary components (PC1–PC3) accounting for 85.2% of the total variance. PC1 was characterized by significant loadings of pH, NH_4^+-N, TSS, and DO. PC2 was associated with Salinity, NH_4^+-N, COD, and TSS, while PC3 was driven by Salinity, TSS, and DO. The results highlight the multi-source nature of water quality variations, particularly for TSS, which is influenced by all three components, whereas Salinity, DO, and NH_4^+-N are governed by dual underlying factors.

Table 6. Sources and variables influencing surface water quality at Ba Lang station

Parameter/PC	PC1	PC2	PC3	PC4	PC5
Sal	-0.189	0.478	0.459	-0.668	-0.023
pH	-0.607	0.233	-0.148	-0.025	0.462
NH_4^+-N	0.424	-0.406	-0.146	-0.580	0.532

COD	-0.294	-0.569	0.271	-0.286	-0.528
TSS	-0.396	-0.459	0.402	0.240	0.443
DO	0.416	0.132	0.715	0.278	0.170
Eigenvalue	2.20	1.89	1.03	0.61	0.24
%var	36.6	31.5	17.1	10.1	4.0
Cum.%var	36.6	68.1	85.2	95.3	99.3

PCA analysis at Cai Con identified two primary components (PC1, PC2) explaining 67.6% of the total variance, with three secondary components contributing an additional 32.5%. PC1 showed strong associations between Salinity, COD, TSS, DO, and pH, while PC2 was primarily driven by DO, pH, and COD. Notably, secondary sources (PC3–PC5) exhibited strong correlations with individual parameters such us Salinity, pH, and TSS. The results indicate that monitored parameters are influenced by multiple pollution sources (2 to 4 factors), implying a complex interplay of environmental pressures that necessitates targeted investigation for effective management.

Table 7. Sources and variables influencing surface water quality at Cai Con station

Parameter/PC	PC1	PC2	PC3	PC4	PC5
Sal	0.427	0.057	0.835	0.338	-0.057
pH	-0.490	-0.362	0.007	0.719	0.335
COD	0.351	-0.691	-0.234	0.157	-0.566
TSS	0.582	-0.261	-0.198	-0.077	0.740
DO	0.340	0.566	-0.457	0.582	-0.129
Eigenvalue	2.14	1.23	0.78	0.56	0.29
%var	42.9	24.7	15.5	11.3	5.7
Cum.%var	42.9	67.5	83.0	94.3	100

PCA analysis results show that at monitoring stations, water quality is affected by 2 to 3 main sources. The indicators of salinity, pH, DO, COD, TSS and NH_4^+-N all have a major influence on water quality. These indicators are affected by 1 to 2 sources of pollution. Therefore, these indicators need to continue to be monitored in the future.

4. CONCLUSIONS

The assessment of surface water quality at Ba Lang and Cai Con stations revealed distinct compliance and contamination patterns. While Salinity, NH_4^+-N, and pH remained within QCVN 08:2023/BTNMT limits (Level A), significant organic and particulate pollution was evident, with TSS classified at Level B, and COD and DO falling to Levels C and D. Spatiotemporal analysis indicated high heterogeneity, with Cluster Analysis (CA) differentiating 2 - 3 temporal groups at Ba Lang and 2 - 4 at Cai Con. Correlation analysis generally showed weak to moderate associations between parameters. Principal Component Analysis (PCA) identified complex pollution dynamics, extracting three and two primary sources driving water quality variations at Ba Lang and Cai Con, respectively.Crucially, the study demonstrates that monitoring frequency can be scientifically optimized from 11 to 6 times per year (January, March, May, July, September, and November) without compromising data representativeness. This proposed methodology provides a cost-effective framework highly applicable to other riverine systems in the Mekong Delta facing budgetary constraints.

REFERENCES

1. Simeonov, V., Stratis, J. A., Samara, C., Zachariadis, G., Voutsa, D., Anthemidis, A., Sofoniou, M. & Kouimtzis, T. (2003). Assessment of the surface water quality in Northern Greece. *Water research*, 37(17), 4119 - 4124.

2. The National Assembly (2020). Law No. 72/2020/QH14 dated November 17, 2020 on

Environmental Protection. The National Assembly, Vietnam.

3. Yang, J., Li, J., Vliet, M. T. H. V., Jones, E. R., Huang, Z., Liu, M. & Bi, J. (2024). Economic risks hidden in local water pollution and global markets: A retrospective analysis (1995 - 2010) and future perspectives on sustainable development goal 6. *Water research*, 252, 121216.

4. Wang, Y. B., Junaid, M., Deng, J. Y., Tang, Q. P., Luo, L., Xie, Z. Y. & Pei, D. S. (2024). Effects of land-use patterns on seasonal water quality at multiple spatial scales in the Jialing River, Chongqing, China. *Catena*, 234, 107646.

5. Ministry of Environment and Natural Resources (MONRE). *National Technical Regulation on Surface Water Quality (QCVN 08-MT/BTNMT)*; Ministry of Environment and Natural Resources: Hanoi, Vietnam, 2015.

6. Ministry of Environment and Natural Resources (MONRE). *National Technical Regulation on Surface Water Quality (QCVN 08: 2023/BTNMT)*; Ministry of Environment and Natural Resources: Hanoi, Vietnam, 2023.

7. Chounlamany, V., Tanchuling, M. A. & Inoue, T. (2017). Spatial and temporal variation of water quality of a segment of Marikina River using multivariate statistical methods. *Water Science Technology*, 76(6), 1510 - 1522.

8. Zeinalzadeh, K. & Rezaei, E. (2017). Determining spatial and temporal changes of surface water quality using principal component analysis. *Journal of Hydrology: Regional Studies*, 13, 1 - 10.

9. Islam, M. S., Nakagawa, K., Abdullah-Al-Mamun, M., Khan, A. S., Goni, M. A. & Berndtsson, R. (2022). Spatial distribution and source identification of water quality parameters of an industrial seaport riverbank area in Bangladesh. *Water*, 14(9), 1356.

10. Balcerowska-Czerniak, G. & Gorczyca, B. (2024). Rapid assessment of surface water quality using statistical multivariate analysis approach: Oder River system case study. *Science of the Total Environment*, 912, 168754.

11. Amador-Castro, F., González-López, M. E., Lopez-Gonzalez, G., Garcia-Gonzalez, A., Díaz-Torres, O., Carbajal-Espinosa, O. & Gradilla-Hernández, M. S. (2024). Internet of Things and citizen science as alternative water quality monitoring approaches and the importance of effective water quality communication. *Journal of Environmental Management*, 352, 119959.

12. Wieczorek, K., Turek, A., Szczesio, M. & Wolf, W. M. (2024). A holistic approach to the spatio-temporal variability investigation of the main river water quality–The importance of tributaries. *Science of the Total Environment*, 906, 167588.

13. Mitryasova, O., Pohrebennyk, V., Cygnar, M. & Sopilnyak, I. (2016). Environmental natural water quality assessment by method of correlation analysis. *International Multidisciplinary Scientific GeoConference: SGEM*, 2, 317 – 324.

14. Siwiec, T., Reczek, L., Michel, M. M., Gut, B., Hawer-Strojek, P., Czajkowska, J., Jóźwiakowski, K., Gajewska, M. & Bugajski, P. (2018). Correlations between organic pollution indicators in municipal wastewater. Archives of Environmental Protection, 44(4), 50 - 57.

15. Son C. T., Giang N. T. H., Thao T. P., Nui, N. H., Lam N. T. & Cong V. H. (2020). Assessment of Cau River water quality assessment using a combination of water quality and pollution indices. *Journal of Water Supply: Research and Technology*, 69, 160-172.

16. Giao, N. T. (2020). Spatial variations of surface water quality in Hau Giang province, Vietnam using multivariate statistical techniques. *Environment Natural Resources Journal*, 18(4), 400 - 410.

17. Giao, N. T., Nhien, H. T. H., Anh, P. K. & Thuptimdang, P. (2022). Combination of water quality, pollution indices, and multivariate statistical techniques for evaluating the surface water quality variation in Can Tho city, Vietnam. Environmental Monitoring Assessment, 194(11), 844.

18. Sanae, B., Mohammed, B. A., Nisrine, I., Youness, G., Nariman, O., Azeddin, E. B., Mustapha, T., Hanane, T. & Zakia, R. (2024). Assessment of surface water quality: Case study of Oued Fez catchment areas (Morocco). *Environmental Sustainability Indicators*, 21, 100326.

19. Syeed, M. M. M., Hossain, M. S., Karim, M. R., Uddin, M. F., Hasan, M. & Khan, R. H. (2023). Surface water quality profiling using the water quality index, pollution index and statistical methods: A critical review. *Environmental Sustainability Indicators*, 18, 100247.

20. Noori, R., Sabahi, M. S., Karbassi, A. R., Baghvand, A. & Zadeh, H. T. (2010). Multivariate statistical analysis of surface water quality based on correlations and variations in the data set. *Desalination*, 260(1-3), 129 - 136.

21. Barakat A., Baghdadi, M. E., Rais, J., Aghezzaf, B. & Slassi, M. (2016). Assessment of spatial and seasonal water quality variation of Oum Er Rbia River (Morocco) using multivariate statistical techniques. *International Soil and Water Conservation Research*, 4(4), 284 - 292.

22. Kushwah, V. K., Singh, K. R., Gupta, N., Berwal, P., Alfaisal, F. M., Khan, M. A., Alam, S., & Qamar, O. (2023). Assessment of the surface water quality of the Gomti River, India, using multivariate statistical methods. *Water*, 15(20), 3575.

23. Department of Natural Resources and Environment of Hau Giang province (2023). Environmental monitoring report, 50 pages.

24. IBM Corp. Released 2011. (2011). IBM SPSS Statistics for Windows, Version 20.0. Armonk, NY: IBM Corp.

25. Primer-E Ltd 2001. (2001). Primer V5: User Manual/Tutorial, Plymouth routines in multivariate ecological research.

26. Mekong River Commission (MRC). (2015). Lower Mekong regional water quality monitoring report. ISSN: 1683 - 1489. MRC Technical Paper No.51.

27. Giao, N. T. & Minh, V. Q. (2021). Evaluating surface water quality and water monitoring parameters in the Tien River, Vietnamese Mekong Delta. *Jurnal Teknologi*, 83(3), 29 - 36.

28. Giao, N. T., Nhien, H. T. H., Anh, P. K. & Ni, D. V. (2021). Classification of water quality in low lying area in Vietnamese Mekong Delta Using set pair analysis method and Vietnamese water quality index. *Environmental Monitoring and Assessment*, 193(6), 1 - 16.

29. Giao, N. T. & Nhien, H. T. H. (2022). Assessment of surface water quality and monitoring in southern Vietnam using multicriteria statistical approaches. *Sustainable Environment Research*, 32(1), 20.

30. Giao, N. T. (2022). Analysis of Surface Water Quality using Multivariate Statistical Approaches: A case study in Ca Mau Peninsula, Vietnam. *Pollution*, 8(2), 463 - 477.

31. Chea, R., Grenouillet, G. & Lek, S. (2016). Evidence of water quality degradation in lower Mekong basin revealed by self-organizing map. *PloS one*, 11(1).

32. Lien, N. T. K., Huy, L. Q., Oanh, D. T. H., Phu, T. Q. & Ut, V. N. (2016). Water quality in mainstream and tributaries of Hau River. *Can Tho University Journal of Science*, 43, 68 - 79.

33. Ly, N. H. T. & Giao, N. T. (2018). Surface water quality in canals in An Giang province, Viet Nam, from 2009 to 2016. *Journal of Vietnamese Environment*, 10(2), 113 - 119.

34. Tuan, D. D. A., Thu, B. A., & Trung, N. H. (2019). Assessing quality of surface water for urban water supply source for Soc Trang city. *Journal of Can Tho university*, 4A, 61 - 70.

35. Giao, N. T. & Nhien, H. T. H. (2023). Evaluating surface water quality using indexes of water quality and plankton diversity. *Civil Engineering Journal*, 9(5), 1187 - 1202.

36. Prathumratana, L., Sthiannopkao, S. & Kim, K. W. (2008). The relationship of climatic and hydrological parameters to surface water quality in the lower Mekong River. *Environment international*, 34(6), 860 - 866.

37. Ongley. E.D. (2009). Chapter 12: Water Quality of the Lower Mekong River. In: Campbell, I.C. (ed.): The Mekong: Biophysical Environment of an International.

WRITING AND SUBMITTING

1. The Vietnam Journal of Agriculture and Environment publishes scientific articles announcing scientific research works with new scientific content, overview articles on the agriculture and rural development sector that have not been submitted for publication in any kind of journals

2. Articles can be written in Vietnamese (published in the Journal by Vietnamese language) or in English (published in the Journal by English language), drafted on a computer, lines separated by 1, 2 (Paragraph/Line spacing Multiple at 1,2), using the font Times New Roman, font size 12, with a length of no more than 10 pages of A4 size paper including references.

3. Keywords are presented in alphabetical order, from 3 to 5 words. Keywords in Vietnamese and English must have the same content and meaning of the word. The abstract must be no more than 350 words in length, without newline, in font size 10, including: Briefly stating the purpose, research method, and main research results. Articles written in Vietnamese must have abstracts in both English and Vietnamese and must not differ in content or meaning.

4. Articles must be presented in the following order: Title of the article in Vietnamese and English, author(s), author(s) agency name, abstract, keywords, content of the article , acknowledgments (if any), references. Author contact must be indicated with office address, email, and phone number on the front page of the manuscript. Vietnamese proper names must have enough accent marks, including articles in English.

5. References are presented in order of citation and numbered in square brackets in the order they appear in the article and in the list of references.

+ For documents that are articles in the Journal, write in full in the following order: Author's name, year of publication, title of article, title of journal, volume, number, page.

+ For documents being books, write in full in the following order: Name of author, year of publication, title of book, publisher, place of publication.

If the article is in English, any references that are not in English must be translated into English and captioned in the original language in parentheses.

6. The Vietnam Journal of Agriculture and Environment implements the submission process, the online review process on the Journal's software system and uses the database of published Journal, to suggest collaborators, reviewers and readers access the website: http://tapchikhoahoc.nnmt.net.vn/ and follow the instructions.

7. For details, please contact: Journal of Agriculture and Environment; No. 10 Nguyen Cong Hoan, Giang Vo, Hanoi; Phone: 024.37711070; 024.38345457; 024.37716634. Email: bbtnongnghiep@gmail.com.